Dimethyl Sulfide and Dimethyl Sulfoxide and Their Oxidation in the Atmosphere

Ian Barnes,*,† Jens Hjorth,‡ and Nikos Mihalopoulos§

Bergische Universität Wuppertal, FB C–Physikalische Chemie, Gauss Strasse 20, 42119 Wuppertal, Germany, European Commission, Joint Research Centre, Institute for Environment and Sustainability, TP 290, 21020 Ispra (VA), Italy, and Environmental Chemical Processes Laboratory, University of Crete, P.O. Box 1470, 71409 Heraklion, Greece

Received February 2, 2005

Contents

1. Introduction

Sulfur plays an important role in both the tropospheric and stratospheric budget of atmospheric gases, and investigation of the atmospheric sulfur cycle has been a subject of intense scientific interest for many years. In industrialized regions such as the United States and most of Europe, anthropogenic sulfur emissions (mainly comprised of SO_2) exceed natural emissions by about 1 order of magnitude.[1−4] On a global scale biogenic emissions become important with contributions to the sulfur budget of 15−20% and 50−60% in the Northern and Southern Hemispheres, respectively.[1,2,4] Of the biogenic contribution one compound, namely, dimethyl sulfide (DMS: CH_3SCH_3), constitutes approximately 50% of the emissions.[1−4]

This review is restricted to reviewing the gas-phase chemistry of dimethyl sulfide and its important oxidation products. Detailed reviews of the kinetics of the gas-phase

† Bergische Universität Wuppertal.
‡ Institute for Environment and Sustainability.
§ University of Crete.

10.1021/cr020529+ CCC: $59.00
Published on Web 02/22/2006

Ian Barnes was born and reared in Northern Ireland. He received his B.Sc. degree in Applied Chemistry from Salford University in the United Kingdom in 1974 and Ph.D. degree in Physical Chemistry from the Queen's University of Belfast in 1977. On completion of his Ph.D. he joined the Physical Chemistry Department of the Bergische University Wuppertal, Germany, where he is presently a Senior Research Scientist. A major portion of his work involves the application of large-scale environmental simulation chambers to investigate atmospheric processes. His research interests lie principally in the areas of gas-phase kinetics and photochemistry, including, in particular, the kinetics and mechanisms for the oxidation of aromatic hydrocarbons and organic sulfur compounds.

Jens Hjorth was born in Denmark and obtained his Ph.D. degree in Chemistry from the University of Odense, Denmark, in 1986. He has since then been employed as a research scientist at the Joint Research Centre of the European Commission in Ispra, Italy, where he presently works in the Climate Change Unit of the Institute for Environment and Sustainability. His research field is atmospheric chemistry, particularly the use of laboratory chamber experiments to gain information about chemical reactions in the troposphere. His work has addressed several aspects of atmospheric chemistry: NO_y chemistry, particularly reactions of the NO_3 radical, as well as the chemistry of biogenic volatile organic compounds (e.g., monoterpenes), organic volatile sulfur compounds (particularly dimethyl sulfide), and fluorinated organic compounds (used as replacements of CFCs). His recent work has been focused on processes leading to the formation of secondary organic aerosol.

oxidation of sulfur compounds, both organic and inorganic and, in particular, DMS, can be found in publications by Wilson and Hirst[5] (up to 1996) and DeMore et al.[6] and Atkinson et al.[7] (up to 1997). Barone et al.[8] and Ravishankara et al.[9] give comprehensive summaries of the situation up to 1997 regarding the kinetics and reaction mechanism of the oxidation of DMS. Detailed articles on the kinetics, products, and mechanisms of the atmospheric oxidation of various types of sulfur compounds prior to 1997 are given (in descending year of appearance) by Urbanski and Wine,[10] Berresheim et al.,[11] Atkinson,[12] Tyndall and Ravishankara,[13]

Nikolaos Mihalopoulos graduated from the University of Athens (1984), and he received his M.Sc. and Ph.D. degrees in Chemistry from the University of Paris 7 (1989). In 1993 he joined the Department of Chemistry of the University of Crete, where he is presently Professor of Atmospheric Chemistry and President of the Department. His research activities focus on photochemistry, biogeochemical sulfur, nitrogen and phosphorus cycles, and aerosol characterization over marine remote locations (Southern Hemisphere) and marine regions strongly influenced by human activities (Mediterranean area).

Plane,[14] Atkinson,[15] and Atkinson and Carter.[16] At the time of writing a review on the volatile organic sulfur compounds, including DMS, appeared by Bentley and Chasteen.[17] This review is, however, mainly restricted to reviewing the knowledge on biosynthetic sources of the sulfur compounds and contains only very rudimentary information on their gas-phase atmospheric degradation pathways.

Since the appearance of the reviews listed above most of the publications in the intervening years on atmospheric sulfur chemistry, encompassing field, laboratory, and theoretical studies, have been largely concerned with different aspects of the chemistry of DMS and DMSO and to a lesser extent CS_2. The present review concentrates to a large extent on reviewing the new data associated with DMS and DMSO. Further, in the interest of brevity, the approach taken in writing this review on the kinetics and mechanistic aspects of the oxidation of the sulfur compounds has been to write a brief synopsis of the situation prior to 1997 and then update this knowledge by inclusion of the information from recent publications followed by an appraisal of the new situation. On the basis of a search of the ISI web of science, almost 350 articles (50% of the total database under the word DMS) have been published on DMS since 1997. Only in instances where it was deemed necessary for the sake of clarity is a detailed historical record given of the development of particular kinetic or mechanistic aspects of DMS chemistry. A list of the meaning of the abbreviations used in the text is given in Table 1. The names of the sulfur compounds, their empirical formulas, and the abbreviations used in the text are listed in Figure 1.

The following few paragraphs serve to highlight the importance of understanding the atmospheric oxidation pathways of DMS. The ocean covers nearly 70% of the Earth's surface, and above the ocean approximately 50% of the sky is covered by stratus clouds. Through reflection of incoming radiation back to space this type of cloud plays a leading role in governing the planetary albedo. Aerosols present in the marine boundary layer, MBL, serve as cloud condensation nuclei (CCN) and are actively involved in regulation of the formation of marine stratus clouds. There are three main sources of aerosol in the remote marine

Table 1. List of the Abbreviations Used in the Manuscript

abbreviation	meaning
	(a) experimental methods
ARFS-LFP	atomic resonance fluorescence spectroscopy-laser flash photolysis
CRDS	cavity ring-down spectroscopy
DF-EPR	discharge flow-electron proton resonance
DF-MS	discharge flow-mass spectrometry
DF-RF	discharge flow-resonance fluorescence
DP-VA	direct photolysis - visual absorption
FP-RF	flash photolysis-resonance fluorescence
FP-VA	flash photolysis-visual absorption
HPTFR-CIMS	high-pressure turbulent flow reactor-chemical ionization mass spectroscopy
LFP-LA	laser flash photolysis-laser absorption
LFP-PLIF	laser flash photolysis-pulsed laser-induced fluorescence
LFP-TDLAS	laser flash photolysis-tunable diode laser absorption spectroscopy
LP-CRDSP	laser photolysis-cavity ring-down spectroscopy
LP-LIF	laser photolysis-laser-induced fluorescence
LP-UV/VIS	laser photolysis-UV−vis absorption spectroscopy
PR-UVRR	pulsed radiolysis-UV absorption spectroscopy relative rate technique
LP-LIF	laser photolysis-laser-induced fluorescence
PLP-LIF	pulsed laser photolysis-laser-induced fluorescence
PLP-PLIF	pulsed laser photolysis-pulsed laser-induced fluorescence
PLP-RF	pulsed laser photolysis-resonance fluorescence
PLP-UV	pulsed laser photolysis-UV absorption spectroscopy
PR-UV	pulsed radiolysis-UV absorption spectroscopy
RR	relative rate technique

boundary layer: sea salt, non-sea-salt (nss) sources, and entrainment of free tropospheric aerosol. The principal component of nss-aerosol is sulfate derived from the oxidation of gaseous dimethyl sulfide produced by phytoplankton in surface water (Charlson et al.,[18] Andreae et al.,[19] Cainey et al.[20]). The relative contributions of the three marine aerosol sources is dependent upon many factors such as wind speed, frequency of occurrence of clouds and precipitation, sea-surface DMS emission rates, oxidation mechanism of DMS to SO_2 and MSA, rate of entrainment of free tropospheric aerosol, etc.

It has been postulated that emission of DMS from the oceans may have a significant influence on the Earth's radiation budget and possibly in climate regulation (CLAW hypothesis, Charlson et al.[18]). Substantial amounts of DMS may also reach the upper troposphere (even the lower stratosphere) over convective regions. Thus, DMS may also influence sulfate aerosol formation in the upper troposphere and lower stratosphere.

The Intergovernmental Panel on Climate Change (IPCC)[21] has classified the coupling between DMS and aerosols as an important component of the planetary climate system which needs to be understood in detail. The major question concerning DMS in the marine atmosphere is the extent it plays in controlling the levels of aerosol in the MBL. Any effect that DMS will have on the climate is critically dependent on the production of gas-phase sulfuric acid (H_2SO_4) and new particles. Despite intensive efforts determination of the quantitative contribution of DMS-derived non-sea-salt sulfate to CCN in the marine boundary layer has remained elusive and model studies of global SO_2 indicate that there may be as yet unaccounted for oxidants involved in the DMS oxidation (Chin et al.[22]). Further progress in the elucidation of the DMS oxidation mechanism requires both further advances in field studies as well as detailed kinetic studies combined with modeling of the field data.

2. Chemistry of Dimethyl Sulfide (DMS)

2.1. Reaction with the OH Radical

2.1.1. Kinetics and Primary Reaction Steps with the OH Radical

The kinetics of the reaction of OH with DMS has been extensively studied using a diverse array of methods including DF-EPR, DF-RF, FP-RF, LP-LIF, and RR. Early FP-RF studies[23−25] suggested that the rate coefficient was well established, was independent of O_2, and that the reaction proceeded by an H-atom abstraction mechanism. However, the situation became confused by the publication of an FP-RF study by Wine et al.,[26] who reported a rate coefficient of 4.3×10^{-12} cm^3 molecule^{-1} s^{-1} for room temperature and observed a small *positive* activation energy. This was followed by numerous investigations on the reaction[27−40] using both absolute and relative kinetic methods. From the studies it emerged that the rate coefficient showed a molecular oxygen dependency.[30,31,33,36] For example, Hynes et al. showed in a comprehensive FP-RF investigation[31] on the reaction of OH with DMS and DMS-d_6 that the effective rate coefficient for OH + DMS and its deuterated analogue was dependent on oxygen and increased as the partial pressure of oxygen was increased. Similar "O_2 enhancements" were observed for DMS and DMS-d_6, showing that there was no isotope effect; a significant *negative* temperature dependence was also found.

The kinetic information is currently interpreted in terms of a two-channel mechanism involving a direct abstraction reaction (O_2 independent) together with reversible adduct formation followed by adduct reaction with molecular oxygen, i.e., for DMS and DMS-d_6

$$OH + CH_3SCH_3 \rightarrow CH_3SCH_2 + H_2O \qquad (1a)$$

$$OH + CH_3SCH_3\ (+\ M) \rightleftharpoons CH_3S(OH)CH_3\ (+\ M) \qquad (1b,1\text{-}b)$$

$$CH_3S(OH)CH_3 + O_2 \rightarrow \text{products} \qquad (2)$$

$$OH + CD_3SCD_3 \rightarrow CD_3SCD_2 + HOD \qquad (3a)$$

$$OH + CD_3SCD_3\ (+\ M) \rightleftharpoons CD_3S(OH)CD_3\ (+\ M) \qquad (3b,\ 3\text{-}b)$$

$$CD_3S(OH)CD_3 + O_2 \rightarrow \text{products} \qquad (4)$$

The current recommendation for the rate coefficient for reaction 1a at 298 K from the review of DeMore et al.,[6] based largely on the measurements in refs 26, 31, 32, 38, and 40 is 5×10^{-12} cm^3 molecules^{-1} s^{-1}. Slightly lower values are to be found in the reviews of Atkinson,[15] Atkinson et al.,[7] and Tyndall and Ravishankara.[13] Theoretical calculations of the rate coefficient for the abstraction of an H atom from DMS have been reported by Sekuŕsak et al.[41] and El-Nahas et al.[42] While the calculated rate of Sekuŕsak et al. is in good agreement with reported literature values, the calculations of El-Nahas et al. give a rate which is a factor of 4 lower than the experimentally determined values.

Equilibrium of pulsed generated OH with a OH·DMS-d_6 adduct has been observed at low pressures and tempera-

Figure 1

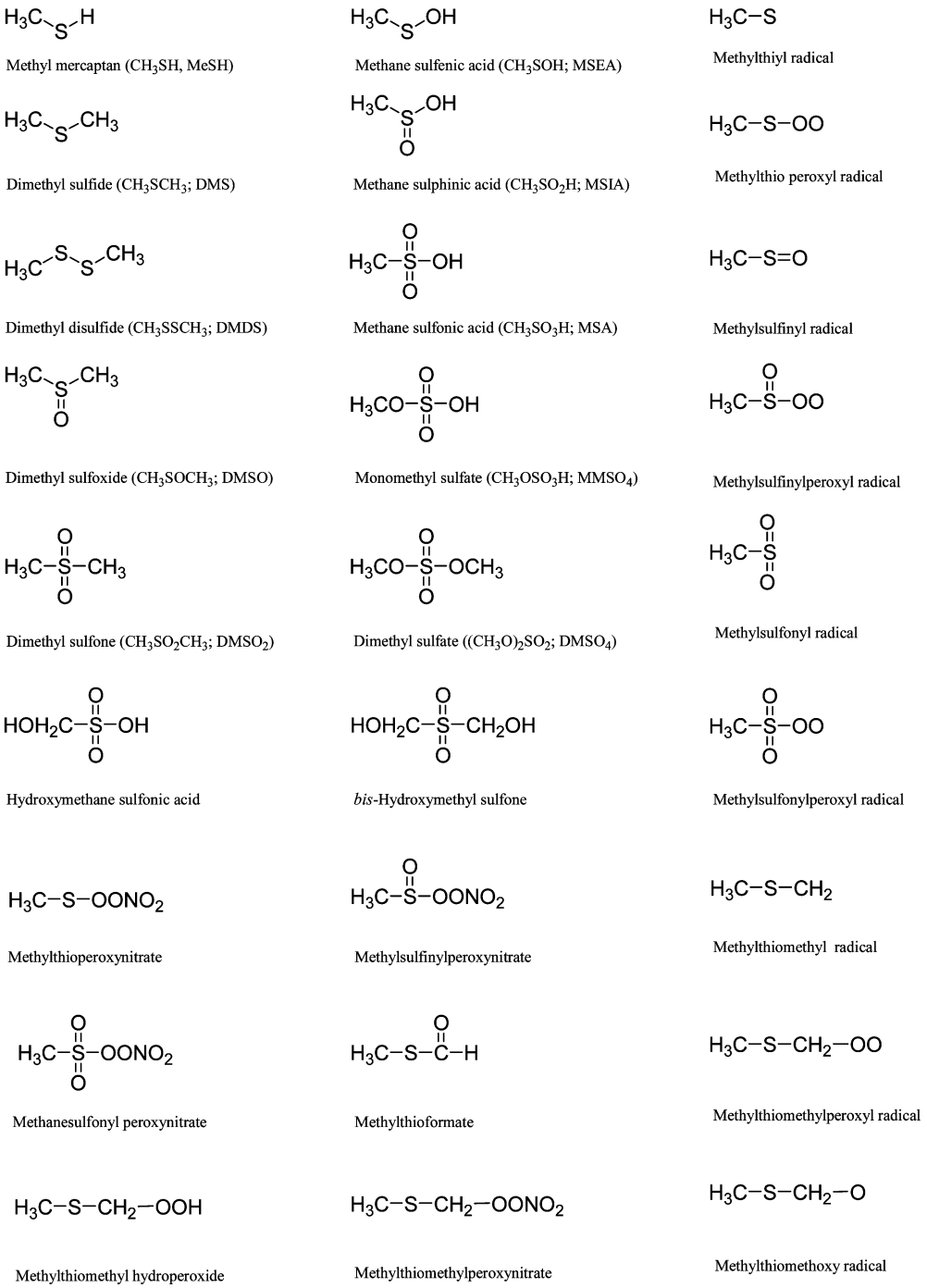

Figure 1. Structural formula and names of organic sulfur compounds and radicals involved in the oxidation of dimethyl sulfide and dimethyl sulfoxide.

tures,[39,40] thus confirming the existence of a stable thermalized adduct. Adduct bond strengths of 13.0, 10.1, and 14 kcal mol^{-1} have been reported by Hynes et al.[31,39,43] and values of 10.2 and 10.7 kcal mol^{-1} by Barone et al.[40] from second- and third-law calculations, respectively.

A computational study by McKee[44] yielded a bound geometry for the OH·DMS adduct with a bond strength of 6.0 kcal mol^{-1}, which is somewhat lower than the experimental values. This study was in contradiction with two other computational studies by Gu and Turecek,[45,46] which suggested that the OH·DMS adduct was not stable. Turecek[47] has since reinvestigated the OH·DMS adduct using DFT-B3LYP and MP2 calculations and finds structures and energetics similar to those of a stable adduct structure identified in a recent study by Wang and Zhang[48] using DFT-B3LYP. Wang and Zhang identified two weakly bound complexes between DMS and OH: (a) a 2-center-3-electron (2c-3e) bonding structure with the O atom pointing to the S atom and (b) a structure with the H atom of the OH radical pointing to the S atom and stabilized by dipole−dipole interaction between the OH and $S(CH_3)_2$. The 2c-3e bonding complex is reported to be more stable at the Gaussian-2 level with −31 kJ mol^{-1} (−7.41 kcal mol^{-1}) relative to OH + DMS. The value is slightly higher than that from McKee[44] but still lower than that obtained by experiment. More recently McKee[49] published a computational comparison of

the gas-phase and solution-phase OH radical oxidation of DMS in which he reports a S−OH binding enthalpy of 8.7 kcal mol^{-1}. The most recent paper on the subject is by Uchimaru et al.,[50] who performed ab initio and DFT investigations on the $(CH_3)_2S-OH$ adduct at the BH&HLYP, B3LYP, MP2, and CCSD(T) levels. For 298 K they report a value of 9.0 kcal mol^{-1} for the dissociation enthalpy of the S−O bond in the $(CH_3)_2S-OH$ adduct.

At the time of writing a theoretical study appeared which examined the geometries of $CH_3S(OH)CH_3$ using ab initio and density functional theories.[51] The studies showed that for an accurate description of the weakly bound adduct relatively large basis sets are required in order to recover a large fraction of the correlation energy. Eight stable $CH_3S(OH)CH_3$ almost identical complexes were identified. In summary, although there is still some uncertainty as to the strength of the S−OH bond in the DMS−OH adduct, its existence has been verified both experimentally and theoretically.

Hynes et al.[39] and Barone et al.[40] measured rate coefficients of $(0.8 \pm 0.3) \times 10^{-12}$ and $(1.00 \pm 0.33) \times 10^{-12}$ cm^3 molecules^{-1} s^{-1}, respectively, for the reaction of the OH·DMS-d_6 adduct with O_2 (reaction 4) independent of both temperature and pressure. From an empirical fit of their complex data set to the two-channel mechanism Hynes et al.[31] derived an expression for the observed rate coefficient for OH + DMS in 1 atm of air

$$k_{obs} = \{T \exp(-234/T) + 8.46 \times 10^{-10} \exp(7230/T) + 2.68 \times 10^{-10} \exp(7810/T)\}/\{1.04 \times 10^{11} T + 88.1 \exp(7460/T)\}$$

where k_{obs} is the overall measured rate coefficient for the abstraction and addition channels.

The branching ratio k_{1a}/k_{obs} is given by $9.6 \times 10^{-12} \exp(-234/T)/k_{obs}$.

Recently a reevaluation of the rate coefficient and branching has been made by the research group of Hynes (Williams et al.[52]) using the PLP−PLIF technique for OH + DMS and OH + DMS-d_6 as a function of O_2 partial pressure at 600 Torr total pressure for temperatures down to 240 K. The reasons given for the reevaluation are observations from measurements of the vibrational deactivation of OH ($v = 2$, 1) by DMS,[53] observation of large enhancements of the rates of reactions 1 and 3 in the presence of nitric acid, and direct observation of the HO·DMS adduct in 600 Torr of N_2.[54] It is argued by Williams et al.[52] that all of these observations are inconsistent with the 1986 data set of Hynes et al.[31]

Williams et al.[52] unfortunately published their results mainly in the form of graphs; however, their graphical results suggest that at low temperatures the rate expression of Hynes et al.[31] underestimates both the effective rate coefficient for the reaction and also the branching ratio between the addition and abstraction reaction channels. With the new data,[52] at 261 K a branching ratio of 3.6 is obtained as opposed to a value of 2.8 based on the 1986 expression of Hynes et al.[31] (branching ratio defined here as $(k_{obs} - k_{1a})/k_{1a}$)). At 240 K the difference is even more crass with a new value of 7.8 as opposed to 3.9. The data of Williams et al. imply a significant change in the product distribution below about 250 K. DMSO is one of the major products from the addition channel, and one would expect a perceptible change in its yield on approaching 240 K.

The data of Williams et al.[52] have been incorporated into the latest IUPAC Gas Kinetic Data Evaluation of the reaction of OH with DMS by Atkinson et al.[55] The IUPAC now currently recommends a value of $k = 1.13 \times 10^{-11} \exp(-253/T)$ cm^3 molecule^{-1} s^{-1} for the reaction $OH + CH_3SCH_3 \rightarrow CH_3SCH_2 + H_2O$ over the temperature range 240−400 K and a value of $k = 1.0 \times 10^{-39} [O_2] \exp(5820/T)/\{1 + 5.0 \times 10^{-30} [O_2] \exp(6280/T)\}$ cm^3 molecule^{-1} s^{-1} for the reaction $OH + CH_3SCH_3 \rightarrow CH_3S(OH)CH_3$ over the temperature range 240−360 K. The above k expressions reproduce the O_2 and T dependence of both Hynes et al.[31] and Williams et al.[52] of k_{obs} at pressures close to 1 atm down to approximately 260 K. Below 260 K the expressions reproduce the measured roll-off in the rate coefficient measured by Williams et al.

At the time of writing a relative kinetic study of the reaction of OH with DMS in a large temperature regulated photoreactor was reported by Albu et al.[56] They studied the reaction over the temperature range 250−299 K at 1 atm total pressure in the presence of different partial pressures of O_2 (0−500 mbar). The photolysis of H_2O_2 was employed as the OH radical source, and the measurements were made relative to three reference compounds. Although the rate coefficients measured by Albu et al.[56] are slightly higher than those reported by Hynes et al.[31] and Williams et al.[52] they are in reasonable agreement with both data sets down to ~260 K. Below 260 K the data of Albu et al.[56] show the same trend with temperature first reported by Williams et al.,[52] i.e., a steep roll-off in the rate coefficient with decreasing temperature. Figure 2a shows plots of k_{obs} for 1 atm of air as a function of temperature, where k_{obs} has been taken from Hynes et al.,[31] the review of Atkinson et al.[55] which included the data from Williams et al.,[52] and the recent study of Albu et al.[56] The branching ratios for the addition and abstraction channels for OH + DMS in 1 atm of air, derived from the data of Hynes et al.,[31] Williams et al.,[52] Atkinson et al.,[55] and Albu et al.,[56] are plotted as a function of temperature in Figure 2b. These plots highlight the good agreement of the data sets at temperatures down to ~260 K and the roll-off in the rate coefficient with decreasing temperature first reported by Williams et al. using an absolute kinetic technique and now confirmed by Albu et al. using a relative kinetic method.

2.1.2. Observed Products from OH + DMS

Although the rate coefficients for the initiation reactions of DMS with the OH radical are now reasonably well established the subsequent chemistry responsible for the observed products and their yields is complex, and many aspects of the mechanism are still not very clear. The identity and yields of the final products depend on the oxidation steps of several intermediates for which a multitude of different possible reaction pathways exist and for which the importance can vary with the prevailing atmospheric conditions. Product information has been derived from both field and laboratory studies.

From field studies, data are now available on measurements of DMS gaseous oxidation products such as sulfur dioxide (SO_2), sulfuric acid (H_2SO_4), dimethyl sulfoxide (CH_3SOCH_3, DMSO), dimethyl sulfone ($CH_3SO_2CH_3$, DMSO$_2$), and methanesulfonic acid ($CH_3S(O)_2OH$, MSA).[11,57−69] Many of these products partition into the condensed phase, and extensive data sets exist for methanesulfonate ($CH_3SO_3^-$, MS) and non-sea-salt sulfate (nss-SO_4^{2-}), the deprotonated

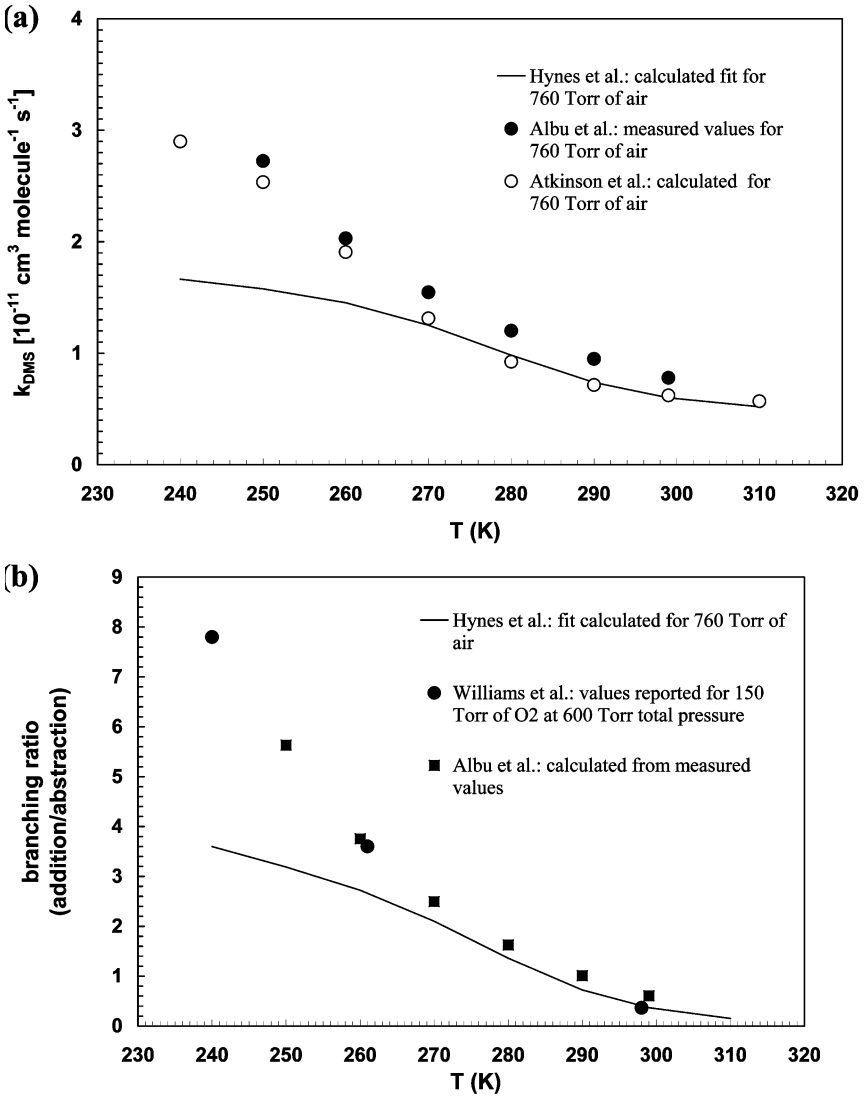

Figure 2. (a) Plots of k_{obs} for the reaction of OH with DMS from the data of Hynes et al.,[31] Williams et al.,[52] Atkinson et al.,[55] and Albu et al.,[56] and (b) plots of the branching ratio for the addition and abstraction channnels ($k_{obs} - k_{abst}/k_{abst}$) from the data of Hynes et al.,[31] Williams et al.,[52] and Albu et al.[56]

forms of MSA and H_2SO_4, respectively.[70−73] Ice core data on these ions are also available.[74−77]

In the laboratory absolute methods have given much useful information on the importance of particular product channels, as will be discussed later, but much of the end product information for the OH + DMS reaction (and indeed other organic sulfur compounds) stems from chamber studies, i.e., photochemical reactors.

In laboratory photoreactor studies at room temperature SO_2, methanesulfonic acid, dimethyl sulfoxide, dimethyl sulfone, and methylsulfonylperoxynitrate (MSPN, CH_3SO_2-$OONO_2$) have been observed as products of the OH-radical-initiated oxidation of DMS.[78−84] Sørensen et al.[80] reported the observation of methanesulfinic acid ($CH_3S(O)OH$, MSIA) in low yield from the reaction of OH with DMS; however, recent results from the study of Arsene et al.[83] support quite a significant yield of MSIA from the secondary oxidation of DMSO. The findings of Arsene et al. are more in line with the results of the LFP-TDLAS study of Urbanski et al.,[85] who determined a CH_3 radical yield of 0.98 ± 0.12 in the reaction and inferred MSIA as the coproduct. Improvements in the collection method for MSIA are invoked to explain the discrepancy with the result of Sørensen et al.[80]

With the continuing improvement in detection limits carbonyl sulfide (OCS) has been consistently detected by in situ long-path FT-IR in chamber product studies of the OH-initiated oxidation of DMS under NO_x free or very low NO_x conditions.[81−86] A formation yield of 0.7 ± 0.2% S has been reported.[86] Possible mechanisms of formation are discussed later. Although the OCS yield is low, because of the relatively high global DMS source strength (15−45 Tg (S) year^{-1}), the result suggests that the oxidation of DMS could possibly represent quite a substantial source of atmospheric OCS with a contribution in the range 0.10−0.28 Tg (OCS) a^{-1}. Methylthiolformate (CH_3SCHO, MTF) is another product which has been detected in chamber studies conducted in the absence of NO_x or when NO_x falls to a low level in the reaction system.[81,83,86] To date, one study on the atmospheric chemistry of MFT exists in the literature.[87]

Most of the chamber product studies have employed high and highly variable NO_x levels, and the chemistry that occurs in these high NO_x systems can be very different from that occurring under the generally much lower NO_x conditions of the atmosphere. Consequently, their is a large variation in the yields of the products reported in the literature, and it is still not possible to make reliable quantitative predictions

of the distribution of DMS oxidation products for specific sets of atmospheric conditions.

Both laboratory and field observations support that SO_2 is a major oxidation product of DMS oxidation, and recent photoreactor studies have demonstrated that it is formed via both the addition and the abstraction channels in OH + DMS. Under NO_x conditions approaching those of the atmosphere, SO_2 molar yields of 70−80% have been reported for photoreactor experiments on OH + DMS.[11,81−84] Similar yields have been deduced from field measurements of DMS and its products. Apart from the gas-phase oxidation with OH radicals to form H_2SO_4(g), the major further fate of SO_2 is uptake in the condensed phase and oxidation to H_2SO_4(l).

2.1.3. Mechanistic Pathways: Chemistry of Intermediate Radical Species

Different approaches have been taken to try and unravel the mechanistic complexities of the reaction of the OH radical with DMS, which are evident from the array of contrary results obtained from laboratory experiments and also observations in the field. All of the approaches, however, attempt to generate chemical mechanisms which best correlate prediction with experimental observation.

From the laboratory side chemical mechanisms have been generated, which attempt to predict the rates and yields of the products formed in the OH-radical-initiated oxidation of DMS based on the end products observed in chamber experiments and best "guestimates" of unknown rates and reactions. The most detailed mechanism developed to date on this principle is that reported by Yin et al.[88,89] Ravishankara et al.[9] adopted a somewhat different approach; they constructed a mechanism based on individual elementary reactions studied in the laboratory, when available, and relied on analogies to estimate the rate coefficients and products of unstudied reactions. The simplified mechanism constructed by the authors was able to explain some of the field observations on the end products of DMS oxidation and their variation with temperature.

Field observations of DMS and its oxidation products have been used to deduce mechanistic information, for example, to obtain SO_2 yields.[57,58,62] However, the interpretation of field data is fraught with difficulties since chemical processes have to be separated from transport processes, aerosol−cloud interactions, etc. The difficulties can be overcome, to a large extent, by use of a model containing a DMS oxidation mechanism in addition to the other important atmospheric processes. The DMS mechanism is evaluated by comparison of the model simulations with the field observations. Modeling studies using comprehensive[90−94] and parametrized[66,68,95,96] versions of DMS oxidation mechanisms are reported in the literature. The comprehensive mechanisms are generally modifications of the Yin et al.[88] mechanism, and the major differences between the various schemes are discussed in the recent paper by Lucas and Prinn.[94] Capaldo and Pandis[97] compared five different DMS mechanisms using nine sets of observations. They found that no single mechanism reproduced all sets of observations and that the predictions of MSA varied very significantly between the mechanisms, indicating that the production pathways for this compound are particularly poorly understood. It is evident from the few remarks above that at present no mechanism is currently in existence which is capable of satisfactorily reproducing the product distributions observed in the DMS oxidation under both field and laboratory conditions.

Table 2. Reported Enthalpies of Formation (in kcal mol^{-1}) of Sulfur Species Involved in the Atmospheric Photooxidation of Dimethyl SulfIde (DMS) and Dimethyl Sulfoxide (DMSO), and Experimental and Calculated Bond Strengths of Dimethyl Sulfide Reaction Adducts $(CH_3)_2S-X$ (X = OH, Cl, Br, ClO, BrO, IO)

species	ΔH°_f (298 K)
CH_3SCH_3	−8.9[55]
CH_3SOCH_3	−(35.95 ± 0.36),[259] −36.2[a]
$CH_3SO_2CH_3$	−89.2[a]
CH_3SCH_2	(32.7 ± 1.4),[175] (35.6 ± 1.0)[180]
CH_3SCH_2O	−(9.8 ± 1.7),[113] −7.4[260]
CH_3SCH_2OO	5.9[261]
CH_3SCH_2OOH	−28.4[113]
$CH_3SCH_2O_2NO$	(3.9 ± 1.2)[113]
$CH_3SCH_2O_2NO_2$	−8.3[113]
$CH_3SCH_2O_2$	(18.2 ± 0.6)[113]
$CH_3SCH_2O_4$	(29.6 ± 0.6)[113]
CH_3SCHO	not available
CH_3S	(29.78 ± 0.44)[261]
CH_3S-O-O	(18.1 ± 1.0)[118]
CH_3SO	−11.9,[113] −(16 ± 2.4)[55]
CH_3SO_2	−38.9,[113] −55[121]
CH_3SO_3	−58.9[113]
CH_3SOH methanesulfenic acid	−35.13,[137] −33.9,[108] −45.4[262]
CH_3SO_2H methanesulfinic acid	−79.1[137]
CH_3SO_3H methanesulfonic acid	−134.6,[137] −134.4[263]
SO	(1.2 ± 0.3)[55]
SO_2	−(70.94 ± 0.05)[55]
SO_3	−94.58[55]
adduct species	adduct binding energy (kcal mol^{-1})
$(CH_3)_2S-OH$	14,[43] 13.0,[31] 10.1,[39] 10.2,[40] 10.7,[40] 8.7,[49] 9.0,[50] 6.0[44]
$(CH_3)_2S-Cl$	12.1,[106] 19, 3,[167] 12.3,[168] 17.7[162]
$(CH_3)_2S-Br$	14.5,[173]12[174]
$(CH_3)_2S-OCl$	2.0[170]
$CH_3)_2S-OBr$	1.7[170]
$CH_3)_2S-OI$	1.3[170]

[a] Calculation at: http://chemistry.anl.gov/compmat/g3xenergies/g3mp2xheatsofformation.htm.

The effects of different levels of NO_x on the DMS oxidation product distributions, as observed in laboratory experiments, will need to be better understood before mechanisms can be constructed, which fit laboratory observations. Once this is achieved more reliable product distribution extrapolations to the conditions encountered in atmospheric conditions can be made. Most product studies have been performed at room temperature. Product studies covering the range of temperatures encountered in the atmosphere are also an important necessity.

Figure 3 shows a simplified OH(NO_3)-radical-initiated oxidation mechanism for DMS which is based loosely upon the schemes presented in Yin et al.[88] and Ravishankara et al.[9] In discussing developments in the mechanism of the reaction of OH radicals with DMS we adopted the following approach; advances in our understanding of the kinetics and product channels of the various radical intermediates and stable products shown in Figure 3 are discussed in relation to experimental and field observations. Table 2 lists published heats of formation (where available) of the major sulfur compounds and radical species discussed in the review within the context of the atmospheric photooxidation mechanisms of DMS and DMSO; the available data on the bond strengths of $(CH_3)_2S-X$ adducts (X = OH, Cl, Br) are also listed in the table. The heats of formation of other non-sulfur-containing species necessary to derive enthalpies of reaction can mostly be found in Atkinson et al.[55]

Kinetic data[7,39,40,98−102] for some of the initial reactions in the OH-radical-initiated oxidation of DMS are listed in Table

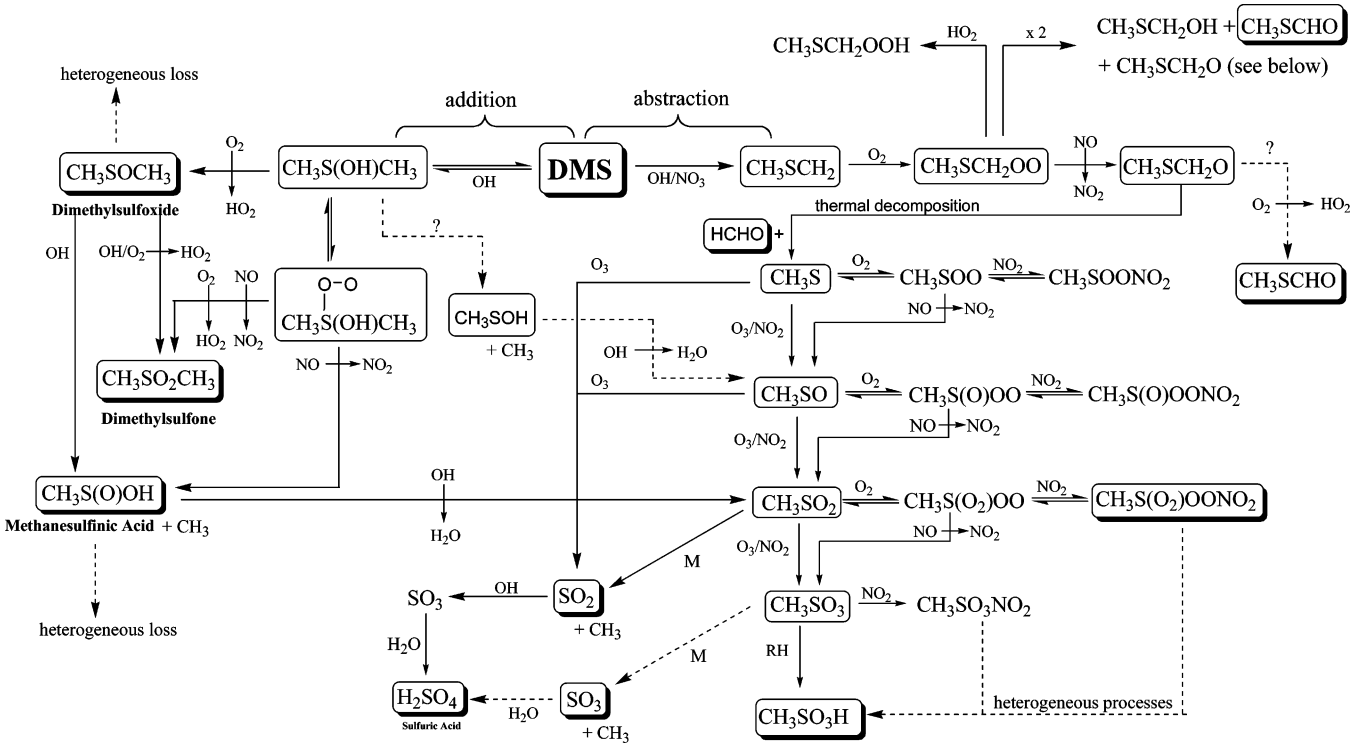

Figure 3. Simplified reaction scheme for the OH and NO_3 radical-initiated oxidation of dimethyl sulfide. Dashed lines represent channels that are uncertain.

Table 3. Kinetic Data for Some Initial Reaction Steps in the OH-Radical-Initiated Oxidation of Dimethyl Sulfide (DMS) at Atmospheric Pressure

reaction	k (298 K) (cm^3 $molecule^{-1}$ s^{-1})	comments	literature
$CH_3SCH_3 + OH \rightarrow CH_3SCH_2 + H_2O$	4.8×10^{-12}	literature evaluation; $k = 1.13\ 10^{-11} \exp(-254/T)$ cm^3 $molecule^{-1}$ s^{-1} over the temperature range 240−400 K	Atkinson et al.[7]
$CH_3SCH_3 + OH \rightarrow CH_3S(OH)CH_3$	1.7×10^{-12}	literature evaluation; $k = 1.7\ 10^{-42}[O_2] \exp(7810/T)/\{1 + 5.510^{-31}[O_2] \exp(7460/T)\}$ cm^3 $molecule^{-1}$ s^{-1} over the temperature range 260−360 K	Atkinson et al.[7]
$CD_3S(OH)CD_3 + O_2 \rightarrow$ products	$(8 \pm 3) \times 10^{-13}$	PLP-PLIF study of H_2O_2/DMS-d_6 mixtures; rate independent of pressure (100−700 Torr of N_2) and temperature (250−300 K)	Hynes et al.[39]
	$(1.0 \pm 0.3) \times 10^{-12}$	PLP-PLIF study of H_2O_2(HONO/DMS-d_6 mixtures; rate independent of pressure (30−200 Torr of N_2) and temperature (222−258 K)	Barone et al.[40] and Ravishankara et al.[9]
$CH_3S(OH)CH_3 + O_2 \rightarrow$ products	$(1.0 \pm 0.3) \times 10^{-12}$	PLP-PLIF study (see above)	Barone et al.[40] and Ravishankara et al.[9]
$CH_3SCH_2 \rightarrow CH_3 + SCH_2$		theoretical study yielding $k = 9.2 \times 10^{13} \exp(-138$ kJ $mol^{-1}/RT)$ s^{-1}	Mousavipour et al.[109]
$CH_3SCH_2 + O_2 + M \rightarrow CH_3SCH_2O_2 + M$	$(5.7 \pm 0.4) \times 10^{-12}$	PR-UV study of SF_6/O_2/DMS gas mixtures at 1000 mbar total pressure	Wallington et al.[98]
	$\sim 2 \times 10^{-13}$	DF-MS study of $NO_3-Cl/Cl_2-DMS-O_2$ and $NO_3-Br/Br_2-DMS-O_2$ systems in 1 Torr He	Butkovskaya and Le Bras[99]
$CH_3SCH_2O_2 + NO \rightarrow$ products	$(1.9 \pm 0.6) \times 10^{-11}$	PR-UV study of SF_6/O_2/DMS/NO gas mixtures at 1000 mbar total pressure; $\Phi(NO_2) = 0.81 \pm 0.15$	Wallington et al.[98]
	$(8.0 \pm 3.1) \times 10^{-12}$	PLP-PLIF study; $\Phi(CH_3S) = 0.81 \pm 0.15$	Turnipseed et al.[100]
	$(1.2 \pm 0.5) \times 10^{-11}$	LFP-TDLAS study of $Cl_2CO-DMS-O_2-N_2$ mixtures with and without NO at 10 Torr total pressure; $k = 4.910^{-12} \exp(263/T)$ over the temperature range 261−400 K; $\Phi(HCHO) = 1.04 \pm 0.13$	Urbanski et al.[102]
$CH_3SCH_2O_2 + NO_2 \rightarrow$ products	$(9.2 \pm 0.9) \times 10^{-12}$	PR-UV study of SF_6/DMS/O_2/NO_2 mixtures; 1000 mbar SF_6	Nielsen et al.[101]
	$(7.1 \pm 0.9) \times 10^{-12}$	300 mbar SF_6	
$CH_3SCH_2O_2 + CH_3SCH_2O_2 \rightarrow$ products	$(7.9 \pm 1.4) \times 10^{-12}$	PR-UV study of SF_6/O_2/DMS gas mixtures at 1000 mbar total pressure	Wallington et al.[98]
	$(1.2 \pm 0.5) \times 10^{-11}$	LFP-TDLAS study of $Cl_2CO-DMS-O_2-N_2$ mixtures at $P = 20$ Torr N_2; $\Phi(HCHO) = 0.97 \pm 0.08$	Urbanski et al.[102]
$CH_3SCH_2O_2 + HO_2 \rightarrow CH_3SCH_2OOH$	(5.0×10^{-12})[a]	DF-MS study of a $Cl/Cl_2-DMS-O_2$ system in 1 Torr He; mass spectroscopic evidence for CH_3SCH_2OOH	Butkovskaya and Le Bras[99]
$CH_3SCH_2O + M$	$> 3 \times 10^4$ s^{-1}	LFP-TDLAS study of $Cl_2CO-DMS-O_2-N_2-NO$ mixtures; value for 261 K and 10 Torr N_2	Urbanski et al.[102]

[a] This is an estimate based on the reported rate coefficients for $RO_2 + HO_2/RO_2$ reactions.

3. With the exception of the LFP-TDLAS study by Urbanski et al.[102] on the reactions of CH_3SCH_2OO and CH_3SCH_2O radicals, all of the reactions have been covered in previous reviews.[6−11]

The reaction of OH with DMS can proceed via the following primary channels

$$OH + CH_3SCH_3 \rightarrow CH_3SCH_2 + H_2O \qquad \Delta H^\circ = -25.2 \text{ kcal mol}^{-1} \quad (1a)$$

$$OH + CH_3SCH_3\ (+\ M) \leftrightarrow CH_3S(OH)CH_3\ (+\ M) \qquad \Delta H^\circ = -10.7 \text{ kcal mol}^{-1} \quad (1b,\text{-}1b)$$

$$OH + CH_3SCH_3 \rightarrow CH_3 + CH_3SOH \qquad \Delta H^\circ = -0 \pm 3 \text{ kcal mol}^{-1} \quad (1c)$$

$$OH + CH_3SCH_3 \rightarrow CH_3S + CH_3OH \qquad \Delta H^\circ = -18.8 \text{ kcal mol}^{-1} \quad (1d)$$

The heats of formation have been taken from the literature and refer to 298 K.[40,103,104] As outlined in section 2.1.1 it is well established that the reaction of OH radicals with DMS proceeds through two channels: H-atom abstraction by OH from a methyl group and OH-radical addition to the S atom. The abstraction channel is *O_2-independent*, whereas the addition channel is *O_2-dependent*. Attack of OH radicals at CH_3 produces water and methylthiomethyl radical (CH_3-SCH_2), while addition to the S atom produces the dimethylhydroxysulfuranyl radical ($(CH_3)_2S-OH$), an adduct which can either dissociate back to reactants or react further with O_2 to form products. The relative importance of the addition versus abstraction channels is temperature dependent.[31,52] The contribution of the addition pathway is approximately 50% and 33% at 285 and 295 K, respectively, i.e., the importance of the *O_2-dependent* channel increases with decreasing temperature.

The reactions discussed above, however, do not consider the possibility of rearrangement of the DMS−OH adduct to form bimolecular products, i.e.

$$OH + CH_3SCH_3\ (+\ M) \leftrightarrow CH_3S(OH)CH_3\ (+\ M) \quad (1b,\text{-}1b)$$

$$CH_3S(OH)CH_3\ (+\ M) \rightarrow H_2O + CH_3SCH_2 \qquad \Delta H^\circ = -0 \pm 3 \text{ kcal mol}^{-1}$$

Such a reaction sequence would make it impossible to decouple the abstraction and addition pathways in the atmosphere. On the basis of a comparison of the measured O_2 behavior of the rate coefficients for the reaction of OH with DMS and DMS-d_6, Ravishankara et al.[9,40] argued that two uncoupled independent reaction channels must exist. The evidence presented by Ravishankara et al. is convincing, and in the following discussion two independent reaction channels, addition and abstraction, are assumed.

2.1.3.1. Addition Channel: Reactions of the $(CH_3)_2S-OH$ Adduct. As reported in section 2.1.1 the $(CD_3)_2S-OH$ adduct has been observed and possesses a binding energy of ca. 10.9 kcal mol^{-1}. A rate coefficient for reaction of the $(CH_3)_2S-OH$ adduct with O_2 of $(1.0\pm0.3) \times 10^{-12}$ cm^3 molecule^{-1} s^{-1} independent of temperature and pressure and the isotopic identity of the hydrogens in DMS has been reported.[9,40] Using ab initio and density functional theories Gross et al.[51] calculated a value of the rate coefficient for the reaction $(CH_3)_2S-OH + O_2 \rightarrow DMSO + HO_2$ at 298 K of $k = 1.74 \times 10^{-12}$ cm^3 molecule^{-1} s^{-1}, which considering the difficulties of such calculations is in fair agreement with the experimental value.

Reaction with O_2 will determine the fate of the $(CH_3)_2S-OH$ adduct in the atmosphere. The reaction pathways are still not well established. Thermodynamically feasible product channels of the $(CH_3)_2S-OH$ adduct with O_2 include

$$(CH_3)_2S-OH + O_2 \rightarrow HO_2 + CH_3S(O)CH_3$$

$$(CH_3)_2S-OH + O_2 + M \rightarrow CH_3S(OH)(OO)CH_3 + M$$

$$(CH_3)_2S-OH + O_2 \rightarrow CH_3OO + CH_3SOH$$

$$(CH_3)_2S-OH + O_2 \rightarrow OH + CH_3S(O)_2CH_3$$

$$(CH_3)_2S-OH + O_2 \rightarrow CH_3 + CH_3S(OH)OO$$

It is now well established that the addition pathway produces DMSO. The results from a recent product study by Arsene et al.[83] support that the major fate of the $(CH_3)_2S-OH$ adduct under NO_x-free conditions is reaction with O_2 to form DMSO. This result is, however, in contradiction with the pulsed laser photolysis/pulsed laser-induced fluorescence and laser flash photolysis/pulsed laser-induced fluorescence studies on the reaction of OH with DMS by Turnipseed et al.[100] and Hynes et al.,[43] who reported similar branching ratios of $\Phi = 0.5 \pm 0.15$ and ~0.5, respectively, for the production of DMSO based on the conversion of the HO_2 produced to OH by reaction with NO. As discussed in Arsene et al.,[83] the reason for the discrepancy is not entirely clear; however, the reason may well lie in the reaction conditions employed in the two studies, i.e., presence or absence of NO in the reaction system. The theoretical study of Gross et al.[51] supports that the dominant channel for the reaction $(CH_3)_2S-OH + O_2$ is formation of DMSO + HO_2 and that the channel forming $CH_3SOH + CH_3O_2$ does not occur.

The OH-radical-initiated oxidation of DMS has been investigated as a function of temperature and different initial NO_x concentration.[83,84] In these chamber studies it was found that the level of NO in the reaction system was a critical factor in determining the yields of DMSO and $DMSO_2$. The yields of DMSO and $DMSO_2$ were observed to be anticorrelated. The data[83,84] support that the major channel for $DMSO_2$ formation is probably reversible addition of O_2 to the DMS−OH adduct formed in OH + DMS followed by sequential reactions with NO and O_2.

$$DMS-OH + O_2 + M \leftrightarrow OH-DMS-O_2 + M$$

$$OH-DMS-O_2 + NO \rightarrow OH-DMS-O + NO_2$$

$$OH-DMS-O + O_2 \rightarrow CH_3S(O)_2CH_3 + HO_2$$

This reaction sequence has been proposed previously in a slightly modified form by Yin et al.[88] In the mechanism of Yin et al. the reaction DMS−OH + O_2 + M was not reversible and a thermal pathway was included

$$OH-DMS-O_2 \rightarrow DMSO + HO_2$$

It is presently difficult to extrapolate the results to typical atmospheric NO concentrations in order to obtain meaningful information about the possible significance of the above reaction sequence in the troposphere. Should the reaction sequence not be significant under tropospheric conditions, this would imply a near unit formation yield of DMSO from the addition channel of the reaction of OH with DMS.

However, under the low NO_x conditions which often prevail in the remote marine atmosphere there remains the possibility of reaction of the OH−DMS−O_2 adduct with HO_2 or other peroxy radicals which may convert it to $DMSO_2$, particularly at low temperature, for which no information presently exists.

2.1.3.2. Abstraction Channel: Reactions of the CH_3SCH_2 Radical. There have been several theoretical studies of the methylthiomethyl radical (MTM; CH_3SCH_2).[105−108] A new theoretical study has been recently reported on the unimolecular dissociation of MTM and also DMS.[109] All the structures have been optimized at the MP2/6-311G)D,p)n level of theory. At the MP4SDTQ/6-311G(D,P) level of theory the barrier height for dissociation of CH_3SCH_2 was found to be 32.42 kcal mol^{-1} (135.5 kJ mol^{-1}). The bond length of CH_3S-CH_2 has been found to be 0.089 Å less than the S−C bond length in DMS. This dissociation has no atmospheric relevance and is not treated further here.

In analogy to the oxidation of alkyl radicals the atmospheric oxidation of the methylthiomethyl radical in the presence of NO will be as follows

$$CH_3SCH_2 + O_2 \rightarrow CH_3SCH_2OO$$

$$CH_3SCH_2OO + NO \rightarrow CH_3SCH_2O + NO_2$$

$$CH_3SCH_2O + M \rightarrow CH_3S + HCHO + M$$

Resende and De Almeida[110] performed an ab initio examination of the mechanism of the reaction between CH_3SCH_2 and O_2 at the UCCSD(T)/6-311+G(2df,2p)/UMP2/6-31G(d) level of theory. They established a bimolecular mechanism and found a transition state for the reaction. However, the calculated negative activation energy of −3.31 kcal mol^{-1} and the high-spin contamination of the transition state precluded the calculation of a rate coefficient for the reaction. Apart from this theoretical study no new significant data on the above reaction sequence has appeared over the past few years. As listed in Table 3, rate coefficients have been measured for the reaction of CH_3SCH_2 with O_2 and the self-reaction of CH_3SCH_2OO and CH_3SCH_2OO with NO, and product yields have been determined for NO_2, CH_3S, and HCHO produced in the reactions. In the LFP-TDLAS study by Urbanski et al.,[102] prompt production of formaldehyde with unit yield was observed at 298 K from both CH_3SCH_2OO + NO and CH_3SCH_2OO + CH_3SCH_2OO at low total pressures. On the basis of time-resolved measurements of HCHO production by Urbanski et al.[102] it is known that the lifetime of the CH_3SCH_2O radical with respect to unimolecular decomposition is less than 30 μs at 261 K and 10 Torr total pressure, and the studies of Turnipseed et al.[100] constrain the lifetime to less than 10 μs at 298 K.

As mentioned above, studies at low total pressure show that the reactions of CH_3SCH_2OO proceeding via intermediate formation of CH_3SCH_2O result in unit yield of HCHO.[102] It is not presently clear whether reaction of the CH_3SCH_2O radical with O_2 might be able to compete with unimolecular decomposition under atmospheric conditions. This reaction would be expected to result predominately in the formation of methylthioformate (MTF; CH_3SCHO)

$$CH_3SCH_2O + O_2 \rightarrow CH_3SCHO + HO_2$$

This compound has been observed consistently in photoreactor studies under conditions of low NO_x.[81−87] In these systems it is not clear whether the MTF is being formed in reaction of CH_3SCH_2O with O_2 or via reaction of CH_3SCH_2OO with HO_2, CH_3SCH_2OO, or other alkyl peroxy radicals which are formed in the system. The observation of MTF in chamber studies in the absence of NO would suggest the alkoxy radical CH_3SCH_2O may be more activated when formed via the CH_3SCH_2OO + NO reaction compared to other formation routes. Reactions of peroxy radicals with NO are exothermic; they occur via the formation of a ROONO complex, which is sufficiently long-lived to allow for energy randomization. Thus, the alkoxy radical produced in these reactions can possess internal excitation, which can lead to unimolecular decomposition of the radical. There are several examples of such reactions in the literature, see, for example, Bilde et al.[111] and references therein.

Under the pristine conditions which prevail in the remote marine boundary layer the concentrations of NO are very low, typically 2−8 pptv. At such low NO concentrations reactions of CH_3SCH_2OO with HO_2 and other alkyl peroxy radicals, in particular CH_3OO, can be potentially important. No direct studies of the reaction of CH_3SCH_2OO with HO_2 have been reported. From a comparison of other HO_2 + RO_2 reactions it would be expected to produce CH_3SCH_2OOH

$$CH_3SCH_2OO + HO_2 \rightarrow CH_3SCH_2OOH + O_2$$

Depending on the further reactions of CH_3SCH_2OOH, this process can potentially short circuit the atmospheric sulfur cycle by returning sulfur prematurely to the aqueous phase.[11] Butkovskaya and Le Bras[99] reported mass spectrometric detection of CH_3SCH_2OOH in flow-tube experiments performed on a Cl/Cl_2 + DMS + O_2 system. Very recently Butkovskaya and Barnes[112] reported tentative FTIR detection of CH_3SCH_2OOH in studies on the UV photolysis of $CH_3SCH_2SCH_3$ in air in a photoreactor. Photolysis of this compound produces CH_3SCH_2 and CH_3S radicals. Four bands belonging to a transient product absent in DMDS/air photolysis and centered approximately at 1290, 1021, 943, and 876 cm^{-1} have been observed. On the basis of the shape and position of the bands a tentative assignment to CH_3SCH_2OOH was made. A theoretical study of the CH_3SCH_2OOH structure was also made using ab initio calculations at the QCISD(T) level with a 6-311g(2d,f) basis set. From the three found conformations the most stable was a structure with a very close location of an oxy-hydrogen to the sulfur atom, i.e.

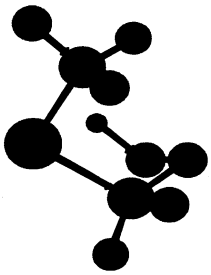

Among the calculated normal modes there are frequencies which can be attributed to the observed peaks. The strong band at 863 cm^{-1} corresponds mainly to an O−O vibration; the medium band at 934 cm^{-1} and the strong band at 1025 cm^{-1} can be assigned to complex O−C−S−C vibrations; and the medium band at 1280 cm^{-1} is nearly pure CH_2 bending. The bands around 3100 cm^{-1} are weak and overlap strongly with other unknown products.

Table 4. Kinetic Data for the Reactions of CH_3S Radicals

reaction	k (298 K) (cm^3 $molecule^{-1}$ s^{-1})	comments	literature
$CH_3S + O_2 + M \leftrightarrow CH_3SOO + M$		equilibrium measured as a function of temperature (216−258 K)	Turnipseed et al.[118]
$CH_3S + O_2 + M \rightarrow$ products (other than CH_3SO_2)	$<3 \times 10^{-18}$	no new data; literature evaluation	DeMore et al.[6]
$CH_3S + O_3 \rightarrow$ products	$(4.6 \pm 0.6) \times 10^{-12}$	LP-LIF study over $T = 259-381$ K and $P = 25-300$ Torr of He yielding $k = (1.02 \pm 0.03) \times 10^{-12} \exp[(432 \pm 77)/T]$ independent of pressure	Martínez et al.[119 a]
	$(5.2 \pm 0.5) \times 10^{-12}$	PLP-LIF study over $T = 295-359$ K and $P = 20-200$ Torr yielding $k = 1.98 \times 10^{-12} \exp[(290 \pm 40)/T]$ cm^3 $molecule^{-1}$ s^{-1}	Turnipseed et al.[103]
	$(5.7 \pm 1.4) \times 10^{-12}$	DF-MS study at 300 K	Dominé et al.[120]
	$(4.1 \pm 2.0) \times 10^{-12}$	PLP-LIF study at 298 K and $P = 38-300$ Torr of N_2 or O_2	Tyndall and Ravishankara[121]
$CH_3S + HO_2 \rightarrow$ products		no data	
$CH_3S + CH_3O_2 \rightarrow$ products		no data	
$CH_3S + NO_2 \rightarrow$ products	$(1.01 \pm 0.16) \times 10^{-10}$	LP-LIF study yielding $k = (4.3 \pm 1.3) \times 10^{-11} \exp[(240 \pm 100)/T]$ cm^3 $molecule^{-1}$ s^{-1} over $T = 222-420$ K and $P = 55-202$ Torr He	Chang et al.[122]
	$(6.6 \pm 1.0) \times 10^{-11}$	LP-LIF study yielding $k = (3.8 \pm 0.3) \times 10^{-11} \exp[(160 \pm 22)/T]$ cm^3 $molecule^{-1}$ s^{-1} over $T = 263-381$ K independent of pressure $P = 30-300$ Torr of He	Martínez et al.[123]
	$(6.1 \pm 1.0) \times 10^{-11}$	LP-LIF study over $T = 240-350$ K yielding $k = (2.06 \pm 0.44) \times 10^{-11} \exp(320 \pm 40/T)$ cm^3 $molecule^{-1}$ s^{-1}	Turnipseed et al.[103]
	$(5.1 \pm 0.9) \times 10^{-11}$	DF-MS study at 297 K in 1 Torr He; $\Phi(NO) = 1.07$ (0.15	Dominé et al.[124]
	$(6.1 \pm 0.9) \times 10^{-11}$	PLP-LIF study at 298 K and $P = 40-140$ Torr of N_2 or O_2; $\Phi(NO) = 0.8 \pm 0.2$	Tyndall and Ravishankara[121]
	$(1.1 \pm 0.1) \times 10^{-10}$	LP-LIF study with $k = (8.3 \pm 1.4) \times 10^{-11} \exp(80 \pm 60/T)$ cm^3 $molecule^{-1}$ s^{-1} over $T = 295-511$ K	Balla et al.[125]

[a] A recommended value of $k(298\ k) = 5.3 \times 10^{-12}$ cm^3 $molecule^{-1}$ s^{-1} with $k = 2.0 \times 10^{-12}\exp(290 \pm 100/T)$ cm^3 $molecule^{-1}$ s^{-1} over the temperature range 290−360 K is given by DeMore et al.[6]

Using the UCCSD(T)/cc-pVTZ//MP2/6-31G(d) level of theory Resende and De Almeida[113] analyzed the thermodynamical properties of the reactions of the $CH_3SCH_2O_2$ radical with NO, NO_2, HO_2, CH_3O, CH_3S, CH_3SO, CH_3SO_2, O, and O_3. They report heats of formation at 298 K (given in brackets in kcal mol^{-1}) for CH_3SO (−11.9), CH_3SO_2 (−38.9), CH_3SO_3 (−58.4), CH_3SCH_2O (−9.8 ± 1.7), $CH_3SCH_2O_2H$ (−28.4), $CH_3SCH_2O_2NO$ (3.9 ± 1.2), $CH_3SCH_2O_2NO_2$ (−8.3), $CH_3SCH_2O_3$ (18.2 ± 0.6), and $CH_3SCH_2O_4$ (29.6 ± 0.6) whereby those for $CH_3SCH_2O_2H$, $CH_3SCH_2O_2NO$, $CH_3SCH_2O_2NO_2$, CH_3SO_3, $CH_3SCH_2O_3$, and $CH_3SCH_2O_4$ are first time estimates. They find that the reactions with NO, NO_2, HO_2, CH_3S, CH_3SO, CH_3SO_2, and O are exothermic and spontaneous. Reactions of O_2 and O_3 with $CH_3SCH_2O_2$ are reported to be thermodynamically unfavorable.

By analogy to other alkyl peroxy radicals NO_2 may be expected to add to $CH_3SCH_2O_2$ and form the equilibrium

$$CH_3SCH_2OO + NO_2 + M \leftrightarrow CH_3SCH_2OO\ NO_2 + M$$

The rate coefficient for the recombination of CH_3SCH_2OO with NO_2 has been determined by Nielsen et al.[101] at 296 K and 300 and 1000 mbar total pressure. The pressure dependence of the reaction is intermediate between that for $CH_3C(O)OO + NO_2$ and $C_2H_5OO + NO_2$. In photoreactor studies of the NO_3-radical-initiated oxidation of DMS by Jensen et al.[114,115] a species observed by FTIR has been tentatively assigned to $CH_3SCH_2OONO_2$. However, Mayer-Figge[116] observed similar bands in studies on the photolysis of CH_3SNO in O_2 where this compound cannot be formed, suggesting that the assignment might be in error. Further, the calculations of Resende and De Almeida[117] suggest that the equilibrium with NO_2 is strongly shifted toward the reactants. The present evidence would suggest that the peroxynitrate is probably not important in the atmosphere.

2.1.3.3. Reactions of CH_3S and CH_3SO_x ($x = 1-3$) Radicals. In this section the role of the reactions of the CH_3S radical and its oxidized forms CH_3SO_x ($x = 1-3$) in determining the DMS oxidation product distribution are considered. The CH_3S radical is formed from reactions of CH_3SCH_2 as discussed above and shown in Figure 3. Kinetic data[6,103,118−125] on the reactions of the methyl thiyl radical CH_3S are listed in Table 4.

Methylthiyl (CH_3S) and Methylthioperoxyl (CH_3SOO) Radicals. The reactions of the methylthiyl radical CH_3S are important in the transformation of DMS to SO_2, MSA, and H_2SO_4. It is established that the reaction of CH_3S with O_2 forms a weakly bound adduct,[118] i.e., the methylthioperoxyl radical, CH_3SOO, with a bond strength of 11 kcal mol^{-1}. Under atmospheric conditions equilibrium between CH_3S and CH_3SOO is rapidly established with approximately 20−80% of CH_3S in the form of CH_3SOO at 298 K.[7] No other reaction channel for this reaction has been positively identified. The equilibrium between CH_3S and CH_3SOO makes it difficult to assess the fate of CH_3S under atmospheric conditions. Current estimates put an upper limit of approximately 3×10^{-18} cm^3 $molecule^{-1}$ s^{-1} at 298 K on the rate coefficient for the reaction of CH_3S with O_2 leading to products other than CH_3SOO.

Rate coefficients for the reaction of CH_3S with other trace gas species such as O_3 [103,119−121] and NO_2 [103,121−125] are reasonably well established (see Table 4), although some discrepancies still remain.[122,129] First-order loss rate coefficients for the CH_3S radical at 298 K through reaction with O_2, O_3 and NO_2 are given in Table 5 for different possible O_3 and NO_2 concentrations. Reaction with NO_2 will only be important at elevated NO_x concentrations. The rate coefficient for the reaction is independent of pressure and displays a negative activation energy. The dominant reaction channel is generation of the methylsulfinyl radical (CH_3SO) and NO[121,124]

$$CH_3S + NO_2 \rightarrow CH_3SO + NO$$

Another possible product methythionitrate, CH_3SNO_2, has

Table 5. Comparison of the First-Order Loss Rates (k[A]) for the Reaction of CH_3SO_x ($x = 0-2$) Radicals with O_2, O_3, and NO_2 at 298 K under Various Atmospheric Conditions

reaction CH_3SO_x + A	k_{298K} (cm^3 molecule^{-1} s^{-1})	[A] (molecules cm^{-3})	k[A] (s^{-1})
$CH_3S + O_2 \rightarrow$ products	$<3.0 \times 10^{-18}$ [a]	5.17×10^{18}	<15.5
$CH_3S + O_3 \rightarrow$ products	5.6×10^{-12}	9.84×10^{11} (40 ppb)	5.5
		2.46×10^{12} (100 ppb)	13.8
$CH_3S + NO_2 \rightarrow$ products	5.6×10^{-11}	2.46×10^{10} (1 ppb)	1.4
		4.92×10^{11} (20 ppb)	27.6
$CH_3SOO + M \rightarrow CH_3 + SO_2 + M$	-		8
$CH_3SOO + O_2 \rightarrow$ products	$<6 \times 10^{-18}$ [b]	5.17×10^{18}	≤31
$CH_3SOO + O_3 \rightarrow$ products	$<8 \times 10^{-13}$	9.84×10^{11} (40 ppb)	≤0.76
		2.46×10^{12} (100 ppb)	≤1.97
$CH_3SOO + NO \rightarrow$ products	1.1×10^{-11}	2.46×10^{8} (10 ppt)	0.003
		4.92×10^{11} (20 ppb)	5.41
$CH_3SOO + NO_2 \rightarrow$ products	2.2×10^{-11}	2.46×10^{8} (10 ppt)	0.005
		4.92×10^{11} (20 ppb)	10.8
$CH_3SO + O_2 \rightarrow$ products	(7.7×10^{-18})[b]	5.17×10^{18}	(40)
$CH_3SO + O_3 \rightarrow$ products	$6\ 10^{-13}$	9.84×10^{11} (40 ppb)	0.6
	(3×10^{-13} new)	2.46×10^{12} (100 ppb)	1.5
$CH_3SO + NO_2 \rightarrow$ products	1.2×10^{-11}	2.46×10^{8} (10 ppt)	0.003
		4.92×10^{11} (20 ppb)	5.9
$CH_3SO_2 + O_2 \rightarrow$ products	(2.6×10^{-18})[b]	5.17×10^{18}	(13)
$CH_3SO_2 + O_3 \rightarrow$ products	3×10^{-13}	9.84×10^{11} (40 ppb)	0.3
		2.46×10^{12} (100 ppb)	0.7
$CH_3SO_2 + NO_2 \rightarrow$ products	2.2×10^{-12}	2.46×10^{8} (10 ppt)	0.0005
		4.92×10^{11} (20 ppb)	1.08

[a] The rate coefficient is for the reaction $CH_3S + O_2$ going to products other than CH_3SOO. The upper limit is not corrected for the $CH_3S + O_2 \leftrightarrow CH_3SOO$ equilibrium. [b] The rate coefficient is an estimate; only the reaction $CH_3SO_x + O_2$ going to products other than CH_3SO_xOO is considered. The rate is not corrected for the $CH_3SO_x + O_2 \leftrightarrow CH_3SO_xOO$ equilibrium.

been observed as a minor product in photoreactor experiments,[114,126] but the pathway leading to its formation in the complex reaction systems is uncertain.

On the basis of the available kinetic data (Tables 4 and 5) reaction with O_2 and O_3 will determine the fate of CH_3S in the atmosphere. Although the kinetics of the reaction of CH_3S with O_3 are well established (Table 4), the mechanism is still very speculative. The following reactions are thermodynamically feasible at 298 K

$$CH_3S + O_3 \rightarrow CH_3SO + O_2 \qquad \Delta H^\circ = -59.09 \text{ kcal mol}^{-1}$$

$$CH_3S + O_3 \rightarrow CH_3 + SO + O_2 \qquad \Delta H^\circ = -28.47 \text{ kcal mol}^{-1}$$

$$CH_3S + O_3 \rightarrow CH_2SO + H + O_2 \qquad \Delta H^\circ = -25.12 \text{ kcal mol}^{-1}$$

$$CH_3S + O_3 \rightarrow CH_2SO + HO_2 \qquad \Delta H^\circ = -74.16 \text{ kcal mol}^{-1}$$

$$CH_3S + O_3 \rightarrow CH_2S + OH + O_2 \qquad \Delta H^\circ = -31.58 \text{ kcal mol}^{-1}$$

$$CH_3S + O_3 \rightarrow CH_3O + SO_2 \qquad \Delta H^\circ = -130.14 \text{ kcal mol}^{-1}$$

The product information for this reaction is very meager; a yield of 15% has been reported for the methylsulfinyl radical (CH_3SO) at 300 K and low pressure along with mass spectrometric evidence for CH_3 and CH_2SO.[120,127] However, due to the exothermicity of the reaction and possible vibrational and/or excited electronic state stabilization the yield of CH_3SO may be considerably higher at atmospheric pressure. Further oxidation of CH_2SO, CH_2S, and SO will probably result eventually in formation of SO_2. The further oxidation of CH_3SO is dealt with below.

As discussed above, between 20% and 80% of CH_3S will be tied up as CH_3SOO in the atmosphere, the partitioning being a strong function of temperature. Rate coefficients for the reaction of CH_3SOO with O_2, O_3, NO, and NO_2 are listed in Table 6.

Another potential fate of the CH_3SOO adduct is isomerization followed by thermal decomposition. To explain their experimental observations Butkovskaya and Barnes,[135] in a model study of the photooxidation of DMDS at a total pressure of 1013 mbar ($N_2 + O_2$) and different partial pressures of molecular oxygen, suggest that the CH_3SOO radical undergoes transformation to $CH_3 + SO_2$ with a frequency of about 8 s^{-1} in synthetic air at room temperature. In view of the existing high equilibrium [CH_3SOO]/[CH_3S] ratio the limiting step of this transformation is the thermal isomerization to a CH_3SO_2 ring structure. The barrier to formation of the three-membered SOO-ring structure, the first step of the isomerization, has been estimated by ab initio calculation to be 21.6 kcal mol^{-1} by McKee.[128] However, this calculation was performed at a low level of theory. For comparison, at this level the CH_3SOO complex is predicted to be unbound by 0.8 kcal mol^{-1}, whereas the experimental equilibrium value is about 11 kcal mol^{-1} below $CH_3S + O_2$. It is quite probable that the barrier for rearrangement to the ring S(O)O structure is less and that it is a thermally effective process at room temperature. Figure 4 shows the energy diagram for the species related to the $CH_3S + O_2$ reaction system.

Since the C−S bond energy in CH_3SO_2 radical is evaluated to be less than 20 kcal mol^{-1}, it is obvious that the release of about 90 kcal mol^{-1} energy after forming two S=O bonds will lead to immediate (with respect to the frequency of collisions) decomposition. Taking into account the high equilibrium [CH_3SOO]/[CH_3S] ratio in air, the CH_3SOO

Table 6. Kinetic Data for the Reactions of CH_3SOO and CH_3SO Radicals

reaction	k (298 K) (cm^3 $molecule^{-1}$ s^{-1})	comments	literature
$CH_3SOO + O_2 \rightarrow$ products	$<6 \times 10^{-18}$	PLP-LIF study over $T = 295-359$ K and $P = 20-200$ Torr.; value corrected for $CH_3S+O_2 \rightarrow CH_3SOO$ equilibrium and extrapolated to 298 K	Turnipseed et al.[103]
	$<4 \times 10^{-17}$	258 K	Turnipseed et al.[118]
$CH_3SOO + O_3 \rightarrow$ products	$<8 \times 10^{-13}$	227 K	Turnipseed et al.[118]
$CH_3SOO + NO \rightarrow$ products	$(1.1 \pm 0.4) \times 10^{-11}$	227−256 K	Turnipseed et al.[118]
$CH_3SOO + NO_2 \rightarrow$ products	$(2.2 \pm 0.6) \times 10^{-11}$	227−246 K	Turnipseed et al.[118]
$CH_3SO + O_2 + M \rightarrow$ products	$<5 \times 10^{-13}$	from a PLP-LIF study at 300 Torr N_2	Tyndall and Ravishankara[121]
$CH_3SO + O_3 \rightarrow$ products	$(3.2 \pm 0.9) \times 10^{-13}$	PLP-LIF study at $P = 140-660$ Torr of N_2 by 300 K; $\Phi(SO_2) = (1.0 \pm 0.12)$ at 660 Torr of N_2	Borissenko et al.[129]
	$(6 \pm 3) \times 10^{-13}$	DF-MS study in 1 Torr He at 300 K; $\Phi(CH_3S) = (0.13 \pm 0.06)$	Dominé et al.[120]
	1×10^{-12}	PLP-LIF study in which the rate coefficient was derived from a complex analysis of the reaction system	Tyndall and Ravishankara[121]
$CH_3SO + NO_2 \rightarrow$ products	$(1.5 \pm 0.4) \times 10^{-11}$	PLP-LIF study at 300 K; k independent of pressure over 1−612 Torr He; $\Phi(SO_2) = 1$ at 1 Torr He, $\Phi(CH_3+SO_2) = (0.33 \pm 0.05)$ at 13 Torr He falling to (0.18 ± 0.03) at 612 Torr He	Kukui et al.[130]
		PLP-LIF study at $P = 140-660$ Torr of N_2 at 300 K; $\Phi(SO_2) = (0.4 \pm 12)$ at 100 Torr N_2 falling to (0.25 ± 0.05) at 664 Torr N_2.	Borissenko et al.[129]
	$(1.2 \pm 0.2) \times 10^{-11}$	DF-MS study at 297 K in 1 Torr He	Dominé et al.[124]
	$(8 \pm 5) \times 10^{-12}$		Tyndall and Ravishankara[121]
	$(3 \pm 2) \times 10^{-11}$		Mellouki et al.[131]

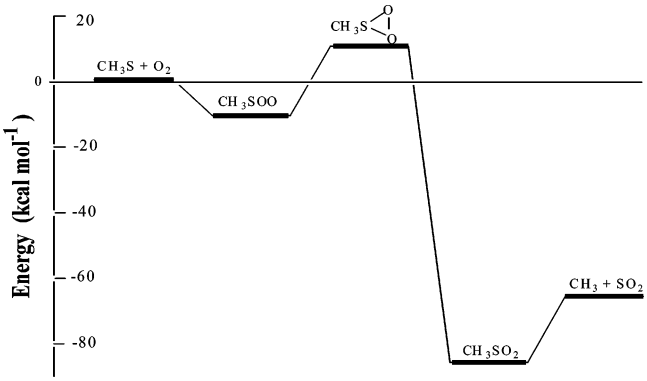

Figure 4. Energy diagram for the species related to the $CH_3S + O_2$ reaction system.

isomerization will be a rate-determining step in the conversion of CH_3S to SO_2.

In analogy with the reaction of NO_2 with alkyl peroxyl radicals, reaction of CH_3SOO with NO_2 would be expected to lead to the formation of an unstable nitrate. In a search for the existence of methylthiomethylperoxynitrate (CH_3SOONO_2) and other sulfur peroxynitrates Mayer-Figge[116] examined the photolysis of CH_3SNO at low temperature. Using in situ FTIR for the analysis of products, the photolysis of CH_3SNO by 258 K in 1013 mbar of O_2 was investigated in the hope that the following reactions would initially dominate

$$CH_3SNO + h\nu \rightarrow CH_3S + NO$$

$$CH_3S + O_2 + M \leftrightarrow CH_3SOO + M$$

$$CH_3SOO + NO_2 + M \leftrightarrow CH_3SOONO_2 + M$$

In the system SO_2 and methanesulfonylperoxynitrate ($CH_3S(O)_2OONO_2$) were positively identified and evidence was found for the presence of a further peroxynitrate compound. However, the IR evidence was more in keeping with the formation of methylsulfinyl peroxynitrate ($CH_3S(O)OONO_2$) rather than CH_3SOONO_2. The conclusion from the study was that either CH_3SOONO_2 is much less thermally stable than, for example, CH_3OONO_2 or the competing reaction of CH_3S with NO_2 was dominating over $CH_3S + O_2$ despite 1 atm of O_2 in the reaction system. A further possibly is a reaction mechanism producing CH_3SO and NO_3 radicals. Table 5 lists first-order loss rates for CH_3SOO for different atmospheric concentrations of the various reactants.

Methylsulfinyl Radical (CH_3SO). Kinetic data[103,118,120,121,124,129−131] on the reactions of CH_3SO radicals are listed in Table 6. In the atmosphere the methylsulfinyl radical (CH_3SO) can undergo a suite of reactions similar to those discussed for CH_3S and CH_3SOO, i.e., reactions of CH_3SO with O_2, O_3, and NO_x and of the methylsulfinylperoxyl radical ($CH_3S(O)OO$), formed from the addition reaction of $CH_3S(O)$ with O_2, with the same species. Because of the low atmospheric concentrations of CH_3SO and $CH_3S(O)OO$ and also HO_2 and alkyl peroxyl radicals, reaction between these species is deemed unimportant in the atmosphere.

There have been no direct studies on the reaction of CH_3SO with O_2. A species has been observed in end product studies which has been tentatively assigned to methylsulfinylperoxynitrate ($CH_3S(O)OONO_2$).[114,115,126] Observation of this species would imply a reaction sequence involving consecutive addition of O_2 and then NO_2 to CH_3SO. However, it is now beyond reasonable doubt that the compound observed in one of the studies[126] was methylsulfonylperoxynitrate ($CH_3SO_2OONO_2$) and not $CH_3S(O)OONO_2$,[116,132,133] and the assignments in the other studies are still open to question. As discussed in the section on CH_3SOO reactions Mayer-Figge[116] observed a product in a study of the photolysis of CH_3SNO at low temperature which is assigned to $CH_3S(O)OONO_2$. In a qualitative study on the thermal stability of the species it was found that the thermal decomposition of the species was more than a factor of 3 faster than that for CH_3OONO_2. Thus, if the species observed in the various systems is indeed $CH_3S(O)OONO_2$, the measurements of Mayer-Figge[116] imply negligible importance for the species under atmospheric conditions.

The rate coefficient for the reaction of CH_3SO with NO_2 is reasonably well established at room temperature. Tyndall and Ravishankara[121] suggested formation of the methylsulfonyl radical (CH_3SO_2) as the main product of the reaction on the basis of the NO yield observed in the photolysis of DMDS in the presence of NO_2. Other studies on the $CH_3S + NO_2$ reaction[131,134] also supported this indirect evidence. In two new studies direct formation of SO_2 has been observed in the $CH_3SO + NO_2$ reaction.[129,130] In both studies the SO_2

Table 7. Kinetic Data for the Reactions of CH_3SO_2 Radicals

reaction	k (298 K) (s^{-1})	comments	literature
$CH_3SO_2 + M \rightarrow CH_3 + SO_2$	1	PLP-LIF study; estimate at 300 K from an analysis of a DMDS/NO_2 system	Borissenko et al.[129]
	(0.4 ± 0.2)	chamber study of the 254 nm photolysis of $CH_3SO_2SCH_3$ with simulation of the products	Butkovskaya and Barnes[135,136]
	100	PLP-LIF and DF-MS studies at 300 K over $P =$ 1−612 Torr of He	Kukui et al.[130]
	510 ± 150	DF-LIF/MS study at 1 Torr in He	Ray et al.[134]
	10	DF-MS study with a fit of experimental and calculated SO_2 profiles	Mellouki et al.[131]
reaction	k (298 K) (cm^3 $molecule^{-1}$ s^{-1})	comments	literature
$CH_3SO_2 + O_2 + M \rightarrow$ products	(2.6×10^{-18})[(ii)]	no measurement; estimate not corrected for $CH_3SO_2 + O_2 + M \leftrightarrow CH_3SO_2OO + M$ equilibrium	Yin et al.[88]
$CH_3SO_2 + O_3 \rightarrow$ products	5×10^{-15}	estimate	Yin et al.[88]
$CH_3SO_2 + NO_2 \rightarrow$ products	$(2.2 \pm 1.1) \times 10^{-12}$	DF-LIF/MS study at 1 Torr in He	Ray et al.[134]
$CH_3SO_2OO + NO \rightarrow CH_3SO_3 + NO_2$	1×10^{-11}	estimate	Yin et al.[88]
$CH_3SO_2OO + NO_2 \rightarrow CH_3SO_2OONO_2$	1×10^{-12}	estimate	Yin et al.[88]
$CH_3SO_3 + HO_2 \rightarrow CH_3SO_3H + O_2$	5×10^{-11}	estimate	Yin et al.[88]

yield was found to be pressure dependent, varying from about 0.4 at 100 Torr to 0.25 at 664 Torr of N_2 and 300 K.[129] This behavior is interpreted in terms of the formation of an activated CH_3SO_2* radical followed by its prompt decomposition or collisional stabilization

$$CH_3SO + NO_2 \rightarrow CH_3S(O)ONO^* \rightarrow CH_3SO_2^* + NO$$

$$CH_3SO_2^* \rightarrow CH_3 + SO_2$$

$$CH_3SO_2^* + M \rightarrow CH_3SO_2 + M$$

The mechanism has been validated theoretically by ab initio calculations.[130]

There is still quite a bit of uncertainty in the rate coefficient for the reaction of CH_3SO with O_3. The value of $(3.2 \pm 0.9) \times 10^{-13}$ cm^3 $molecules^{-1}$ s^{-1} from the recent PLP-LIF measurement by Borissenko et al.[129] is approximately a factor of 2 lower than the value of $(6 \pm 3) \times 10^{-13}$ cm^3 $molecules^{-1}$ s^{-1} determined in the DF-MS study of Dominé et al.;[120] the values, however, do agree within the large uncertainty limits. Thermodynamically feasible channels for the reaction of O_3 with CH_3SO at 298 K include[10]

$$CH_3SO + O_3 \rightarrow CH_3S + 2O_2 \qquad \Delta H^\circ = -9.09 \text{ kcal mol}^{-1}$$

$$CH_3SO + O_3 \rightarrow CH_2SO + OH + O_2 \qquad \Delta H^\circ = -42.82 \text{ kcal mol}^{-1}$$

$$CH_3SO + O_3 \rightarrow CH_3SO_2 + O_2 \qquad \Delta H^\circ = -95.22 \text{ kcal mol}^{-1}$$

$$CH_3SO + O_3 \rightarrow CH_3 + SO_2 + O_2 \qquad \Delta H^\circ = -75.84 \text{ kcal mol}^{-1}$$

$$CH_3SO + O_3 \rightarrow CH_2SO_2 + H + O_2 \qquad \Delta H^\circ = ? \text{ kcal mol}^{-1}$$

$$CH_3SO + O_3 \rightarrow CH_2SO_2 + HO_2 \qquad \Delta H^\circ = ? \text{ kcal mol}^{-1}$$

$$CH_3SO + O_3 \rightarrow CH_3O + SO_3 \qquad \Delta H^\circ = -131.34 \text{ kcal mol}^{-1}$$

In the DF-MS low pressure (1−2 Torr of He) study by Dominé et al.[120] a branching ratio of 0.13 ± 0.06 was obtained for the channel forming the CH_3S radical and a limit of ~0.10 was put on the channel forming CH_2SO. However, in a new PLP-LIF study on DMS/O_3/NO_2 mixtures by Borissenko et al.[129] where SO_2 was measured directly a yield of (1.0 ± 0.12) at 660 Torr of N_2 has been determined. As for the studies on $CH_3SO + NO_2$,[131,134] Borissenko et al.[129] interpret their results in terms of an activated CH_3SO_2* radical followed by its prompt decomposition or collisional stabilization

$$CH_3SO + O_3 \rightarrow CH_3SO_2^* + O_2$$

$$CH_3SO_2^* \rightarrow CH_3 + SO_2$$

$$CH_3SO_2^* + M \rightarrow CH_3SO_2 + M$$

If the reaction is proceeding via an activated CH_3SO_2* complex, then the high yield of SO_2 observed at high pressure would imply that collisional stabilization at atmospheric pressure is not efficient enough for thermalization. Interestingly, if the yield of SO_2 in the $CH_3SO + O_3$ reaction is unity as reported,[129] then the only reaction that can compete and prevent C−S bond scission is the formation of an O_2 adduct, $CH_3S(O)O_2$.

Methylsulfonyl Radical (CH_3SO_2). As discussed above, the methylsulfonyl radical (CH_3SO_2) is a potential product of the oxidation of CH_3S and CH_3SO radicals by O_2 and other reactive trace gas atmospheric constituents. In addition to the competition between OH addition to and hydrogen abstraction from DMS the atmospheric fate of CH_3SO_2 has been proposed to be an additional factor controlling the observed temperature dependence of the [MSA]/[SO_4^{2-}] ratio in the atmosphere. The critical factor concerns the branching ratio between thermal decomposition of CH_3SO_2 and reaction to form the CH_3SO_3 radical. Kinetic data[129−136] on the reactions of CH_3SO_2 radicals are listed in Table 7. Considering the potential importance of the CH_3SO_2 radical the kinetic database for its atmospheric reactions, as listed in Table 7, is very sparse. Experimental kinetic information is available only on the thermal decomposition of CH_3SO_2[129−136] and its reaction with NO_2;[134] all other kinetic information is based on educated guesses.[88]

As can be seen in Table 7 the value for the thermal decomposition of CH_3SO_2 has oscillated between low[129,131,135,136] and high values[130,134] with the newest determinations favoring a low value.[129,135,136] It would now appear that the high values for the thermal decomposition are in error[129] and that the value is <1 s^{-1}.[129,135,136] In any event, it

Table 8. Arrhenius Parameters for $CH_3SO_2OONO_2 + M \rightarrow CH_3SO_2OO + NO_2 + M$ for $M = N_2$

P (mbar)	k (298 K) (s^{-1})	A (s^{-1})	E_a (kJ mol^{-1})	literature
1013	0.0119	2.25×10^{18}	115.6 ± 10.8	Hjorth et al.[132]
1013 ± 1	0.0135	2.7×10^{15}	98.7 ± 2.8	Mayer-Figge[116]
100.9 ± 0.7	0.0113	5.7×10^{14}	95.3 ± 3.6	
10.4 ± 0.2	0.0065	3.7×10^{13}	89.9 ± 4.9	

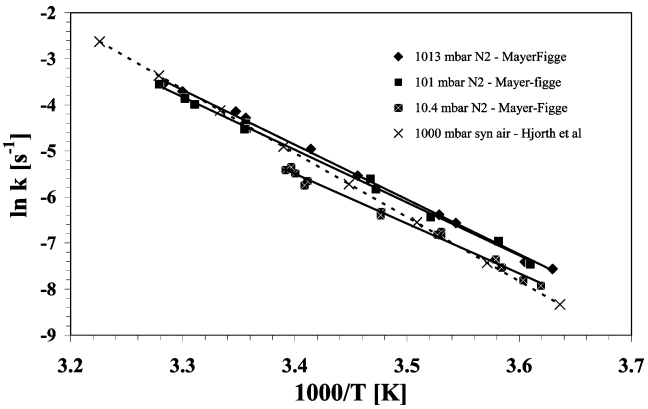

Figure 5. Arrhenius plot of the rate of thermal decomposition of $CH_3SO_2OONO_2$ by different total pressures of N_2.

is extremely difficult to explain the high yields of MSA observed by Bukovskaya and Barnes[135,136] in their study on the UV photolysis of $CH_3SO_2SCH_3$ and also other "NO_x-free" chamber studies without invoking a low value for the thermal decomposition of CH_3SO_2. The use of a lower value for the thermal decomposition of CH_3SO_2 in atmospheric models of DMS chemistry would lead to somewhat higher formation yields of MSA and slightly lower SO_2 yields.

It seems beyond reasonable doubt that the identity of one of the peroxynitrates observed in many chamber studies is methanesulfonylperoxynitrate ($CH_3SO_2OONO_2$). This is evident from the behavior of IR absorption bands assigned to the compound as monitored in many photoreactor systems using different precursors (refs 81, 82, 84, and 114−116 and references therein). Kinetic information on the thermal decomposition of $CH_3SO_2OONO_2$ is listed in Table 8. The data are plotted in Figure 5.

As can be seen from Figure 5, the results from the studies of Hjorth et al.[132] and Mayer-Figge[116] are in good agreement at 1013 mbar total pressure and 298 K. However, the values of Hjorth et al.[132] deviate quite significantly from those of Mayer-Figge[116] at lower temperatures. The activation energies determined by Hjorth et al. are significantly higher than those determined by Mayer-Figge. The preexponential factor determined by Hjorth et al. is abnormally large; however, their determination was made over a small temperature interval (282−306 K), and the uncertainty on the preexponential factor is large, i.e., almost 2 orders of magnitude. For a thermal decomposition reaction of this type a value 2 orders of magnitude smaller than that quoted by Hjorth et al. would normally be expected.

Wang and Zhang[137] made calculations on the enthalpies of formation of CH_3SO_xH ($x = 1-3$) and H_2SO_y ($y = 2,3$) using the Gaussian-3 (G3) method with B3LYP/6-31G(d) and MP2/cc-pVTZ geometries. With the isodesmic reaction procedure using G3//MP2, they report $\Delta_f H_{298}°$ values of −134.69, −79.19, −35.17, −126.32, and −69.38 kcal mol^{-1} for CH_3SO_2OH, $CH_3S(O)OH$, CH_3SOH, H_2SO_3, and HOSOH, respectively. The results are generally consistent with other available experimental and theoretical values summarized in the paper. On the basis of the calculated enthalpies of formation the O−H BDEs of MSA, MSIA, and CH_3SOH at 298 K, when dissociated into the most stable radicals, are estimated using G3//MP2 calculations to be 112.68, 81.34, and 71.53 kcal mol^{-1}, respectively.

Hydrogen abstraction from H−R species by the $CH_3S(O)_2$ radical is energetically possible only from HONO. Hence, it is unlikely that $CH_3S(O)OH$ will be produced from H-abstraction reactions of $CH_3S(O)_2$ radicals. Given the much higher BDE of H−O in MSA compared to MSIA, H-abstraction reactions appear more likely to be of importance in the case of the CH_3SO_3 radical. The bond dissociation energies of CH_3SO_2 and CH_3SO_3 to form SO_2 and SO_3, respectively, together with a CH_3 radical have been estimated as 17.2 and 22 kcal mol^{-1};[88] thus, it seems likely that the rate of dissociation of CH_3SO_3 to form SO_3 will be similar or much slower than that of CH_3SO_2 to form SO_2. The observations of MSA formation in the studies of Bukovskaya and Barnes[135,136] on CH_3SO_2 radicals in a laboratory photoreactor are indicative that H-abstraction reactions by CH_3SO_3 forming MSA were occurring under the conditions of their experiments. The dissociation reaction of CH_3SO_3, leading to formation of SO_3 and thus H_2SO_4 in the atmosphere, is of interest as a potential direct pathway to the formation of H_2SO_4. There has been no report of any direct experimental evidence for the occurrence of this reaction. Bukovskaya and Barnes[135,136] were only able to model their studies on the CH_3SO_2 radical assuming a negligible thermal decomposition rate for CH_3SO_3. The indirect circumstantial evidence supports that the thermal decomposition of CH_3SO_3 to form CH_3 and SO_3, if occurring, is probably of negligible atmospheric importance.

2.2. Reaction with the NO_3 Radical

The NO_3 radical is formed in the atmosphere by the reaction between NO_2 and ozone. While it is rapidly removed by photolysis at daytime, its concentration may build up at night, which combined with its high reactivity makes it an important oxidizing species in the troposphere. The reaction between DMS and nitrate radicals is sufficiently fast to make it become a potentially important sink for DMS.

2.2.1. Kinetics and Primary Reaction Step with the NO_3 Radical

The rate coefficient of the primary step in the reaction of the NO_3 with DMS has been determined by several techniques (see Table 9). The value recommended in the review by De More et al.[6] is derived from a composite fit to the data obtained by the FP-VA study by Wallington et al.,[138,139] the DP−VA study by Tyndall et al.,[140] and the DF-LIF study by Dlugokencky and Howard[141]

$$k = 1.9 \times 10^{-13} \exp((500 \pm 200)/T) \text{ and } k_{298} = 1.0 \times 10^{-12}\ \text{cm}^3\,\text{molecule}^{-1}\,\text{s}^{-1}$$

This value is in good agreement with the room-temperature RR study by Atkinson et al.[142] An absolute determination of the rate coefficient for the reaction between NO_3 and *trans*-2-butene allowed the rate constant to placed on an absolute basis, leading to a value of $(9.92 \pm 0.02) \times 10^{-13}$ cm^3 $molecule^{-1}$ s^{-1}. Also, the room-temperature rate coefficients found in the FP-VA studies by Wallington et al.[138,139] and Daykin and Wine[143] are in reasonable agreement with the recommendation by De More et al.[6] The determinations of

Table 9. Kinetic Data for the Reaction of the NO_3 Radical with Dimethyl Sulfide (DMS)

$k(NO_3+DMS)$ ($cm^3 molecule^{-1} s^{-1}$)	T (K)	P (Torr)/bath gas	comments	literature
$(5.4 \pm 0.7) \times 10^{-13}$	296	735/N_2	RR, relative to *trans*-2-butene, $k_{trans-2-butene}=1.89 \times 10^{-13}$[a]	Atkinson et al.[142]
$(10 \pm 2) \times 10^{-13}$	278-3 18	20/N_2	DP-VA	Tyndall et al.[140]
$(7.5 \pm 0.5) \times 10^{-13}$	298	50−400/He	FP-VA	Wallington et al.[138]
$(8.1 \pm 1.3) \times 10^{-13}$	280−350	50−100/N_2	FP-VA, Arrhenius expression determined: $(4.7 + 2.6/-1.7)\ 10^{-13} \exp[(170 \pm 130)/T]$ $cm^3 molecule^{-1} s^{-1}$ for $T = 280-350$ K	Wallington et al.[139]
$(10.6 \pm 1.3) \times 10^{-13}$	298	0.46−5/He	DF-LIF, Arrhenius expression determined: $(1.79 + 0.22) \times 10^{-13} \exp[(530 \pm 40)/T]$ $cm^3 molecule^{-1} s^{-1}$ for $T = 256-376$ K	Dlugokencky and Howard[141]
$(13 \pm 3) \times 10^{-13}$	298	20−500/air	LP-LA	Daykin and Wine[143]

[a] Atkinson et al.[264]

the reaction rate coefficient were carried out over a wide range of pressures, and all evidence suggests that it is independent of pressure in the range between 0.5 Torr and atmospheric pressure (Tyndall and Ravishankara[144]).

The inverse temperature dependence of the rate coefficient suggests that the reaction proceeds via reversible formation of a NO_3−DMS adduct

$$CH_3SCH_3 + NO_3 \leftrightarrow CH_3S(ONO_2)CH_3 \qquad \Delta H = -7.0 \text{ kcal mol}^{-1}$$

Daykin and Wine[143] and Jensen et al.[145] used the FP-VA and the RR techniques, respectively, to determine the kinetic isotope effect of deuterium substitution. Comparing the rate coefficient of the reaction of NO_3 with CH_3SCH_3 and that of its reaction with CD_3SCD_3 they found k_H/k_D values of 3.5 and 3.8, respectively, which suggests a mechanism involving hydrogen abstraction. Thus, the overall reaction should be

$$CH_3SCH_3 + NO_3 \rightarrow CH_3SCH_2 + HNO_3 \qquad \Delta H^\circ = -8.4 \text{ kcal mol}^{-1}$$

possibly via the intermediate formed in reaction 1a followed by

$$CH_3S(ONO_2)CH_3 \rightarrow CH_3SCH_2 + HNO_3$$

A subsequent study by Butkovskaya and Le Bras[99] used chemical titration of the primary formed radical to show that the hydrogen-abstraction reaction is predominant. In a DF-MS study carried out using He as carrier gas at 1 Torr total pressure the primarily formed radical was titrated by Br_2 and Cl_2 via the reaction

$$CH_3SCH_2 + X_2 \rightarrow CH_3SCH_2X + X$$

where X is the halogen atom. Products were measured by mass spectrometry with electron impact ionization. Four possible reaction pathways were considered: adduct formation, hydrogen abstraction, and the reactions

$$CH_3SCH_3 + NO_3 \rightarrow CH_3S(O)CH_3 + NO_2 \qquad \Delta H = -20.0 \text{ kcal mol}^{-1}$$

$$\rightarrow CH_3SONO_2 + CH_3 \qquad \Delta H = -7.0 \text{ kcal mol}^{-1}$$

The results showed that alternative channels to the hydrogen-abstraction reaction could not account for more than at most 6% of the overall reaction. The reaction forming dimethyl sulfoxide was estimated to account for approximately 3%, while the contribution of a pathway forming methyl radicals was estimated to be less than 2% of the overall reaction.

The outcome of this study was in agreement with evidence obtained in previous studies of the reaction between DMS and NO_3 that failed to observe either dimethyl sulfoxide (Jensen et al.[146]) or NO_2 (Dlugokencky and Howard;[141] Tyndall et al.[140]) as products of the reaction between NO_3 and DMS but in some disagreement with a recent product study of Arsene et al.[147] In the EUPHORE chamber facility in Valencia, Spain, using FTIR for product identification Arsene et al. found DMSO as well as small amounts of $DMSO_2$ among the products in an investigation of the reaction of NO_3 with DMS. The results suggest that an addition channel leading to the formation of DMSO and NO_2 is also operative and could account for 11−12% of the overall reaction. This contradicts the results of the above-mentioned studies. However, the results of Arsene et al. need independent validation. If the results are valid the reaction of NO_3 with DMS should be examined as a function of temperature since the DMSO formation channel pathway will probably increase in importance with decreasing temperature.

2.2.2. Products and Mechanism of the NO_3 + DMS Reaction

Since the initial step in the reaction of NO_3 with DMS appears to be predominantly a hydrogen-abstraction reaction, it can be expected that the reaction products are identical to those formed by the OH-initiated H-atom-abstraction reaction.

The published product studies of this reaction have been carried out at relatively high NO_x levels. This is the case for the early study by MacLeod et al.[148] as well as for the studies by Jensen et al.,[145,146] who used concentration levels of NO_2 of a few ppm. In a recent study by Arsene et al.[147] NO_x concentrations up to approximately 1 ppm were applied. Yin et al.[77] report the results of two smog chamber runs, using a large all Teflon chamber, with initial NO_x concentrations closer to ambient levels and more than an order of magnitude below those of the other studies. The yields of SO_2 determined by Yin et al. (55−68%) are significantly higher than those determined in the other studies (10−35%). Yin et al. find low yields of MSA (0−0.5%), while Jensen et al. find high yields (around 50%) of MSA when sampling by bubbling the reaction mixture through water. Later results have indicated that the high yield of MSA found by Jensen et al. is an artifact caused by the sampling system where MSA is produced by the degradation of a peroxynitrate intermediate in liquid water.[133] This peroxynitrate intermedi-

Table 10. Literature Rate Coefficients for the Reaction of Cl Atoms with Dimethyl Sulfide (DMS) at Room Temperature

$10^{10} \times k$ (cm^3 $molecule^{-1}$ s^{-1})	T (K)	P (Torr)/bath gas	comments	literature
3.3 ± 0.5	297	700/N_2	FP-RF	Stickel et al.[156 d]
<1.8	297	3/N_2		
0.69 ± 0.13	298	1/He 0.5−1/He	DF-MS	Díaz-de-Mera et al.[160 e]
3.6 ± 0.2	298	760/N_2	CRDS[a]	Enami et al.[162]
3.61 ± 0.21	298 ± 3	(760 ± 10)/N_2	RR [relative to k(n-butane) = 1.94×10^{-10} cm^3 $molecule^{-1}$ s^{-1}][b]	Kinnison et al.[157]
4.03 ± 0.17	298 ± 3	(760 ± 10)/air	RR [relative to k(n-butane) = 1.94×10^{-10} cm^3 $molecule^{-1}$ s^{-1}][b]	Kinnison et al.[157]
3.22 ± 0.30	295	740/N_2	RR [relative to k(cyclohexane) = 3.11×10^{-10} cm^3 $molecule^{-1}$ s^{-1}][c]	Nielsen et al.[155]
3.16 ± 0.33	298	760/N_2	RR [relative to cyclohexane, propene and n-butane][f]	Arsene et al.[161]
3.78 ± 0.36	298	760/air	RR[relative to cyclohexane, propene and n-butane][g]	Arsene et al.[161]

[a] Estimated from an analysis of the time profiles of the Cl-DMS adduct. [b] Aschmann and Atkinson.[265] [c] Atkinson and Aschmann.[266] [d] Temperature dependence observed in the range 240−421 K, but no Arrhenius equation reported; rate increases with decreasing temperature. [e] Arrhenius expression reported $k(T) = (2.0 \pm 1.2) \times 10^{-10} \exp[-(332 \pm 173)/T]$ cm^3 $molecule^{-1}$ s^{-1} valid for 257−364 K and 0.5−1/He. [f] Arrhenius expression reported $k(T) = 1.87 \times 10^{-13} \exp[2204/T]$ cm^3 $molecule^{-1}$ s^{-1} valid for 283−303 K and 1000 mbar N2. [g] Arrhenius expression reported $k(T) = 3.40 \times 10^{-13} \exp[2081/T]$ cm^3 $molecule^{-1}$ s^{-1} valid for 283−303 K and 1000 mbar synthetic air.

ate, $CH_3S(O_2)OONO_2$ (discussed in section 2.1.3.3), is found in particularly high concentrations in experiments with high [NO_x]. The low SO_2 yields found in some studies may be a result of the fact that ppm-level NO_x concentrations inhibit the formation of SO_2, e.g., by the sequence of reactions

$$CH_3SO_2 + O_2 + M \leftrightarrow CH_3S(O_2)OO + M$$

$$CH_3S(O_2)OO + NO_2 + M \leftrightarrow CH_3S(O_2)OONO_2 + M$$

that competes with

$$CH_3SO_2 \rightarrow CH_3 + SO_2$$

and reactions leading to the formation of CH_3SO_3 and MSA, as discussed previously (section 2.1.3.3).

At the ppt-level NO_x concentrations typical of remote marine atmospheres, formation of SO_2 and some MSA will likely dominate in the reaction of NO_3 with DMS, but based on recent evidence[147] formation of low yields of DMSO cannot be completely ruled out.

2.3. Reactions with Halogen Atoms and Halogen Oxides (X/XO)

Halogen atoms and their oxides are potential oxidants for DMS in the marine troposphere. In the case of the halogen atoms, the fast reaction of DMS with chlorine is of particular interest since peak concentrations of chlorine as high as 10^4−10^5 molecules cm^{-3} have been measured and predicted by models (Pszenny et al.,[149] Singh,[150] Singh et al.,[151] Spicer et al.[152]). With respect to the halogen oxides, it has been found that the reaction between DMS and BrO radicals could be particularly important under some conditions, based on what is known about the atmospheric concentration of this radical (Toumi,[153] Finlayson-Pitts, and Pitts[154]).

2.3.1. Kinetics of the Cl + DMS Reaction

Kinetic studies on the DMS + Cl reaction[155−162] are listed in Table 10. There is good agreement between the values determined at high pressure. The relative rate studies of Kinnison et al.[157] and Arsene et al.[161] at 1 atm show that the overall rate is sensitive to the O_2 partial pressure with somewhat higher values being obtained in synthetic air compared to N_2 as the bath gas.

Stickel et al.[156] showed that the reaction proceeds via two channels; a pressure-dependent $(CH_3)_2S$−Cl adduct-forming channel and a pressure-independent H-atom-abstraction channel. They found a low-pressure limit of $\sim 1.8 \times 10^{-10}$ cm^3 $molecule^{-1}$ s^{-1} at 3 Torr for the reaction which increased to a value of $(3.3 \pm 0.5) \times 10^{-10}$ cm^3 $molecule^{-1}$ s^{-1} at 700 Torr of N_2. The high-pressure value is in good agreement with the high-pressure relative rate studies. Enami et al.[162] recently studied the kinetics of the Cl + DMS reaction in the pressure range 20−300 Torr N_2 using CRDS analyses of time profiles of the $CH_3)_2S$−Cl adduct to obtain the kinetic information. The pressure dependence is in reasonable agreement with that of Stickel et al.[156] However, Díaz-de-Mera et al.,[160] in a recent low-pressure DF-MS study, measured a rate coefficient for the DMS + Cl reaction at 0.5 Torr which is over a factor of 2 lower than that reported in the FP-LP study by Stickel et al.[156] at 3 Torr. In addition, Díaz-de-Mera et al. also measured a slightly positive activation energy of (0.67 ± 0.36) kcal mol^{-1} (2.8 ± 1.5kJ mol^{-1}) for the reaction, whereas Stickel et al.[156] found an overall negative activation for the reaction. An overall reaction negative activation has also been found in the recent relative kinetic study by Arsene et al.[161] Enami et al.[162] reported a negative temperature dependence for the forward reaction forming the adduct (Cl + DMS → Cl−DMS) in the temperature range 278−318 K.

Díaz-de-Mera et al.[160] argue that at the low pressure in their experiments they are measuring the pressure-independent channel, i.e., an H-atom abstraction from a methyl group, whereas in the other studies the measured rate and activation energy represents the combination of the pressure-independent and pressure-dependent channels. However, because of the complexity of the reaction of Cl with DMS, this interpretation of the present state of the available kinetic data needs independent experimental confirmation. If the interpretation of Díaz-de-Mera et al.,[160] is correct then at atmospheric pressure and room temperature this would imply that approximately 20% of the Cl + DMS reaction will be occurring by H-atom abstraction and the remaining 80% by adduct formation.

Rate coefficients of $(1.19 \pm 0.18) \times 10^{-11}$ and $(2.7 \pm 0.41) \times 10^{-11}$ cm^3 $molecule^{-1}$ s^{-1} have been measured at 155 Torr total pressure and room temperature for the reactions of the Cl−DMS adduct with NO and NO_2, respectively.[165]

Molecular chlorine is known to react with DMS and that is the reason why it is not used as a photolytic Cl atom source in photoreactor studies of Cl + DMS chemistry. Using a

flow tube coupled with UV photoelectron spectroscopy, a rate coefficient of $(3.4 \pm 0.7) \times 10^{-14}$ cm^3 molecule^{-1} s^{-1} has been measured for the reaction[163] at (294 ± 2) K between 1.6 and 3.0 Torr total pressure. The reaction has been found to proceed through an intermediate, $(CH_3)_2SCl_2$, to give CH_3SCH_2Cl and HCl as products.

2.3.2. Products and Mechanism of the Cl + DMS Reaction

The following channels are possible for the reaction of Cl with DMS

$$\begin{aligned} Cl + CH_3SCH_3 &\rightarrow CH_3SCH_2 + HCl \\ &\rightarrow [(CH_3)_2S{-}Cl]^* \\ [(CH_3)_2S{-}Cl]^* + M &\rightarrow CH_3S + CH_3Cl + M \\ &\rightarrow CH_3SCl + CH_3 + M \\ &\rightarrow (CH_3)_2S{-}Cl + M \end{aligned}$$

The DF-MS study of Butkovskaya et al.[158] supports that at $T = 298$ K and $P \approx 1$ Torr the unique channel in the DMS + Cl reaction is the H-atom-abstraction reaction giving CH_3SCH_2 + HCl. Stickel et al.[156] found that hydrogen abstraction is the dominant pathway at low pressure and that stabilization of a $(CH_3)_2S{-}Cl$ adduct becomes an increasingly important pathway with increasing pressure. Their results supported that at 298 K and 760 Torr total pressure only about 40−50% of the overall Cl + DMS reactivity could be attributed to an H-atom-abstraction pathway. As indicated in the previous section, however, based on the results of Díaz-de-Mera et al.[160] the contribution of the abstraction pathway may be only around 20%.

The fate of the $(CH_3)_2S{-}Cl$ adduct under atmospheric conditions is still very uncertain. Zhao et al.[159] showed that dissociation of the $(CH_3)_2S{-}Cl$ adduct to $CH_3 + CH_3SCl$ is very minor, and the work of Langer et al.[164] showed that the dissociation pathway to give CH_3S and CH_3Cl is also very minor at atmospheric pressure.

Urbanski and Wine[165] used LFP/UV−vis absorption spectroscopy to perform a spectroscopic and kinetic study of the $(CH_3)_2S{-}Cl$ adduct. The gas-phase spectrum of the adduct possesses a strong, broad, unstructured absorption extending from ca. 450 to 280 nm with λ_{max} at ≈340 nm ($\sigma_{max} = (3.48 \pm 1.04) \times 10^{-17}$ cm^2 molecule^{-1}). Under their experimental conditions they did not observe a reaction between the adduct and O_2 and estimated a rate coefficient of $<4 \times 10^{-18}$ cm^3 molecule^{-1} s^{-1} for this reaction at 298 K. Enami et al.[162] in a recent CRDS study of the $(CH_3)_2S{-}Cl$ adduct could also not detect any perceptible change in the adduct profile on adding 10 Torr of O_2 to their reaction system at a total pressure of 100 Torr N_2, which agrees with the observations of Urbanski and Wine.[165] Enami et al.[162] using a theoretically calculated equilibrium constant of $K_{ClDMS} = 2.8 \times 10^{-12}$ cm^3 molecule^{-1} s^{-1} for Cl + DMS ↔ Cl−DMS in combination with an experimentally determined value for the forward reaction have estimated a value of 90 ± 20 s^{-1} for the back reaction at room temperature and a total pressure of 300 Torr which corresponds to a lifetime of 0.01 s for the adduct. This lifetime taken in conjunction with the kinetic data of Urbanski and Wine[165] would support that the atmospheric fate of $(CH_3)_2S{-}Cl$ is not direct reaction with O_2. Thompson et al.[169] used variational RRKM theory to predict the thermal decomposition rate of the stabilized adduct back to the starting reactants and obtained a value of 0.02 s^{-1}. With this decomposition rate a rate coefficient for reaction of O_2 with the $(CH_3)_2S{-}Cl$ adduct of $\sim 10^{-21}{-}10^{-22}$ cm^3 molecule^{-1} s^{-1} would suffice to make this process competitive with the decomposition channel.

The differences observed in the rate coefficients measured for Cl + DMS in N_2 and synthetic air at atmospheric pressure by Kinnison et al.[157] and Arsene et al.[161] support that an interaction between the $(CH_3)_2S{-}Cl$ adduct and O_2 must be occurring. Arsene et al.[166] recently measured the products of the Cl + DMS reaction as a function of temperature and O_2 partial pressure. They observe formation of DMSO and SO_2. The yield of DMSO was found to increase with increasing O_2 partial pressure and also with increasing temperature. At 293 K they measured DMSO and SO_2 molar yields of 52% and 39%, respectively, the DMSO being corrected for secondary consumption by Cl atoms. The most plausible reaction forming DMSO is reaction of the $(CH_3)_2SCl$ adduct with O_2

$$(CH_3)_2S{-}Cl + O_2 \rightarrow CH_3SOCH_3 + ClO$$

As indicated earlier, the present kinetic data would indicate that about 80% of the Cl + DMS reaction is proceeding via adduct formation under these conditions. According to the results of Arsene et al. this would imply that the fate of the $(CH_3)_2SCl$ adduct under these conditions is ca. 75% reaction with O_2 to form DMSO.

There have been five theoretical studies on the Cl + DMS reaction to date performed at different levels of theory.[106,162,167−169] McKee[106] determined the $(CH_3)_2S{-}Cl$ adduct structure at the UHF/6-31G* level of geometry optimization and the energetics at the PMP2/6-31G*//UHF/3-21G* level and reported a binding energy of 12.1 kcal mol^{-1}. This value is considerably lower than the $\Delta H^{298} = -19.3$ kcal mol^{-1} reported by Wilson and Hirst[167] calculated at the MP2(Full)/6-311G** level but in good agreement with a value of 12.3 kcal mol^{-1} reported by Resende and De Almeida[168] at the UQCISD-(T)/DZP//UMP2/DZP level of calculation. The most recent value of 17.7 kcal mol^{-1}, reported by Enami et al.,[162] at the QCISD(T)/MP/6-311++G-(2df.2p) level lies between the previous determinations. Thompson et al.[169] reported values of $\Delta_r H°$ for formation of the $(CH_3)_2S{-}Cl$ adduct which are in good agreement with the value of Wilson and Hirst[167] but not with the calculated values of by McKee[106] or Resende and De Almeida.[168]

Of the four possible reaction channels investigated by Resende and De Almeida[168] the calculations gave that the channels leading to $(CH_3)_2S{-}Cl$ adduct formation and the hydrogen-abstraction channel leading to CH_3SCH_2 + HCl are the most favorable. The calculations predicted that direct formation of CH_3Cl and CH_3S is considerably hindered. The calculations also predicted that under atmospheric conditions the channel forming the adduct reaches equilibrium more quickly than the abstraction channel and that the concentration of the adduct will be very small. From this they conclude that the abstraction channel will be the most important under atmospheric conditions. The calculations do not, however, consider stabilization of the adduct by another species such as O_2.

2.3.3. Kinetics of the ClO + DMS Reaction

The rate coefficient of this reaction has been determined in two studies, both applying the DF-MS technique and He

Table 11. Literature Rate Coefficients for the Reaction of ClO Atoms with Dimethyl Sulfide (DMS) at Room Temperature

$10^{15} \times k$ (cm^3 $molecule^{-1}$ s^{-1})	T (K)	P (Torr)/bath gas	comments	literature
9.5 ± 2.0	298	0.4−5.1 Torr/He	DF-MS, Arrhenius expression, $k_3 = (1.2 \pm 0.7) \times 10^{-15}$ $\exp[(354 \pm 163)/T]$ cm^3 $molecule^{-1}$ s^{-1}, valid for the temperature interval 259−335 K, was reported	Barnes et al.[172]
3.9 ± 1.2	298	0.5−2 Torr/He	DF-MS	Díaz-de-Mera et al.[160]

as bath gas (see Table 11). Although very similar techniques were applied, the results at room temperature differ by a factor of 2. There does not seem to be any obvious explanation for this disagreement. A rate coefficient of 3×10^{-15} cm^3 $molecule^{-1}$ s^{-1} been computed at high levels of theory at 298 K and 60 Torr by Sayin and McKee[170] and is in good agreement with the lower of the experimental values reported by Diaz-de-Mera et al.[160] However, in the computational study only the bimolecular pathway for the reaction $CH_3SCH_3 + ClO \rightarrow CH_3SCH_2 + HOCl$ was considered as the calculated binding enthalpy of the ClO−DMS adduct of 2.0 kcal mol^{-1} could not compensate for the loss of entropy associated with its formation. In addition the computational study predicts a positive activation barrier which is in contradiction with the very small negative activation found in the experimental study of Barnes et al.[172]

Barnes et al.[172] suggested that the relatively low preexponential factor and negative temperature dependence they observed may be explained by the formation of an association complex, which may either decompose or react to form products. In light of the recently calculated low binding enthalpy of the ClO−DMS adduct, Gravestock et al.,[171] in a detailed analysis of the trends of XO + DMS (X = Cl, Br, I), argue that while the ClO + DMS reaction may proceed via a weakly bound intermediate, it is probably the barrier to products which controls the reaction.

No kinetic studies under close to ambient atmospheric conditions are reported in the literature. The reaction appears to be too slow to be of atmospheric importance.

2.3.4. Products and Mechanism of the ClO + DMS Reaction

Barnes et al.[172] detected DMSO as a product of the reaction between ClO and DMS in a discharge flow-mass spectrometric study but made no quantification of its yield. In the study by Diaz-de-Mera et al.[160] DMSO was observed as a product of the reaction at 298 K but not quantified. However, in separate experiments at 335 K losses of DMSO in the system were minimized and its signal was calibrated. The yield of DMSO could be calculated, after correction for a wall reaction also forming this product, and was found to be 0.90 ± 0.49. The dominating pathway of the reaction under these conditions would appear to be some form of efficient oxygen-atom transfer via a weakly bound ClO−DMS adduct, e.g.

$$CH_3SCH_3 + ClO \leftrightarrow [(CH_3)_2S(OCl)] \rightarrow CH_3S(O)CH_3 + Cl \quad \Delta H_{298} = -30.26 \text{ kcal mol}^{-1}$$

even though a H-abstraction pathway would be expected to be favored by the low-pressure and high-temperature conditions applied in the study of Diaz-de-Mera et al.[160]

Because of the lack of studies under atmospheric conditions it is not known whether the ClO−DMS adduct may react with O_2 to any significant extent under ambient conditions.

2.3.5. Kinetics of the Br + DMS Reaction

Wine et al.[173] showed, by a flash photolysis-resonance fluorescence study, that the dominating reaction pathway below 310 K is formation of an adduct

$$CH_3SCH_3 + Br + M \leftrightarrow (CH_3)_2SBr + M$$

$$\Delta H = -12 \pm 1 \text{ kcal mol}^{-1} \text{ (Nakano et al.[174])} \quad \Delta G = -23 \pm 4 \text{ cal (Nakano et al.[174])}$$

while at high temperatures (>375 K) the decomposition of the adduct is so rapid that only the H-abstraction pathway is of importance

$$CH_3SCH_3 + Br \rightarrow CH_3SCH_2 + HBr$$

$$\Delta H^\circ = 5.4 \pm 1.4 \text{ kcal mol}^{-1} \text{ (Jefferson et al.[175])}$$

The high-temperature (386−604 K) study by Jefferson et al.[175] showed an almost unity yield of HBr and a strong kinetic isotope effect of deuteration, thus confirming that H abstraction dominates under such conditions.

Enami et al.[162] report a value of $(1.02 \pm 0.07) \times 10^{-4}$ s^{-1} for the unimolecular decomposition (Br−DMS → DMS + Br). The rapid unimolecular decomposition of the Br−DMS adduct under ambient conditions implies that only the reaction with O_2 may be sufficiently fast to compete with this. However, Nakano et al.[174] determined an upper limit for the reaction

$$(CH_3)_2SBr + O_2 \rightarrow DMSO + BrO$$

of 1×10^{-18} $cm^3 molecule^{-1} s^{-1}$, which implies that it will be negligible under ambient conditions. The experimental evidence shows that the Br−DMS adduct is less stable than the Cl−DMS adduct. As pointed out by Nakano et al.,[174] this indicates that the halogen−S bond strength in the Cl−DMS adduct should be higher than in the Br−DMS adduct, which implies that the values calculated by McKee[106] and Resende and De Almeida[168] of 12.1 and 12.3 kcal, respectively, for Cl−DMS are too low while the higher values calculated by Wilson and Hirst,[167] Enami et al.,[162] and Thompson et al.[169] are in better agreement with the experimental results.

The apparent disagreement between the values of the rate coefficient given in Table 12 can be explained by the fact, that they do not refer to the same reaction: The value given by Jefferson et al.[175] is for the H-abstraction reaction, while the values found by Ingham et al.[176] and Nakano et al.[174] are for the reaction leading to formation of the Br−DMS adduct. The upper limit determined by Maurer et al.[177] and the value determined by Ballesteros et al.[178] apply to the overall, irreversible reaction DMS + Br → products.

A bond strength of 14.5 ± 1.2 kcal mol^{-1} was estimated for the $(CH_3)_2S$−Br bond in the study by Wine et al.,[173] while Nakano et al.[174] report an experimentally determined bond strength of 12 ± 1 kcal mol^{-1}.

Table 12. Literature Rate Coefficients at Room Temperature for the Reaction of Br Atoms with Dimethyl Sulfide (DMS), and the Equilibrium Constant for the Formation of the Adduct, Br + DMS ↔ Br−DMS

k(Br + DMS) (cm^3 molecule^{-1} s^{-1})	K_{eq} (10^{15} cm^3 molecule^{-1} s^{-1})	T (K)	P (Torr)/bath gas	comments	literature
3×10^{-14}		298	20−200/N_2	LP-LIF; k at 298 K is extrapolated from 386 to 604 K using the Arrhenius expression $(9.0 \pm 2.9)10^{-11}$ [exp((−2386 ± 151)/T] cm^3 molecule^{-1} s^{-1}; valid for 386 K < T < 604 K	Jefferson et al.[175]
$(6.36 \pm 0.43) \times 10^{-11}$	6.24 ± 0.56	295	100/N_2	PLP-RF	Ingham et al.[176]
$\leq 1 \times 10^{-13}$		298	750 Torr $N_2 + O_2$	RR (relative to acetylene, k(acetylene) depends on [O_2] and [M][a])	Maurer et al.[177]
$(5.0 \pm 0.2) \times 10^{-11}$	4.1 ± 0.3	300 K	100/N_2	LP-CRDS	Nakamo et al.[174]
$(4.9 \pm 1.0) \times 10^{-14}$		293 K	740 Torr/air	RR (relative to k(ethene) = $(1.4 \pm 0.2) \times 10^{-13}$ cm^3 molecule^{-1} s^{-1} [b])	Ballesteros et al.[178]

[a] Barnes et al.[268] [b] Barnes et al.[268] and Yarwood et al.[269]

Table 13. Literature Rate Coefficients at Room Temperature for the Reaction of BrO radicals with dimethyl sulfide (DMS)

k(BrO + DMS) (10^{13} cm^3 molecule^{-1} s^{-1})	T (K)	P (Torr)/bath gas	comments	literature
(2.7 ± 0.5)	298	0.4−5.1/He	DF-MS	Barnes et al.[172]
2.6	298	1/He	DF-MS, $k = (1.5 \pm 0.4) \times 10^{-14}$ exp[(845 ± 175)/T] cm^3 molecule^{-1} s^{-1} for T = 233−320 K	Bedjanian et al.[179]
(4.40 ± 0.66)	295	60, 100, 200/N_2	PLP-UVA	Ingham et al.[176]
4.2	300	100, 200/N_2 100/SF_6	LP-CRDS $k = (1.3 \pm 0.1) \times 10^{14}$ exp[(1033 ± 265)/T] cm^3 molecule^{-1} s^{-1} for T = 278−333 K	Nakamo et al.[174]

The concentration of Br−DMS under typical atmospheric conditions ([Br] = 5×10^5 molecules cm^{-3}, [DMS] = 5×10^9 molecules cm^{-3}) will be 10 molecules cm^{-3}. As pointed out by Nakano et al., this combined with the slow reaction with O_2 implies that the adduct has no atmospheric importance. The rate constants found by Maurer et al.[177] and Ballesteros et al.[178] show that the reaction of Br with DMS is not of importance under atmospheric conditions.

Product studies (see section 2.3.6) suggest that the overall reaction between DMS and Br, leading to stable products, occurs via a Br−DMS intermediate. Thus, the overall rate coefficient can be written as $k_{overall} = k_a k_b/(k_{-a} + k_b) \approx K_{eq} k_b$, where k_a and k_{-a} are the forward and backward reactions for the adduct formation, K_{eq} the equilibrium constant for this reaction, and k_b the irreversible decomposition of the adduct. Using 5×10^{-15} cm^3 molecule^{-1} s^{-1} for K_{eq} [174] and the value determined by Ballesteros et al.[178] for $k_{overall}$ gives a value for k_b of 10 s^{-1}. Recently a value of 7.7×10^{-15} cm^3 molecule^{-1} s^{-1} has been calculated for K_{eq} [162] which is in good agreement with the experimentally determined value of Nakano et al.[174]

2.3.6. Products of the Br + DMS Reaction

The formation of reaction products was investigated in the FTIR chamber study by Maurer et al.[177] in N_2/O_2 mixtures at 750 Torr. Maurer et al. considered three possible decomposition channels for the Br−DMS adduct

$$CH_3S(Br)CH_3 \rightarrow CH_3SCH_2 + HBr$$
$$\rightarrow CH_3Br + CH_3S$$
$$\rightarrow CH_3SBr + CH_3$$

On the basis of the IR spectra, SO_2, DMSO, and CH_3SBr were identified as major sulfur-containing products and also OCS and $DMSO_2$ were found. The observed time dependence of the concentrations showed that DMSO and CH_3-SBr appear to be primary reaction products, while SO_2, $DMSO_2$, and OCS are formed with some delay, indicating that they are secondary products.

The first channel can be considered negligible because if it occurred it would lead to direct primary formation of SO_2 and not secondary formation, which is experimentally observed. The second channel is unimportant since CH_3Br was not detected among the products. Thus, the third channel appears to be the major reaction route. It was found that the observed formation of DMSO could best be explained by the generation of BrO radicals by the reaction of Br with RO_2 radicals, followed by the fast reaction of BrO with DMS, leading to DMSO.

Ballesteros et al.[178] in another FTIR chamber study in air at 296 K and atmospheric pressure, observed time-dependent product formation in good agreement with the findings of Maurer et al.[177] Also in this case CH_3Br could not be detected, while CH_3SBr was found to be a major product. The yield of DMSO, corrected for its reaction with Br, goes through a maximum early in the experiment, suggesting a complex mechanism for its formation.

2.3.7. Kinetics of the BrO + DMS Reaction

The determinations of the rate constant of the reaction BrO + DMS at room temperature show very good agreement among the studies carried out at low pressure in helium (Barnes et al.,[172] Bedjanian et al.[179]) as well as among those carried out at higher pressures in N_2 (Ingham et al.,[176] Nakano et al.[174]) (Table 13). There is, however, a clear difference between the values determined at low and higher pressures, with a significantly faster reaction at higher pressures. Ingham et al. as well as Nakano et al. found no pressure dependence for the reaction at the pressures applied in their studies (60−200 Torr N_2, 100 Torr SF_6), indicating that the reaction has reached its high-pressure limit under the conditions of their experiments. In a computational study at high levels of theory Sayin and McKee[170] calculated rate coefficients for the oxygen-atom-transfer (OAT) and hydrogen-abstraction pathways of 8.7×10^{-13} and 8.9×10^{-15} cm^3

molecule s^{-1}, respectively, at 298 K and 760 Torr, which corresponds to a branching ratio of 0.98 for the oxygen-transfer pathway. The computed value of the rate coefficient for the OAT channel is in fair agreement with the experimental values.

The temperature dependence of the reaction at a total pressure around 1 Torr He was studied by Bedjanian et al.[179] over the temperature range 233−320 K in a discharge flow-mass spectrometric study. BrO atoms were generated by the same procedure as in the study by Barnes et al., and Bedjanian et al. also used an excess of DMS to obtain pseudo-first-order conditions. A negative temperature dependence was observed, and the Arrhenius expression $k = (1.5 \pm 0.4) \times 10^{-14} \exp[(845 \pm 175)/T]$ cm^3 $molecule^{-1}$ s^{-1} valid in the range 233−320 K was derived from the experimental data, which gives a value of $k = 2.6 \times 10^{-13}$ cm^3 $molecule^{-1}$ s^{-1} at 298 K, in excellent agreement with the value from the study by Barnes et al.[172] Ballesteros et al.[178] investigated the effect of deuterization on the kinetics of BrO with DMS. No significant kinetic isotope effect was found.

A negative temperature dependence for the reaction has also been found in the higher pressure studies of Nakano et al.[174] The negative temperature dependence observations of Bedjanian et al.[179] and Nakano et al.[174] and the higher rate coefficients determined at the higher pressures of the laser photolysis studies compared to the lower pressure flow tube studies have been taken as indicating that the reaction proceeds via an association complex mechanism. The observed pressure and temperature dependence agrees with a mechanism involving the formation of a $(CH_3)_2S-OBr$ adduct that is more efficiently stabilized by thermalization in the systems at higher pressures than those applied in the discharge flow-mass spectrometric studies.

A binding enthalpy of 1.7 kcal mol^{-1} has recently been computed for the BrO−DMS adduct, i.e., much weaker than the $(CH_3)_2S-Br$ complex. Using this binding energy and applying a Lindemann-type reaction scheme Gravestock et al.[171] argue that the Lindemann scheme is not consistent with the experimental evidence. They argue that the binding energy is too small, even allowing for calculation uncertainties, to allow collisional stabilization of the excited adduct and that the Lindemann scheme, which predicts a decrease in the DMSO yield with increasing pressure, is not borne out experimentally where a DMSO yield of unity has been observed at all pressure up to 200 Torr by Ingham et al.[176] They conclude from these observations that the difference of approximately two between the rate coefficients for BrO + DMS measured at low pressure[172,179] and those measured at higher pressure[174,176] is not due to pressure stabilization of a complex intermediate. They add, "that if a complex intermediate is formed, then it must be weakly bound, and could explain a pressure independent rate coefficient with a small activation energy." The temperature dependent studies, which have been performed over a relatively narrow range, report a small negative activation barrier (Table 13). Finally, Gravestone et al.[171] propose that the reactions kinetics of BrO + DMS are controlled by the formation of a weakly bound intermediate with no barrier to reaction.

A possible influence of O_2 on the rate coefficient, such as a reaction between the $(CH_3)_2S-OBr$ adduct and O_2, has not been investigated. However, the fact that the product formation does not seem to be affected by the presence of O_2 (see section 2.3.8) suggests that such a reaction is not of importance.

2.3.8. Products of the BrO + DMS Reaction

Barnes et al.[172] detected DMSO as a product of the reaction in a discharge flow-mass spectrometric study (see section 2.3.1) but could not quantify this yield. Three subsequent product studies all showed that DMSO is the predominant product of the reaction over a wide range of conditions: Bedjanian et al.[179] measured the formation of DMSO in a discharge flow-mass spectrometric study and determined a yield of 0.94 ± 0.11 at a total pressure of 1 Torr He and 320 K; Ingham et al.[176] found a DMSO yield of 1.17 ± 0.34 in N_2 at 60−200 Torr pressure and 295 K; Ballesteros et al.[178] found DMSO to be formed with a near unit yield in synthetic air at atmospheric pressure and 295 K.

In light of the product studies and the discussion in the preceding section it would appear that the overall reaction, which probably involves a weakly bound adduct, leads to the formation of DMSO, i.e.

$$CH_3SCH_3 + BrO \leftrightarrow \{(CH_3)_2S-OBr\} \rightarrow CH_3S(O)CH_3 + Br \quad \Delta H_{298} = -30.26 \text{ kcal mol}^{-1}$$

2.3.9. Kinetics of the I + DMS Reaction

Shum and Benson[180] (1985) investigated the I_2-catalyzed decomposition of DMS at 630−650 K. The data obtained by this pyrolysis study, carried out at low pressures (typically <10 Torr), allowed determination of an Arrhenius expression for the H-abstraction reaction

$$CH_3SCH_3 + I \rightarrow CH_3SCH_2 + HI$$

of $2.62 \times 10^{-10} \exp(-13436 \pm 269 \text{ K}/T)$ cm^3 $molecule^{-1}$ s^{-1}. This gives a very low value of 6.9×10^{-30} cm^3 $molecule^{-1}$ s^{-1} for the rate constant of this reaction at 298 K. In fact, by analogy to the Cl and Br reactions with DMS, the dominating pathway at room temperature can be expected to be formation of an $(CH_3)_2S-I$ adduct. Considering the trend observed when going from Cl to Br it may be expected that the iodine−sulfur bond in the adduct is very weak and consequently that the adduct very rapidly dissociates to reform the reactants. Neither a binding enthalpy for the $(CH_3)_2S-I$ adduct nor determinations of the rate coefficient for the DMS + I reaction at room temperature are, to the best of our knowledge, available in the literature.

2.3.10. Products of the I + DMS Reaction

To the best of our knowledge, no product information is available in the literature on this reaction.

2.3.11. Kinetics of the IO + DMS Reaction

The first investigations of this reaction were a DF-MS study by Martin et al.[181] and a study by Barnes et al.[182] where the rate coefficient was determined as a best numerical fit to experimental 'smog chamber' data, applying a complex chemical reaction scheme. The two studies gave rather similar results (1.5×10^{-11} and 3.0×10^{-11} cm^3 $molecule^{-1}$ s^{-1}, respectively), but later work has shown that the value of the rate coefficient determinations were in error, apparently because some of the gas-phase chemistry as well as the heterogeneous chemistry were not accounted for in the derivation of the rate constants.

Table 14. Literature Rate Coefficients at Room Temperature for the Reaction of IO Radicals with Dimethyl Sulfide (DMS)

k(IO + DMS) × 10^{14} (cm^3 molecule^{-1} s^{-1})	T (K)	P (Torr)/bath gas	method	literature
<3.5	298 ± 2	40−300/N_2+O_2	LFP-UV−vis; only upper limit determined	Daykin and Wine[183]
(1.5 ± 0.2)	298	1.1−1.8/He	DF-MS	Maguin et al.[184]
(0.88 ± 0.27)	298	0.−-5.1/He	DF-MS	Barnes et al.[172]
(1.6 ± 0.3)	298	2.5−2.7/He	DF-MS	Knight and Crowley[185]
(25 ± 2)	298[a]	200/N_2	CRDS	Nakano et al.[186]
(2.0 ± 0.5)	296[b]	5−300/He	PLP-LIF	Gravestock et al.[171]

[a] $k = (1.2 + 4.5/-1.0) \times 10^{-16} \exp(2230 \pm 460/T)$ cm^3 molecule^{-1} s^{-1} for T = 273−312 K. [b] $k = (9.6 \pm 8.8) \times 10^{-12} \exp\{1 - (1816 \pm 397]/T\}$.

The LFP-UV−vis study by Daykin and Wine[183] (Table 14) put a limit of <3.5 × 10^{-14} cm^3 molecule^{-1} s^{-1} on the reaction, and no evidence for a pressure dependence could be found. Later DF-MS studies provided absolute values for the rate coefficient at low pressure which were in reasonable agreement, particularly the studies by Maguin et al.[184] and Knight and Crowley.[185] The latter study applied IO concentrations that were sufficiently low so as not to require corrections for the self-reaction of the IO radicals, in contrast to the two other DF-MS studies.

At this point it was generally accepted that the reaction of IO with DMS was too slow to be of importance in the sulfur and iodide cycles in the marine boundary layer (MBL), and a value of $k = (1.3 \pm 0.2) \times 10^{-14}$ cm^3 molecules s^{-1} at 298 K was recommended[55] for the reaction coefficient. However, in 2003 a paper appeared by Nakano et al.[186] which indicated that reaction with IO was a dominant sink for DMS in the MBL. Nakano et al.[186] used cavity ring-down spectroscopy (CRDS) to monitor IO and measured a room-temperature rate coefficient for the reaction of $k = (2.5 \pm 0.2) \times 10^{-13}$ cm^3 molecules s^{-1}, which was more than an order of magnitude greater than the recommended value at that time. In addition, they found a pressure dependence and a negative activation energy for the reaction which suggested an association complex mechanism. They reported an Arrhenius expression $k = (1.2 + 4.5/-1.0) \times 10^{-16} \exp(2230 \pm 460/T)$ cm^3 molecules s^{-1} for the reaction, valid in the temperature range 273−312 K which gives a negative activation energy of $E_a = -4.42 \pm 0.91$ kcal mol^{-1}. In the following year Sayin and McKee[170] published a computational study of the reactions of halogen oxides with DMS in which their rate coefficients for the reactions of ClO and BrO with DMS were in reasonable agreement with the experimental values but their value for IO with DMS of $k = 1.5 \times 10^{-11}$ cm^3 molecules s^{-1} was approximately 3 orders of magnitude greater than the preferred values.[55] Sayin and McKee[170] also reported a binding enthalpy for the $(CH_3)_2S$−OI adduct of only 1.3 kcal mol^{-1}.

The computational study of Sayin and McKee[170] suggests a reactivity trend for XO + DMS of IO > BrO > ClO. On the basis of thermodynamics arguments one might expect the order of reactivity to be IO ≈ BrO > ClO, which the results of Nakano et al.[174] would support. Using the current recommended IUPAC rate coefficients[55] for XO + DMS gives the reactivity trend BrO > ClO ≈ IO. The uncertainty in the rate coefficient for IO + DMS brought about by the experimental study of Nakano et al. and the computational study of Sayin and McKee have lead to a recent detailed study on the kinetics of the IO + DMS reaction by Gravestock et al.[171] using a PLP-LIF technique. These authors studied the reaction over a very wide temperature range, T = 296−468 K, at total pressures between 5 and 300 Torr of helium. They observed a positive activation energy for the reaction with $k = (9.6 \pm 8.8) \times 10^{-12} \exp\{-(1816 \pm 397)/T\}$ cm^3 molecules s^{-1}. No dependence on pressure was observed for the reaction over the pressure range investigated. At 296 K they determined a rate coefficient of $k = 2.0 \times 10^{-14}$ cm^3 molecules s^{-1} which is more than an order of magnitude smaller than the value of Nakano et al. but in reasonable agreement with the previous literature values (Table 14). Gravestock et al.[171] discuss in great length potential interferences from secondary chemistry in both their own investigations and those of Nakano et al.[186] The conclusion of the paper is that their own study is subject to negligible interference from undesirable chemistry and that the work of Nakano et al. has the most potential for interference from unwanted chemistry and the results are most probably flawed. The authors are aware of another independent study (as yet unpublished) which also supports the lower rate coefficient for the IO + DMS reaction.

2.3.12. Products of the IO + DMS Reaction

DMSO was detected as a product in several studies; the only quantitative estimate of the yield has been by Barnes et al.,[172] who reported a yield of (84 ± 40)%. No other oxidation products regarding this reaction have been reported in the literature.

The pressure dependence and negative activation energy reported by Nakano et al.[186] implied a mechanism involving a strongly bound $(CH_3)_2S$−OI adduct. In light of the computational determination of the binding energies for the $(CH_3)_2S$−OX complex and the finding of the recent kinetic study of Gravestock et al.,[171] this seems extremely unlikely. Gravestock et al. measured the temperature dependence of the reaction over a very wide temperature range, and in the absence of interfering chemistry accurate Arrhenius parameters are to be expected from the work. The authors write that the positive activation energy and the absence of a pressure dependence observed by them suggests that the reaction proceeds via a bimolecular reaction mechanism and that it is the barrier to products that is controlling the temperature dependence. The observation of DMSO as the major product, however, supports that some form of weakly bound intermediate must be involved in the mechanism

$$CH_3SCH_3 + IO \rightarrow [(CH_3)_2S{-}OI] \rightarrow CH_3S(O)CH_3 + I \quad \Delta H_{298} = -32 \text{ kcal mol}^{-1}$$

2.4. Short Summary

The major intent of this paper is to review the available kinetic and product data available on the atmospheric photooxidation of DMS rather than to critically review the implications of the information for the role of DMS in atmospheric chemistry. The implications of much of the newer aspects of the chemistry presented here have been

Table 15. Estimated Tropospheric Chemical Lifetime τ of DMS, DMSO, and $DMSO_2$ with Respect to Their Gas-Phase Reactions with Br, BrO, Cl, ClO, IO, NO_3, and OH under Remote Conditions

species	environment	oxidant level[a]	DMS k value (lifetime(	DMSO k value (lifetime)	$DMSO_2$ k value (lifetime)
Br	arctic BL	$(1\text{-}10) \times 10^7$	4.9×10^{-14} [e] (2.4−23.6 days)	$<6 \times 10^{-14}$ [e] (>1.9−19 days)	$<1 \times 10^{-15}$ [e] (>116−1157 days)
BrO	arctic and antarctic BL	$\leq 7 \times 10^8$	4.4×10^{-13} [f] ($\geq$0.9 h)	1.0×10^{-14} [e] ($\geq$1.7 days)	$<3 \times 10^{-15}$ [e] (>5.5 days)
	mid lat. marine BL	$\leq 5 \times 10^7$	($\geq$12.6 h)	($\geq$23.1 days)	(>77 days)
Cl	arctic BL	$(1-10) \times 10^4$	3.3×10^{-10} [g] (0.4−3.5 days)	7.4×10^{-11} [i] (1.6−15.6 days)	2.4×10^{-14} [l] ($(4.8-48) \times 10^3$ days)
	remote marine BL	$(1-15) \times 10^3$	(2.3−35 days)	(10−156 days)	($(3.2-48) \times 10^4$ days)
ClO	arctic BL	$(3-52) \times 10^8$ [b]	9×10^{-15} [f] (5.9 h to 4.3 days)	$<1.6 \times 10^{-14}$ [k] (>3 h)	
IO	coastal areas	$\leq 1.5 \times 10^8$	1.3×10^{-14} [f] ($\geq$5.9 days)		
NO_3	remote marine BL	$<7 \times 10^7$ to $5\ 10^8$ [c]	1.110^{-12} [f] (0.5 to >3.6 h)	1.7×10^{-13} [j] (3.2 to >23.3 h)	$<2 \times 10^{-15}$ [l] (>12 to >83 days)
OH	global average[c]	$1.1\ 10^6$ [d]	6.1×10^{-12} [h] (1.7 days)	1×10^{-10} [f] (2.5 h)	$<3 \times 10^{-13}$ [l] (>35 days)

[a] Platt and Hönninger.[270] [b] Tuckermann et al.[271] (1997). [c] Finlayson-Pitts and Pitts.[154] [d] Prinn et al.[272] [e] Ballesteros et al.[178] [f] Atkinson et al.[55] [g] Kinnison et al.[157] and Arsene et al.;[161] measurements in air at atmospheric pressure. [h] Hynes et al.[31] [i] Barnes et al.[86] and Falbe-Hansen et al.[196] [j] Barnes et al.[199] [k] Only upper limits available by Martinez et al.[203] and Riffault et al.[204] [l] Falbe-Hansen et al.[196]

examined in some recent model studies,[22,94,95,187−189] and these should be consulted in combination with the literature referenced in these studies for details on possible atmospheric implications.

Many major advances have been made in our understanding of the atmospheric oxidation of DMS via OH, NO_3, halogen atoms, and halogen oxides and also on the chemistry of its important reaction intermediates. The investigations have helped to give better insights into many aspects of the DMS oxidation mechanisms by these oxidants and allow in some cases at least tentative mechanistic conclusions to be drawn. For example, the evidence from laboratory studies suggests that the major fate of the CH_3S radical in the atmosphere will most likely be reaction with O_3 and formation of SO_2. However, validation of this conclusion is needed since there are still large uncertainties surrounding the $CH_3S + O_2$ reaction and direct product information on the $CH_3S + O_3$ reaction under atmospheric conditions is still lacking. There are still large uncertainties in the product distributions of many of the reactions which compose the DMS atmospheric photooxidation system and the dependence of the product branching ratios upon the reaction conditions. This is particularly true of the OH-radical-initiated oxidation of DMS where the product yields show a complex O_2 and NO_x dependence. Kinetic data are also required for many of the reactions of photooxidation intermediates in the OH photooxidation. Lack of this information is a major factor affecting the effectiveness of mechanism reduction, which is required for the representation of DMS chemistry in atmospheric models.

A lot of new information, both kinetic and mechanistic, has emerged on the halogen atom and halogen oxide oxidation of DMS. Halogen−DMS adduct formation competes with H abstraction in the reactions of Cl as well as Br with DMS; at room temperature adduct formation appears to dominate in the case of Br, while H abstraction seems to be a significant, though minor, pathway in the case of Cl. There are, to our knowledge, no experimental data regarding the reaction of I atoms with DMS at room temperature. The fate of the Cl−DMS adduct under atmospheric conditions is still very uncertain; the recent study by Arsene et al.[160] suggests that the main reaction will be with O_2 to form DMSO. The main fate of the Br−DMS adduct appears to be dissociation to form CH_3SBr and CH_3.

The atmospheric lifetimes of DMS due to reaction with the oxidant species discussed in this review have been calculated for different atmosphere regions and are given in Table 15 (lifetime is defined as $\tau = 1/[X]$, where X is the concentration of the oxidant species). The lifetimes show that for most marine regions where DMS is emitted reactions with OH radicals during the day and NO_3 radicals during the night will be major DMS sinks as is often assumed in model representations of DMS chemistry. Recent field measurements in the Mediterranean area, however, have shown that during the passage of polluted air parcels reaction with NO_3 can be the dominant sink for DMS. On the basis of the present state of knowledge this change in the main oxidant species will probably change quite significantly the SO_2 and MSA product yields and thus the potential for CCN formation, i.e., the experimental evidence discussed in this review suggests that larger SO_2 yields and thus higher H_2SO_4 formation are more probable in the NO_3 + DMS oxidation which proceeds via an H-atom-abstraction mechanism than in the OH + DMS oxidation which proceeds via a complex addition and abstraction mechanism.

Of the halogen species reaction with BrO will also be of importance. The importance of this oxidation pathway for DMS may be more important than has been previously thought since measurements of BrO indicate that levels of BrO of around 2 ppt may be ubiquitous throughout the troposphere.[270] The atmospheric chemistry of the reaction of BrO with DMS is reasonably well established, and its importance has been highlighted in recent model studies.[188,189] It would appear that a recently reported high rate coefficient for the reaction of IO + DMS,[186] which would have made this reaction important in the marine boundary layer, is flawed[171] and that the earlier slower values are to be preferred. The reactions of I and IO with DMS, therefore, have no atmospheric importance. Reactions of DMS with Cl will only be important in regions where elevated Cl atom concentrations occur, and reactions with ClO will be of negligible importance since sufficiently high ClO radicals have only been observed in the Arctic boundary layer[270] where the DMS concentrations are very low anyway.

3. Chemistry of Dimethyl Sulfoxide

Dimethyl sulfoxide (DMSO) is considered to be an important intermediate in the atmospheric oxidation of DMS. Despite its importance as a DMS oxidation product, the chemical behavior of DMSO in the atmosphere has received relatively little attention. It has been observed in laboratory chamber studies of the OH-radical-initiated oxidation of DMS[80−84,86] and in the marine boundary layer.[190−192,231] The reported DMSO yields from the various chamber studies are very variable.

As discussed in section 2.1.3, the production of DMSO in the OH-radical-initiated photooxidation of DMS is thought

Table 16. Product and Kinetic Data for the Reaction of OH Radicals with Dimethyl Sulfoxide

reaction	k (298 K) (cm^3 $molecule^{-1}$ s^{-1})	comments	literature
$CH_3SOCH_3 + OH \rightarrow$ products	$(6.5 \pm 2.5) \times 10^{-11}$	competitive kinetic study using $CH_3ONO/NO/N_2/O_2$ or NO_x/hydrocarbon/N_2/O_2 as OH radical sources at $T = 298$ K and $P = 760$ Torr; high yield of SO_2 observed and lesser yields of $DMSO_2$	Barnes et al.[193]
	$(1.0 \pm 0.3) \times 10^{-10}$	PLP-PLIF study $H_2O_2/DMSO/N_2$ or O_2 mixtures, rate independent of buffer gas and $P = 25-700$ Torr and also isotopic identity of the H atoms in DMSO, i.e., H or D; Arrhenius expression derived from four data points: $k = 10^{-11.2\pm0.7} \exp(800 \pm 540/T)$ cm^3 $molecule^{-1}$ s^{-1}.	Hynes and Wine[194]
	$(8.7 \pm 1.6) \times 10^{-11}$	LFP-TDLAS study of $H_2O_2/DMSO/N_2/CH_4$ gas mixtures at 298 K; $\Phi(CH_3) = (0.98 \pm 0.12)$	Urbanski et al.[85]
	$(5.9 \pm 1.5) \times 10^{-11}$	competitive kinetic study using $CH_3ONO/NO/N_2/O_2$ as the OH radical source; $T = 295 \pm 2$ K and $P = 740 \pm 5$ Torr; $\Phi(SO_2) = (20 \pm 15)$ and $\Phi(DMSO_2) = (22 \pm 10)$	Falbe-Hansen et al.[196]
	$(8 \pm 2) \times 10^{-11}$	HPTR-CIMS study at 300 K at $P = 100-500$ Torr	Kukui et al.[197]

to involve addition of the OH radical to the sulfur atom of DMS to form an adduct which can either decompose back to reactants or react with molecular oxygen to form DMSO and other products. Turnipseed et al.[100] and Hynes et al.[43] in pulsed laser photolysis/pulsed laser-induced fluorescence studies on the reaction of OH + DMS reported branching ratios of $\Phi = 0.5 \pm 0.15$ and ~0.5, respectively, for HO_2 production from the DMS−OH + O_2 reaction. They assumed that HO_2 was formed via H-atom abstraction from the hydroxyl group of the DMS−OH adduct and that the coproduct was DMSO. In contrast, Arsene et al.[83] measured a near unit molar formation yield for DMSO in a smog chamber study under NO_x-free conditions. In a later study Arsene et al.[84] showed that the DMSO yield is sensitive to the NO concentration and in the presence of NO obtained yields similar to those of Turnipseed et al. and Hynes et al. Although the absolute yield of DMSO under atmospheric conditions is still uncertain, all of the studies confirm that its yield will be quite substantial.

3.1. Reaction with the OH Radical

3.1.1. Kinetics of the OH-Radical Reaction

Kinetic data on the reaction of OH radicals with dimethyl sulfoxide are tabulated in Table 16.[85,193−196] As can be seen there is substantial variability in the reported rate coefficient which stems mainly from experimental difficulties in handling this sticky compound. The last reported value by Kukui et al.[197] is in agreement with the two direct measurements[85,194] within the experimental error limits, while the values from the relative kinetic measurements give somewhat lower values. The rate constant for the reaction of OH with DMSO at room temperature and atmospheric pressure is approximately 15 times faster than that for OH with DMS. Since the reaction of DMSO with the OH radical is fast, this removal process is very likely an important atmospheric sink for this compound. However, as discussed in section 5.3, physical removal of DMSO involving uptake by aerosol and cloud droplets and heterogeneous reactions[64,66,190,191,198] may be even more significant and could dominate the fate of DMSO.

3.1.2. Products and Mechanism of the OH + DMSO Reaction

The products of the OH-radical-initiated oxidation of DMSO in the atmosphere are poorly characterized. Products observed in smog chamber studies include sulfur dioxide (SO_2), dimethyl sulfone ($DMSO_2$), methanesulfonylperoxynitrate (MSPN, $CH_3S(O)_2OONO_2$), methanesulfonic acid (MSA, $CH_3S(O)_2OH$), and methanesulfinic acid (MSIA, $CH_3S(O)OH$).[80,199] However, the values of the product yields reported in the various studies differ significantly. Production of significant amounts of SO_2 and lesser amounts of $DMSO_2$ were observed by Barnes et al.[199] in a long-path FT-IR study. In 1996 Sørensen et al.[80] found production of SO_2 and $DMSO_2$ in roughly equal amounts, and they reported a MSIA formation yield of ≤0.3%. There are four exothermic product channels in the reaction of OH with DMSO[200]

$$CH_3S(O)CH_3 + OH \rightarrow (CH_3)_2S(O)\text{-}OH \qquad \Delta H^\circ_{298} = -12.13 \text{ kcal mol}^{-1}$$

$$\rightarrow CH_3S(O)OH + CH_3 \qquad \Delta H^\circ_{298} = -15.79 \text{ kcal mol}^{-1}$$

$$\rightarrow CH_3S(O)CH_2 + H_2O \qquad \Delta H^\circ_{298} = -15.22 \text{ kcal mol}^{-1}$$

$$\rightarrow CH_3SO + CH_3OH \qquad \Delta H^\circ_{298} = -130.17 \text{ kcal mol}^{-1}$$

Urbanski et al.[85] investigated the mechanism and kinetics of the OH + DMSO reaction at 298 K using the 248 nm laser flash photolysis of H_2O_2 in the presence of DMSO and time-resolved tunable diode laser spectroscopy for the detection of CH_3, CH_4, and SO_2. They obtained a yield for CH_3 of 0.98 ± 0.12 in the absence of O_2. From the observed unit yield of CH_3 and the near zero yields of CH_4 and SO_2 they concluded that the dominant OH + DMSO reaction channel was OH-radical addition to DMSO followed by very rapid DMSO−OH adduct decomposition to CH_3 and the associated coproduct MSIA. This implied a near unit yield of MSIA, which was in marked disagreement with the very low yield of MSIA observed in the chamber study of Sørensen et al.[80] However, subsequent chamber studies using cryogenic sample trapping and ion chromatography by Arsene et al. detected high yields of MSIA in the reaction of both OH with DMSO[201] and also OH with DMS.[83] Although the yield information of Arsene et al.[201] is only semiquantitative, the data support an MSIA yield between 80% and 99% in the OH + DMSO reaction which is in line with the results of Urbanski et al.[85] Arsene et al.[201] attribute the failure of Sørensen et al.[80] to detect MSIA in high yields to the sampling procedure employed.

Very recently MSIA has been detected directly by Kukuiet al.[197] using the HPTR-CIMS technique. The reactions of OH radicals with DMSO ($CH_3S(O)CH_3$) and MSIA ($CH_3S(O)$-OH) have been studied at 300 K in the pressure range 100−500 Torr using a turbulent flow reactor coupled to a detection system consisting of an ion molecule reactor and a mass spectrometer. The mechanisms of the reactions of OH with DMSO and MSIA have been derived directly from the kinetics of OH, DMSO, MSIA, SO_2, and CH_3 measured from the corresponding ion signal intensities of OH^-, $DMSO^+$, $CH_3S(O)OHF^-/CH_3S(O)OH^+$, $FSO_2^-/F_2SO_2^-$, and CH_3^+, respectively. The above positive and negative ions are formed in the ion molecule reactions with Xe^+ and SF_6^- primary ions, respectively. The charge-transfer reactions of DMSO and MSIA with Xe^+ and of MSIA with SF_6^- proceeding with formation of $DMSO^+$ and $CH_3S(O)OH^+$, respectively, have been observed for the first time in this study.

Kukuiet al.[197] report that the reaction of OH with DMSO forms predominantly MSIA, and a rate coefficient of $(1 \pm 0.2) \times 10^{-10}$ cm^3 molecule^{-1} s^{-1} was determined for OH + MSIA at room temperature. The work is the first determination for the OH + MSIA rate coefficient, and the product analysis showed that under the high OH radical concentration conditions of the experiments SO_2 was formed in unit yield. Kukui et al.[197] suggested a mechanism for the reaction of OH with MSIA involving either direct abstraction of an H atom and formation of excited CH_3SO_2* radicals or OH addition to S followed by H_2O elimination and formation of CH_3SO_2* radicals followed by prompt dissociation of CH_3-SO_2* leading to formation of CH_3 and SO_2

$$CH_3S(O)OH + OH \rightarrow (CH_3S(O)OH{-}OH) \rightarrow CH_3S(O)O^* + H_2O$$

$$CH_3S(O)O^* + M \rightarrow CH_3 + SO_2$$

Since the rate coefficient for the reaction of OH with MSIA is so fast addition to the S atom is the more likely the initial reaction channel. An alternative to the addition mechanism proposed by Kukuiet al.[197] would be rapid elimination from the MSIA−OH adduct of CH_3 to yield H_2SO_3, which is unstable in the gas phase and would rapidly decompose to SO_2 and H_2O. If the initial step is addition to the sulfur atom, reaction of the MSIA−OH adduct with O_2 could yield MSA if it could compete with decomposition reactions of the adduct under atmospheric conditions.

The study of Arsene et al.[201] shows that the formation of SO_2 and $DMSO_2$ in the OH + DMSO reaction is secondary in nature and provides further indirect support for MSIA as the primary product in OH + DMSO. The secondary formation of SO_2 is now supported by a product study on OH + DMSO[202] at the EUPHORE outdoor chamber in Spain. The yields of SO_2 and $DMSO_2$ reported in the study of Arsene et al.[201] are only of the order 5−10%, and under the low OH radical concentration conditions of the EUPHORE experiments the yield of SO_2 was only of the order of 20%. Due to the rapid further oxidation of MSIA by OH, which according to the study of Kukui et al.[197] results mainly in SO_2 formation, much larger yields of SO_2 would be expected. This would suggest that under the conditions of the photoreactor experiments and also probably in the atmosphere as other loss routes for MSIA must be occurring such as, for example, possibly reactions of an MSIA−OH adduct with O_2 to form MSA as discussed above. The aerosol yield in the EUPHORE experiments was extremely low, showing that aerosol formation or loss to particles cannot account for the observed behavior. More studies are needed on the atmospheric fate of MSIA.

Wang and Zhang[200] performed ab initio calculations on the gas-phase reaction of DMSO with OH radicals using the GAUSSIAN 98 program. They calculate that the product forming $CH_3S(O)OH + CH_3$ has an overall negative reaction activation energy and that the reaction could proceed by formation of an adduct $(CH_3)_2S(O)\cdot OH$ with subsequent decomposition to MSIA and CH_3. The negative activation energy is consistent with the slightly negative temperature dependence for the reaction observed experimentally by Hynes and Wine.[194] On the basis of their calculations Wang and Zhang postulate that the $CH_3S(O)OH + CH_3$ forming channel is the dominant reaction pathway for the OH + DMSO reaction. Two other product channels $CH_3S(O)CH_2 + H_2O$ and $CH_3SO + CH_3OH$ had energy barriers of 12.4 and 78.4 kJ mol^{-1} above OH + DMSO, respectively.

3.2. Reaction with the NO_3 Radical

3.2.1. Kinetics of the NO_3 + DMSO Reaction

The information in the literature on this reaction comes from the studies carried out by Falbe-Hansen et al.,[196] where a rate coefficient of $(5.0 \pm 3.8) \times 10^{-13}$ cm^3 molecule^{-1} s^{-1} was determined at 298 K and atmospheric pressure, and the study by Barnes et al.,[199] who obtained a value of $(1.7 \pm 0.3) \times 10^{-13}$ cm^3 molecule^{-1} s^{-1} at 500 Torr pressure and 298 K. Both studies were carried out in synthetic air and used the relative rate technique with FT-IR detection of reactants. Falbe-Hansen et al. used ethene as reference compound, while Barnes et al. used isobutene. Despite the relatively large difference between the two determinations, there is overlap within the large reported uncertainty intervals. The rate coefficient appears to be fast enough that the reaction is of potential importance under tropospheric conditions (see Table 15).

3.2.2. Products of the NO_3 + DMSO Reaction

Both Falbe Hansen et al.[196] and Barnes et al.[199] could only identify $DMSO_2$ as a product of this reaction; formation of SO_2 was not observed, thus suggesting that H abstraction is not important. Only Falbe-Hansen et al. reported yields for $DMSO_2$; however, these were found to be highly variable (10−94% molar). The variability could not be explained by wall losses of either DMSO or $DMSO_2$, and Falbe-Hansen et al. suggest that secondary chemistry or formation of a long-lived intermediate may be occurring.

3.3. Reactions with Halogen Atoms and Halogen Oxides

3.3.1. Kinetics of the Cl + DMSO Reaction

Kinetic studies on the reaction of Cl with DMSO are tabulated in Table 17.[196,199,202−205] The first relative rate studies on the reaction in 1 atm of synthetic air and 298 K were in good agreement, giving a rate coefficient of approximately 7.4×10^{-11} cm^3 molecule s^{-1} for the reaction. Two recent determinations at low pressure, both using the DF-MS technique, by Martínez et al.[203] and Riffault et al.[204] gave a value of around 2×10^{-11} cm^3 molecule^{-1} s^{-1} at 1 Torr total pressure of He and 298 K. A very recent relative rate investigation by Arsene et al.[205] found a very high value

Table 17. Literature Rate Coefficients for the Reaction of Cl Atoms with Dimethyl Sulfoxide (DMSO)

$10^{11} \times k$ (cm^3 $molecule^{-1}$ s^{-1})	T (K)	P (Torr)/bath gas	technique	ref
7.4 ± 1.0	295 ± 2	740 ± 5/air	RR [relative to k(n-ethane) = 5.7×10^{-11} and k(n-propane) = 1.4×10^{-10} cm^3 $molecule^{-1}$ s^{-1}][a]	Falbe-Hansen et al.[196]
7.4 ± 1.8	298	760/air	RR [relative to k(propene) = 24.4×10^{-11} cm^3 $molecule^{-1}$ s^{-1}][b]	Barnes et al.[199]
26.7 ± 2.7		760/air	RR[d]	Arsene et al.[205]
1.7 ± 0.3	273−335	0.5−3/He	DF-MS	Martínez et al.[203]
2.05 ± 0.40	298	1/He	DF-MS[e]	Riffault et al.[204]
<10	298	600/N_2	ARFS-LFP[f]	Wine et al.[206]

[a] DeMore et al. (1997). [b] Atkinson and Aschmann (1985). [c] Rate was found to be independent of pressure within the range investigated. [d] Different reference hydrocarbons and Cl atom sources used which gave consistent results; a positive activation energy was observed for the reaction (283−303 K). [e] A branching ration of 0.91 ± 0.15 was found for the channel producing HCl + CH_3SCH_2 and 0.10 ± 0.02 for the channel producing CH_3 + $CH_3S(O)Cl$. [f] Reaction studied as a function of temperature and pressure; detailed rate information was not available at the time of writing.

of 2.67×10^{-10} cm^3 $molecule^{-1}$ s^{-1} for the reaction in 1 atm of air at 298 K. A variety of different reference compounds and Cl-atom sources were used in these investigations. The reaction was investigated as a function of O_2 partial pressure (0−500 mbar) and over the temperature range 283−308 K. Arsene et al.[205] found good agreement between the various reference compounds employed (cyclohexane, n-butane, and propene). They observed only a very minor dependence on the O_2 partial pressure with a very slight increase in the rate coefficient with increasing O_2 partial pressure, which was within the experimental error limits. They measured a positive activation energy for the reaction with $k_{(Cl+DMSO)} = 3.9 \times 10^8 \exp(-1406/T)$ for 1 atm of synthetic air valid over 283−308 K. The lack of an O_2 effect on the rate coefficient and the positive activation energy contrast sharply with the Cl + DMS reaction where an O_2 effect is observed and overall negative activation energy is observed for atmospheric conditions.

At the time of writing information on a detailed kinetic and mechanistic study of the Cl + DMSO reaction by Wine et al.[206] was obtained. Using time-resolved atomic resonance fluorescence spectroscopy coupled with laser flash photolysis of $Cl_2CO/DMSO/N_2$ mixtures they studied the kinetics of the reaction over a wide range of temperatures and pressures and observed pressure-dependent and pressure-independent channels for the reaction. At T < 300 K both channels are operative, whereas at T > 400 K only the pressure-independent pathway was observed, and the rate coefficients are considerably slower than those measured at T < 300 K. At T = 298 K and P = 600 Torr the overall rate coefficient was $\sim 1 \times 10^{-10}$ cm^3 $molecule^{-1}$ s^{-1} with a pressure-dependent adduct-forming channel accounting for 85−95% of the observed reactivity. The result resolves the differences observed in the previous determined rates at low and high pressure and validates the high value of the rate determined by Arsene et al.[205] There is, however, a need for further kinetic investigations to determine more precisely the rate coefficient under atmospheric conditions.

Wine et al.[206] were able to study the equilibrium between the Cl−DMSO adduct and the reactants and from a "third-law analysis" of the results derived a value of 73 ± 10 kJ mol^{-1} at 298 K for the bond-dissociation energy of Cl−DMSO which is less than that for the Cl−DMS adduct. Rate coefficients for the reaction of the Cl−DMSO adduct with O_2, NO, and NO_2 at 298 K of $<1 \times 10^{-18}$, 1.6×10^{-11}, and 2.0×10^{-11} cm^3 $molecule^{-1}$ s^{-1}, respectively, are also reported. These rate coefficients are very similar to those measured for the same reactions with the Cl−DMS adduct.[165]

3.3.2. Products of the Cl + DMSO Reaction

At low pressure Riffault et al.[204] observed in their DF-MS study CH_3 and HCl as primary products

$$CH_3S(O)CH_3 + Cl \rightarrow HCl + \text{products}$$
$$\rightarrow CH_3 + \text{products}$$

From measurements of the product concentrations as a function of the consumed concentration of Cl atoms they report branching ratios of 0.91 ± 0.09 for the HCl producing channel and 0.10 ± 0.02 for the CH_3 producing channel. The observation of HCl would imply formation of $CH_3S(O)CH_2$ as the coproduct via an abstraction reaction channel.

In the chamber study of Arsene et al.,[205] dimethyl sulfone ($DMSO_2$) and SO_2 have been observed as products of the Cl + DMSO reaction. At room temperature and 1 atm of synthetic air a constant molar yield of approximately 12% was observed for $DMSO_2$, whereas the molar yield of SO_2 was observed to increase with increasing reaction time. Product yields have also been reported in two other chamber studies by Falbe-Hansen et al.[196] and Barnes et al.[199] under similar conditions. Falbe-Hansen et al.[196] reported molar yields of (8 ± 2)% and (28 ± 12)% for $DMSO_2$ and SO_2, respectively. Barnes et al.[199] reported molar yields of 14% and 42% for $DMSO_2$ and SO_2, respectively. Neither of these studies reported the time behavior of the yields. The molar yields of $DMSO_2$ are very similar for all three chambers, and the variation of the SO_2 yield with time observed by Arsene et al.[205] would explain the differences in the reported SO_2 yields.

3.3.3. Kinetics of the ClO + DMSO Reaction

The reaction has been studied by the discharge flow-mass spectrometry method at 1 Torr total pressure of helium by Martinez et al.[203] and Riffault et al.;[204] only upper limits of $k_{ClO+DMSO} < 6 \times 10^{-14}$ and 1.6×10^{-14} cm^3 $molecule^{-1}$ s^{-1}, respectively, could be established.

3.3.4. Products of the ClO + DMSO Reaction

To the best of our knowledge, no information is available in the literature on the products of this reaction.

3.3.5. Kinetics of the Br + DMSO Reaction

Two kinetic studies of this reaction have been reported in the literature: the FTIR study by Ballesteros et al.[178] and the DF-MS study by Riffault et al.[204] (Table 18). The results of Ballesteros et al.[178] indicated a value of $k_{DMSO+Br}$ in the range $(1-5) \times 10^{-14}$ cm^3 $molecule^{-1}$ s^{-1}; however, due to

Table 18. Literature Rate Coefficients at Room Temperature for the Reactions of Br and BrO with Dimethyl Sulfoxide

k(Br + DMSO) cm^3 molecule^{-1} s^{-1})	T (K)	P (Torr)/bath gas	comments	literature
$<6 \times 10^{-14}$	296 ± 3	740/air	RR, relative to ethene, $k_{Br + ethene} = (1.4 \pm 0.2) \times 10^{-13}$ cm^3 molecule^{-1} s^{-1} [a]	Ballesteros et al.[178]
$(1.2 \pm 0.3) \times 10^{-14}$	298	1/helium	DF-MS	Riffault et al.[204]
k(BrO + DMSO)	**T (K)**	**P (Torr)/bath gas**	**comments**	**literature**
$(1.0 \pm 0.3) \times 10^{-14}$	296 ± 3	740/air	RR, relative to DMDS and DMS-d_6 (see text)	Ballesteros et al.[178]
$<4 \times 10^{-14}$	298	1/helium	DF-MS	Riffault et al.[204]

[a] Average of values from Barnes et al.[268] and Yarwood et al.[269]

considerable scatter in the data, only an upper limit of the rate constant was reported. The value of $(1.2 \pm 0.3) \times 10^{-14}$ cm^3 molecule^{-1} s^{-1} determined by Riffault et al.[204] using DF-MS lies at the lower end of the rate coefficient spread reported by Ballesteros et al.[178]

The reaction of DMSO with Br thus appears to be approximately 3−4 orders of magnitude slower than its reaction with Cl; this is similar to what is observed for the corresponding reactions with DMS. The data are not sufficient to establish whether the reaction exhibits a pressure or O_2 dependence.

3.3.6. Products of the Br + DMSO Reaction

The only published study of the products of the reaction is by Ballesteros et al.[178] $DMSO_2$ was formed with a yield of about 4%. Methanesulfonyl bromide, CH_3SO_2Br, was identified as a product based on its characteristic IR absorption bands but could not be quantified. Experiments where Br was reacted with $DMSO_2$ showed that methanesulfonyl bromide does not come from the further degradation of $DMSO_2$; Ballesteros et al. propose a formation reaction initiated by the addition of Br to DMSO.

3.3.7. Kinetics of the BrO + DMSO Reaction

The only kinetic information reported in the literature regarding this reaction is the chamber relative rate study by Ballesteros et al.[178] using FTIR and the low-pressure DF-MS study by Riffault et al.[204] (Table 18). Ballesteros et al. used DMDS and deuterated DMS as reference compounds after $k_{DMDS+Br}$ and k_{DMS-d6} had been determined using DMS as reference compound, assuming $k_{DMS+Br} = 3.2 \times 10^{-13}$ cm^3 molecule^{-1} s^{-1}. The upper limit of Riffault et al. is in agreement with the rate coefficient determined by Ballesteros et al.

3.3.8. Products of the BrO + DMSO Reaction

Ballesteros et al.[178] found a close to unity yield of $DMSO_2$, which suggests a reaction mechanism similar to that for the reaction between DMS and BrO.

3.4. Short Summary

The atmospheric lifetimes of DMSO due to gas-phase reaction with the oxidant species discussed in this review have been calculated for different atmosphere regions and are given in Table 15. It is evident from the table that the main gas-phase fate of DMSO will be oxidation with OH radicals. As discussed in the next section, uptake and oxidation of DMSO to the aqueous phase/particles may be an important competing pathway. Laboratory studies have now firmly established MSIA as an important DMS secondary oxidation product via the further OH-radical oxidation of DMSO. The question as to whether the gas-phase OH-radical-initiated oxidation of DMSO in the atmosphere produces MSIA or $DMSO_2$ is important since MSIA can readily oxidize to MSA whereas $DMSO_2$ oxidation is not expected to produce MSA. $DMSO_2$ has often been assumed to be the main product in atmospheric models. The new studies show quite convincingly that MSIA is the dominant product, probably with near unit yield. There are several possible fates for MSIA in the atmosphere. MSIA is a low volatility acidic compound and can be readily taken up by existing aerosols and droplets where it is now known that it will be quickly oxidized to MSA (see section 4.3). On the other hand, the gas-phase reaction of OH radicals with MSIA has been predicted to be rapid,[88] and this has now been confirmed experimentally.[197] The experiments indicate that SO_2, a precursor of cloud condensation nuclei (CCN), is the major product. Therefore, the atmospheric fate of MSIA may well be a balance between the relative competitiveness between uptake and gas-phase oxidation by OH. Since in the marine atmosphere where DMS occurs the OH levels are generally low, uptake will probably often dominate. The fate of MSIA from the gas-phase oxidation of DMSO will influence the atmospheric methanesulfonate (MS^-)/nss-SO_4^{2-} ratio and may partly explain the large variation observed in this ratio in field experiments (see section 4). Obviously only further investigations on the chemistry of MSIA will be able to unambiguously establish its major atmospheric fate.

While the reaction of OH with DMSO is about 10 times faster than its reaction with DMS, the available experimental data all suggest that reactions of halogens and halogen oxides with DMSO are slower than the corresponding reactions with DMS. Thus, halogen and halogen oxide reactions with DMSO will be even less important under atmospheric conditions than in the case of DMS (see lifetimes in Table 15). The rate coefficient for the reaction of Cl with DMSO is, however, still very uncertain.

The main channel of the reaction of Cl atoms with DMSO at room temperature has been found to be formation of an adduct. Little is known about the reaction of Br with DMSO, but the observed products suggest that also in this case the halogen atom adds to DMSO at room temperature. The further reactions of the Cl−DMSO adduct in air have not yet been elucidated; the observed formation of $DMSO_2$ may possibly be explained by a reaction with O_2, while the pathways leading to formation of SO_2 need to be clarified. To our knowledge there is no information available on the reaction of I atoms with DMSO.

Very little is known about the reactions of halogen oxides with DMSO; they all appear to be too slow to be of atmospheric relevance (Table 15). The only available product study on the reaction of BrO with DMS showed a close to

unit yield of $DMSO_2$ in air at atmospheric pressure and room temperature.

4. Present State of Measurements in the Field and Their Interpretation

4.1. Multiphase Chemistry Involved in the Atmospheric Oxidation of DMS

To quantitatively understand the relation between gas-phase DMS and cloud condensation nuclei (CCN) and to test the important hypothesis that there is a feedback loop between DMS emissions and climate, detailed information must be acquired on the chemical transformation and reaction intermediates that link DMS to its final oxidation products. There is increasing evidence, from numerous field and modeling studies (see below), which strongly suggests that gas-phase reactions alone cannot fully explain the atmospheric DMS oxidation rate and the measured distribution of its oxidation products. To correctly represent the atmospheric chemistry of DMS, multiphase chemistry needs be considered both for DMS oxidation products as well as for DMS itself. As remarked by Ravishankara,[206] a differentiation should be made between "heterogeneous chemistry", which involves reactions of species coming from the gas phase onto a surface, and "multiphase chemistry", which involves reactions occurring in a liquid. Because diffusion in solids is slower than in liquids, to a first approximation the reactions involving solids are confined to the surface, whereas in a multiphase reaction a gas-phase reactant is likely to enter a liquid and then react with one or more constituents.

It is attempted to summarize here what is known about the aqueous-phase chemistry of the compounds involved in the atmospheric oxidation of DMS. The summary will contain three parts. The first part will present evidence for multiphase reactions from field observations. The second part will summarize the actual knowledge on multiphase reactions of DMS and its oxidation products. As seen in the section of the review dealing with gas-phase reactions, DMS can react in this phase with OH, NO_3, halogen, and halogen oxide radicals, giving SO_2, DMSO, $DMSO_2$, MSIA, and MSA. This section of the review will be limited to the multiphase reactions of DMS, DMSO, $DMSO_2$, MSIA, and MSA since extensive literature already exists for the aqueous-phase reactions of SO_2 (see, for instance, Finlayson-Pitts and Pitts[154] and Seinfeld and Pandis[207] and references therein). Finally, the third part will deal with the atmospheric implications of the multiphase reactions in the fate of DMS and its oxidation products.

4.2. Evidence from Field and Modeling Studies on the Role of Multiphase Reactions in the DMS Cycle

Since the publication of the CLAW hypothesis several field campaigns have been conducted which were aimed at elucidating the fate of DMS and its oxidation products in the atmosphere. From these campaigns convincing evidence has emerged which supports that multiphase reactions can play an important role in the atmospheric DMS cycle.

(1) For instance, recent modeling of field campaign data, in which only gas-phase DMS oxidation pathways by OH radicals are considered, overestimates measured levels of DMS and its oxidation products in the marine boundary layer (see, for instance, Chin et al.,[95] Yvon et al.,[209] Sciare et al.,[210] James et al.[211]). Consideration of halogen-atom- and halogen-oxide-initiated DMS oxidation could resolve the difference between modeling and measurements, especially since observations of sea salt debromination and large diurnal cycles for O_3 in the marine atmosphere offer evidence that significant Br radical chemistry could take place in such environments (see, for example, Vogt et al.,[212] Ayers et al.,[213] Dickerson et al.,[214] von Glasow et al.,[215] von Glasow and Crutzen[216]). Sciare et al.[210] pointed out that BrO at concentrations of the order of 2−3 pmol mol^{-1} in the MBL can reproduce the amplitude of the observed DMS diurnal variation. Satellite observations have shown the presence of BrO in the troposphere with global background vertical columns of about $(1-3) \times 10^{13}$ molecule cm^{-2} corresponding to BrO mixing ratios of 0.5−2 pmol mol^{-1} if uniformly mixed in the troposphere.[217,218] Comparisons with balloon- and ground-based measurements in the mid- and high-northern latitudes (between 42 and 68°N) indicate that tropospheric BrO is mainly located within the free troposphere.[219] Model studies reported that the 24 h average mixing ratio of BrO in the MBL is only 0.1−0.3 pmol mol^{-1},[215] which indicates that halogen oxide alone cannot fully resolve the model shortfalls. Another alternative, which has not so far been considered in most of the modeling studies, is the implication of multiphase reactions for DMS.

(2) In field studies in which simultaneous measurements of gaseous and particulate MSA have been performed it has been concluded that the observed gaseous MSA concentrations can only explain a minor part (less than 10%) of the observed particulate MSA levels.[64,66] It is worthwhile noting that these campaigns were performed under completely different conditions (Antarctic and equatorial Pacific). Davis et al.[64,66] and Bardouki et al.[220] suggested that multiphase reactions of DMSO on particles could account for the majority of the observed MS^- levels in the aerosol phase. Sciare et al.[221] and Legrand et al.,[222] who performed simultaneous measurements of DMS and DMSO at Amsterdam Island (sub-tropical Indian Ocean) and Antarctica, found that model studies considering only gas-phase chemistry significantly underestimate the observed DMSO levels. A good agreement between model and observation was obtained only by assuming a heterogeneous loss rate of DMSO proportional to the OH radical concentration. Under these conditions the heterogeneous loss of DMSO was estimated to be of at least the same order of importance as the DMSO + OH gas-phase oxidation. Finally, Legrand et al.[222] from simultaneous measurements of DMSO and MSA concluded that the multiphase oxidation of DMSO on aerosols could account for the observed MS^- levels in the aerosol phase.

(3) Several authors have reported that the MS^-/nss-SO_4^{2-} ratio varies both seasonally and latitudinally with higher values at higher latitudes and during summer (see, for instance, Saltzman et al.,[223] Savoie and Prospero,[224] Bates et al.,[225] Legrand and Pasteur[226]). From aerosol data collected during an oceanographic cruise from high to low latitudes under pure clean marine conditions Bates et al.[225] proposed an empirical equation relating the MS^-/nss-SO_4^{2-} ratio inversely with temperature. In recent years several authors have tried to model and understand the temperature dependences of the DMS oxidation mechanism and especially the variation of MSA/nss-SO_4^{2-} ratio as a function of temperature (see, for instance, Barone et al.[8] and Ayers et al.[227]). This is because the ratio of MSA/nss-SO_4 has often been used to estimate the contribution of DMS to the sulfur budget

from measurements of MSA and nss-SO_4 at a given temperature. Campolongo et al.[228] performed simulations of the MSA/nss-SO_4 ratio at several altitudes in which they switched the multiphase chemistry on and off. The model outcomes have been compared with the observational data reported by Bates et al.[225] When only the homogeneous chemistry was considered in the model the MSA/nss-SO_4 ratios were an order of magnitude lower compared to the observational data due to underestimation of MSA formation. The agreement between model predictions and observational data was significantly improved by the addition of multiphase chemistry.

The above results highlight the very important role of multiphase atmospheric chemistry, not only for SO_2 but also for the other oxidation products of DMS and, possibly, DMS itself. Therefore, the following section reviews the physicochemical properties of DMS, DMSO, $DMSO_2$, MSIA, and MSA relevant to multiphase reactions (Henry's law and mass accommodation coefficients) and the kinetics of their aqueous-phase reactions.

4.3. Aqueous Phase Reactions of DMS, DMSO, $DMSO_2$, MSIA, and MSA

4.3.1. Henry's Law and Mass Accommodation Coefficients

DMS is not very soluble in water. Several authors have studied the variation of the Henry's law coefficient as a function of temperature.[229] At 298 K the Henry's law coefficient for DMS was found to be about 0.48 M atm^{-1} and increases to 1.5 M atm^{-1} at 273 K. On the other hand, DMSO, $DMSO_2$, MSIA, and MSA are very soluble in water. Watts and Brimblecombe[230] reported a lower limit of 5×10^4 M atm^{-1} for the Henry's law coefficient of DMSO, and Lee and Zhu[231] reported a lower limit of 10^6 M atm^{-1}. Campolongo et al.[228] used for DMSO and $DMSO_2$ a Henry's law coefficient equal to 10^7 M atm^{-1} with an uncertainty of 50%. From field studies where DMSO was measured both in the gas and particulate phases[222] an effective Henry's law coefficient in the range of 10^7 M atm^{-1} was estimated. In this review a Henry's law coefficient of 10^7 M atm^{-1}, as suggested by Campolongo et al.,[228] has been adopted for use in calculations on both DMSO and $DMSO_2$.

Clegg and Brimblecombe[232] estimated a lower limit of 2×10^7 M atm^{-1} for the Henry's law coefficient of MSA. Campolongo et al.[228] used a value of 10^9 M atm^{-1} with an uncertainty of 50%. The value adopted by Campolongo et al. is smaller than that of HNO_3 (effective H for HNO_3 = $10^{10}-10^{12}$ M atm^{-1} depending on the pH; Sander[233] and Jacob[234]). Note, however, that MSA is a stronger acid than HNO_3 (K_a of MSA = 47 M, i.e., is 3 times higher compared to K_a = 22 for HNO_3; Clegg and Brimblecombe[232]). From field experiments where MSA was measured both in the gas and particulate phases[64−66] the partition of MSA between the aqueous and particulate phases ($C_{aqueous}/C_{total}$) was found to be higher than 0.95, a value which is comparable to the HNO_3 partition reported for the marine atmosphere. In this review, therefore, a Henry's law coefficient for MSA of 10^9 M atm^{-1} reported by Campolongo et al.[228] will be used in calculations on MSA; it should be kept in mind that this estimation could be a lower limit.

For MSIA no estimation of the Henry's law coefficient exists. MSIA is a much weaker acid than MSA ($K_a = 2.2 \times 10^{-2}$). The Henry's law coefficient for MSIA is expected to be higher than that of DMSO and lower than that of MSA. In this review a Henry's law coefficient of 10^8 M atm^{-1} has been adopted for MSIA.

De Bruyn et al.[198] estimated mass accommodation coefficients (α) for DMSO, $DMSO_2$, and MSA. The mass accommodation coefficient represents the probability that a given molecule impacting the surface will be absorbed in the bulk aqueous phase (Nathason et al.[235]). For DMSO, $DMSO_2$, and MSA, α at 273K are in the range from 0.1 for DMSO to 0.14 for MSA and increase with decreasing temperature (Kolb et al.[236]). For such highly soluble gases it is expected that their uptake by clouds droplets ($d \approx 10\ \mu$m) will tend to be diffusion limited ($\sim dD_g^{-1}A^{-1}$, where D_g and A are the gas-phase molecular diffusion coefficient and aerosol surface, respectively). Under these conditions the time constant is of the order of seconds and shows little dependence on α. On the other hand, in the case of noncloud aerosol ($d \approx 0.1\ \mu$m) the uptake tends to be limited by the free molecular collision rate ($\sim u\ \alpha\ An/4$, where u is the mean molecular speed and n is the bulk gas-phase concentration far from the gas-particle interface). Under these conditions the time constant varies inversely with α and is of the order of few minutes in the lower troposphere (Jacob;[234] Dentener and Crutzen[237]).

4.3.2. Overview of the Aqueous-Phase Reactions of DMS, DMSO, $DMSO_2$, MSIA, and MSA

Table 19 lists the most important reactions of DMS, DMSO, $DMSO_2$, MSIA, and MSA reported for the aqueous phase.

4.3.2.1. DMS. DMS reacts very rapidly with OH radicals in the aqueous phase via a complex reaction mechanism forming mainly DMSO.[238] Bonifacic et al.[238] reported a diffusion-limited second-order rate constant of 1.9×10^{10} $M^{-1}\ s^{-1}$ for the reaction which proceeds via the following reaction sequence

$$(CH_3)_2S + OH \rightarrow (CH_3)_2S{\cdot}OH$$

$$(CH_3)_2S{\cdot}OH \rightarrow CH_3SCH_2^{\bullet} + H_2O$$

$$CH_3SCH_2^{\bullet} \rightarrow \text{(deprotonation)}\ CH_3SCH_2^{+}$$

$$CH_3SCH_2^{+} + H_2O \rightarrow (CH_3)_2SO + H^+$$

A very rapid reaction between DMS and O_3 in the aqueous phase with rate coefficients of 6.1 and 8.6×10^8 $M^{-1}\ s^{-1}$ (more than 10^6 times faster than in the gas phase) has been reported by Lee and Zhu[231] and Gershenzon et al.,[239] respectively. Contrary to the gas phase, the aqueous-phase reaction leads to DMSO formation with 100% yield. As suggested by Gershenzon et al.,[239] DMSO formation occurs because there is no C−S bond scission and the reaction proceeds via a polar adduct $(CH_3)_2S^{d+}OOO^{d-}$. A polar solvent will stabilize the adduct and facilitate its conversion to DMSO.

DMS is also oxidized by H_2O_2 to DMSO via a first-order reaction with respect to both DMS and H_2O_2 which is subject to catalysis by strong acids.[273] The rate coefficient is fairly constant (3.4×10^{-2} $M^{-1}\ s^{-1}$) between pH values of 2 and 6 and increases by almost a factor of 2.5 (8.1×10^{-2} $M^{-1}\ s^{-1}$) at pH 1 and below. In addition, it decreases substantially at pH 7 (1.4×10^{-2} $M^{-1}\ s^{-1}$). Various hydroperoxides such as peroxo formic acid (HCO_3H), peroxo acetic acid (CH_3CO_3H), peroxo monosulfuric acid anion (PMS; HSO_5^-), etc.,

Table 19. Summary of the Aqueous Phase Reactions of DMS, DMSO, $DMSO_2$, MSIA, and MSA

reaction	products	k ($M^{-1}s^{-1}$) at 295 ± 2 K	ref
OH + DMS	DMSO, MS^-	1.9×10^{10}	Bonifacic et al.[238]
O_3 + DMS	DMSO	$6.1-8.6 \times 10^8$	Lee and Zhou,[231] Gershenzon et al.[239]
H_2O_2 + DMS	DMSO	$1.4-8.1 \times 10^{-2}$[a]	Adewuyi and Garmichael[272]
ROOH + DMS	DMSO	310−4780[b]	Amels et al.[246]
OH + DMSO	MSI^-	$(6 \pm 1) \times 10^9$	Milne et al.,[248] Bardouki et al.,[247] Zhu et al.[249]
Cl + DMSO		6.3×10^9	Zhu et al.[254]
Cl_2^- + DMSO		1.6×10^7	Zhu et al.[254]
SO_4^-+ DMSO		2.8×10^9	Zhu et al.[255]
H_2O_2 + DMSO	$DMSO_2$	$0.5-4.5 \times 10^{-5}$	Amels et al.,[246] Bardouki et al.[247]
ROOH + DMSO	$DMSO_2$	$2.7-3.4 \times 10^{-3}$[b]	Amels et al.[246]
OH + $DMSO_2$	MS^-	3.0×10^7	Milne et al.[248]
		$<1.7 \times 10^7$	Zhu et al.[249]
Cl + $DMSO_2$		8.2×10^5	Zhu et al.[254]
Cl_2^- + $DMSO_2$		8.2×10^3	Zhu et al.[254]
SO_4^-+ $DMSO_2$		$<3.9 \times 10^6$	Zhu et al.[255]
OH + MSI^-	MS^-	1.2×10^{10}	Bardouki et al.[247]
Cl_2^- + MSI^-		8.2×10^8	Zhu et al.[254]
H_2O_2 + MSI^-	MS^-	1.2×10^{-2}	Bardouki et al.[247]
OH + MS^-	SO_4^{2-}	5.6×10^7	Milne et al.[248]
		1.3×10^7	Olson and Fessenden[250]
		1.2×10^7	Zhu et al.[249]
Cl + MS^-		4.9×10^5	Zhu et al.[254]
Cl_2^- + MS^-		3.9×10^3	Zhu et al.[254]
SO_4^-+ MS^-		1.1×10^4	Zhu et al.[255]
H_2O_2 + MS^-		$<1 \times 10^{-5}$	Bardouki et al.[247]

[a] pH dependent, see text. [b] Depends on the peroxides, see text.

will also react with DMS similarly to H_2O_2 with pH-dependent rates.[246] For example, in the case of HCO_3H, the rate constant will range from 62 M^{-1} s^{-1} for the peroxo formic anionic form to 1950 M^{-1} s^{-1} for the acidic form.

From a consideration of the rate constants of DMS with the various reactants in the liquid phase reported in Table 19 and their concentrations the relative contributions of the aqueous-phase reactions of DMS can be assessed. The H_2O_2 levels in rainwater are such that the rate of oxidation of DMS by H_2O_2 is too slow to compete with other multiphase pathways, namely, reactions with OH and O_3 (Table 19). It is unlikely, for example, that the aqueous-phase oxidation of DMS by H_2O_2 can account for the presence of DMSO in rain observed by Andreae[240] and Sciare et al.[192] A clear conclusion for the reaction of DMS with other peroxides cannot be drawn mainly due to the absence of measurements of ROOH in the marine atmosphere. However, even for the fastest reaction of DMS with the PMS anion ($k = 4780$ M^{-1} s^{-1}) and considering PMS levels of the order of few μM as estimated by Jacob[241] and Kleiman[242] it seems unlikely that reactions of DMS with ROOH will have any significant atmospheric implications.

Brimblecombe et al.[243] and Brimblecombe and Shooter[244] studied the fate of DMS in seawater. Although these reactions have little atmospheric interest, they could play a significant role in the cycling of DMS in seawater. These authors reported that DMS oxidation by H_2O_2 is first order with respect to DMS and catalyzed by sea-salt metals. In seawater (pH = 8) at 20 °C and with $H_2O_2 = 4 \times 10^{-5}$ M the first-order rate constant was found to be 5.7×10^{-6} s^{-1}. Brimblecombe and Shooter[244] also reported that aqueous DMS is photooxidized in the presence of photosensitizers or humic acid and rose Bengal, which occur naturally in seawater. With $[DMS]_0 = 6.8 \times 10^{-5}$ M in seawater samples containing natural photosensitizers they obtained a first-order rate constant of 2.4×10^{-5} s^{-1} for photooxygenation in sunlight. DMSO was the final product of the DMS photooxidation, which was found to be quite resistant to further photooxidation.

4.3.2.2. DMSO, $DMSO_2$, MSI^-, and MS^-. DMSO, $DMSO_2$, MS^-, and MSI^- are highly water soluble. Multiphase reactions are expected to play an important role in determining the fate of these compounds in the atmosphere. Table 19 lists our actual state-of-knowledge on the aqueous-phase reactions of these compounds.

(i) Reactions of DMSO, $DMSO_2$, MSI^-, and MS^- with H_2O_2 and Other Peroxides. DMSO, $DMSO_2$, MSI^-, and MS^- are very stable in pure water or in solutions containing H_2O_2 at various pH.[245] For the reaction of DMSO with H_2O_2, Amels et al.[246] obtained a rate coefficient of 2.7×10^{-6} M^{-1} s^{-1} at 298 K. For the same reaction Bardouki et al.[247] obtained rate coefficients ranging between 4.5×10^{-5} and 5×10^{-6} M^{-1} s^{-1}, with the higher value considered as an upper limit. Bardouki et al.[247] reported a rate coefficient of 1.2×10^{-2} M^{-1} s^{-1} at 303 K for the reaction of MSI^- with H_2O_2. Methanesulfonate MS^- has been identified as the exclusive oxidation product of the MSI^- + H_2O_2 reaction with a yield of almost unity. Finally, for the reaction of MS^- with H_2O_2 the same authors reported an upper limit of 4.5×10^{-5} M^{-1} s^{-1} for the rate constant.

(ii) Reactions of DMSO, $DMSO_2$, MSI^-, and MS^- with OH Radicals. Milne et al.[248] and Zhu et al.[249] reported rate coefficients for the reactions of DMSO, $DMSO_2$, and MS^- with OH radicals. Milne et al.[248] concluded that the reaction rates decrease in the order DMSO > MS^- > $DMSO_2$. Zhu et al.[249] reported only an upper limit for the reaction of $DMSO_2$ with the OH radical. Although there is very good agreement for the reaction rate of OH + DMSO between these two studies, Milne et al. reported reaction rates for the reactions of OH + MS^- and OH + $DMSO_2$ which are 4.7 and at least 1.8 times faster, respectively, compared to those reported by Zhu et al. (see Table 19). The low value for the reaction of OH with MS^- reported by Zhu et al.[249] is in excellent agreement with the value obtained in a pulse radiolysis experiment by Olson and Fessenden.[250] Zhu et al.[249] put the discrepancy between their work and that of Milne et al.[248] down to higher impurity levels in the samples used by Milne et al.

Bardouki et al.[247] studied the kinetics and product distribution of the reactions of OH radicals with DMSO and MSI^- in the aqueous phase and confirmed that DMSO reacts very fast ($k = 4.5 \times 10^9$ M^{-1} s^{-1}) with OH radicals. MSI^- was identified as the main intermediate product, while MS^- and sulfate were the final products due to the very fast further reaction of MSI^- with OH radicals ($k = 1.2 \times 10^{10}$ M^{-1} s^{-1}).

Bardouki et al.[247] proposed that oxidation of DMSO by OH radicals could proceed through the following pathway

$$(CH_3)_2SO + OH \rightarrow CH_3S(O)OH + CH_3$$

$$CH_3S(O)OH + OH \rightarrow CH_3S\cdot(O)(OH)_2\ (+ O_2) \rightarrow CH_3S(O)_2OH + {}^{\bullet}HO_2$$

$$CH_3S(O)_2OH + OH \rightarrow H_2SO_4 + {}^{\bullet}CH_3$$

DMSO, which has its S atom at the center of a pyramidal structure with a free electron pair to one corner, is easily accessible to electrophilic attack by the OH radical. In the mechanism the initially formed MSI^- ion reacts further with OH radicals to form MS^-. Bardouki et al.[247] measured the rate constant for the reaction of the $MSI^- + OH$ relative to benzoate ($k_{benzoate} = 5.9 \times 10^9$ $M^{-1}s^{-1}$; Ross et al.[251]) and determined a rate constant of $k = 1.2 \times 10^{10}$ M^{-1} s^{-1} for the reaction. This value is almost 2 times higher than the value of $(6.2 \pm 0.7) \times 10^9$ M^{-1} s^{-1} reported by Sehested and Holcman.[252] Presently, there is no explanation for this disagreement. MS^- was identified as the main oxidation product of the $MSI^- + OH$ reaction by Bardouki et al. with a stoichiometry of 1:1.

Both the $OH + DMSO_2$ and $OH + MS^-$ reactions are several hundred times slower than the OH + DMSO reaction.[245,248,252] Preliminary results by Bardouki[245] based on product distributions indicate that both reactions proceed via addition of an OH radical followed by elimination of the CH_3 radical (as in the case of DMSO). Bardouki[245] suggested that the reaction of $DMSO_2 + OH$ will lead to MS^- formation, which will further react with OH radicals, forming SO_4^{2-}. Since these results are only preliminary, additional studies on these two reactions are clearly needed.

(iii) Reaction of DMSO with O_3. Lee and Zhu[231] and Gershenzon et al.[239] studied the kinetics of the reaction of DMSO with O_3. The reported rate coefficients range between 4.3 and 5.7 M^{-1} s^{-1} (Table 19).

(iv) Reactions of DMSO, $DMSO_2$, MSI^-, and MS^- with Cl Atoms and Cl_2^-. Zhu et al.[254] applied a laser flash photolysis-long path UV−vis absorption technique to investigate the kinetics of the aqueous-phase reactions of Cl atoms and Cl_2^- radicals with DMSO, $DMSO_2$, MSI^-, and MS^- . The measured reaction rate coefficients, which are listed in Table 19, take the order DMSO > $DMSO_2$ > MS^- and MSI^- > DMSO > $DMSO_2$ >MS^- for the Cl atom and Cl_2^- radical reactions, respectively.

(v) Reactions of DMSO, $DMSO_2$, and MS^- with SO_4^- Radicals. Zhu et al.[255] applied a laser flash photolysis-long path UV−vis absorption technique to investigate the kinetics of the aqueous-phase reactions of SO_4^- radicals with DMSO, $DMSO_2$, and MS^- . The measured reaction rate coefficients, as listed in Table 19, take the approximate order DMSO > $DMSO_2$, MS^- since only an upper limit has been reported for $DMSO_2$.

4.4. Atmospheric Implications of the Aqueous-Phase Reactions of DMS, DMSO, MSIA, and MSA

Multiphase reactions can compete with the analogous gas-phase reactions when the species are highly soluble or the reaction rates are significantly enhanced in the aqueous medium. The reaction of DMS in aqueous medium with O_3 falls in the second category. DMSO and MSI^- are possible candidate species for multiphase reactions due to their high reactivity in the aqueous phase and high Henry's law coefficients. Finally, $DMSO_2$ and MS^-, although they have high Henry's law coefficients, are not as reactive as DMSO and MSI^-.

Following the approach presented by Gershenzon et al.,[239] under conditions of gas−liquid equilibrium when the gas- and aqueous-phase reaction rates for two species A and B are equal

$$(RT)^2 H_A H_B L[A][B]k_{aq} = [A][B]k_{gas} \qquad (1)$$

where [A] and [B] are the gas-phase concentrations of A and B in (mol L^{-1}), H_A and H_B are their Henry's law constants, k_{aq} and k_{gas} are the gas- and aqueous-phase reaction rate constants in M^{-1} s^{-1}, R is the gas constant, 0.082 L atm K^{-1} mol^{-1}, and L is the fractional liquid water content which ranges from 5×10^{-7} cm^3 cm^{-3} in tropospheric clouds to 3×10^{-11} cm^3 cm^{-3} in sea salt aerosols. At $T = 298$ K and for tropospheric clouds eq 1 is simplified to

$$H_A H_B (k_{aq}/k_{gas}) = 5300$$

Using this information in combination with the kinetic data for the gas and aqueous phase oxidation processes the following conclusions can be drawn on the fates of DMS, DMSO, and MSA.

(1) For DMS, k_{aq}/k_{gas} is 7.3 and $>10^6$ for the reactions with OH radicals and O_3, respectively. Using Henry's law coefficients at 298 K of 25, 0.48, and 1.1×10^{-2} M atm^{-1} for OH, DMS, and O_3, respectively, it can be seen that although the role of aqueous-phase reaction of DMS with OH will be minor (less than 3% of the total atmospheric DMS oxidation at 298 K and about 10% at 273 K), this is not the case for the reaction with O_3. With these Henry's law constants the oxidation rate of DMS by O_3 in clouds has at least the same importance as the gas-phase reaction at 298 K and is a factor of 6 higher at 273 K due to the negative temperature dependence of Henry's law constants. Note also that in-cloud DMS oxidation by O_3 occurs during the entire day, in contrast to the gas-phase oxidation of DMS by OH and NO_3 radicals, which occurs mainly during the day and night, respectively. In a recent modeling study Boucher et al.[256] and von Glasow and Crutzen[188] found that aqueous-phase oxidation of DMS by O_3 could contribute ≤6.2% to the total DMS oxidation, which is a factor of 2 higher than the contribution from the DMS gas-phase reaction with O_3. At high latitudes the combined aqueous- and gas-phase oxidation of DMS by O_3 can contribute up to 30−40% to the total atmospheric DMS loss.

(2) For the reactions with OH radicals, although ($k_{aq}/k_{gaseous}$) is 0.1 and 0.2 for DMSO and MSIA, respectively, the very high Henry's law constant for both species ($>10^6$ M atm^{-1}) implies that the oxidation rate of DMSO and MSIA by OH in clouds is at least 1000 times higher than in the gas phase. Note that even considering a fractional liquid

Table 20. Lifetimes of DMS, DMSO, MSIA, and MSA Due to Gas and Aqueous Oxidation Processes in the Atmosphere Reactant[a]

lifetime (h)	OH(g)	OH(aq)	O_3(g)	O_3(aq)	Cl(g)	Cl(aq)	Cl_2^-(aq)	SO_4^-(aq)
DMS	46	2400	>400	320	172			
DMSO	3−5	0.6	>170		730	3.5	14 (70)[a]	233 (0.7[a]
$DMSO_2$	>960	>200			$>2.3 \times 10^6$	$>2.7 \times 10^4$	$>2.7 \times 10^4$ (1.4×10^5)*	>570 (1.9×10^5)*
MSA/MS	slow	340	slow	slow	slow	4.5×10^4	5.7×10^4 (2.9×10^5)*	2.5×10^5 (8.3×10^7)*
MSIA/MS	3−5	0.5	slow	slow	fast		0.3 (1.5)*	1.2 (400)*

[a] Estimated global diurnally averaged gas-phase OH, O_3, and Cl concentrations have been derived from Krol et al.,[274] Logan et al.,[275] Pszenny et al.,[149] and Wingenter et al.[276] and are equal to OH = 10^6 cm^{-3},O_3 = 6.5×10^{11} cm^{-3}, and Cl = 5×10^3 cm^{-3}. Typical diurnally averaged OH(aq), Cl(aq), Cl_2^-(aq), and SO_4^-(aq) concentrations in marine boundary layer cloud droplets are derived from Herrmann et al.[277] and Lelieveld and Crutzen[278] and are equal to OH = 6×10^{-13} M, Cl = 1×10^{-13} M, Cl_2^- = 2×10^{-12} M, and SO_4^- = 3×10^{-15} M. For aqueous levels of O_3 an equilibrium with the gas phase and Henry's law coefficients at 298 K of O_3 = 1.1×10^{-2} M atm^{-1} were assumed (Logan et al.[275]). The asterisk (*) indicates lifetimes calculated using the levels of Cl_2^- and SO_4^- radicals reported by Zhu et al.[254] for the marine atmosphere.

water content of 3×10^{-11}, which is characteristic of sea salt aerosol (Sander[257]), the oxidation rate of DMSO and MSIA by OH in aerosols is of comparable importance with the gas-phase reaction. The same conclusion is valid for the reaction of DMSO with Cl atoms for which ($k_{aq}/k_{gaseous}$) is also 0.1.

(3) The higher oxidized species $DMSO_2$ and MS^- are not as reactive as DMSO and MSIA/MSI^- in either the gas or the aqueous phase; thus, uptake into condensed phases is the most efficient removal process from the gas phase.

The rate constant in time^{-1} for multiphase reactions is given by the following equation

$$k_A = k_{aq} p_B H_A H_B L R T \quad (2)$$

where A is the compound of interest, B is the reactant, and p_B is the partial pressure of the reactant in the atmosphere. This equation is valid only for compounds existing in equilibrium in both the gaseous and the aerosol phases.

Table 20 lists the estimated lifetimes of DMS, DMSO, $DMSO_2$, MSIA, and MSA with respect to (i) gas-phase reactions with OH, O_3, and Cl radicals and (ii) aqueous-phase reactions with OH, Cl, Cl_2^-, and SO_4^- radicals at 295 K. The aqueous-phase lifetimes were calculated from the rate coefficients given in Table 19 and reasonable estimates of the radical concentrations of interest. Note that (i) concentrations of radicals in the aqueous phase estimated from bulk chemistry considerations can dramatically underestimate the true concentrations because essentially small atmospheric droplets do not contain enough radicals for chain termination reactions to occur (Mozurkewich[258]) and (ii) the reported radical concentrations are subject to considerable variability depending on the time of the day, season, and location. Finally, since eq 2 introduces a high degree of uncertainty (the fractional liquid water content (L) varies up to a factor of 10^4 in the atmosphere), it has been assumed for the calculation of the lifetime in the condensed phase that aerosol particles spend only a fraction of their time (3 h/day) as aqueous droplets (Katoshevski et al.[259]).

The following conclusions can be drawn from the lifetimes of the various organic sulfur species reported in Table 20:

(i) In the aqueous phase, DMSO is oxidized mainly by OH radicals. However, contributions from Cl_2^- and SO_4^- radicals could be significant if the levels of Cl_2^- and SO_4^- radicals reported by Zhu et al.[254] are valid for the marine atmosphere. The lifetime of DMSO in the aqueous phase is estimated to be around 35 min, which is much faster than gas-phase oxidation; its uptake into the condensed phase is estimated to be of the order of a few hours. More precisely, the atmospheric lifetimes calculated using eq 2 for multiphase reactions of DMSO would vary from a few seconds due to reactions in tropospheric clouds (almost diffusion limited) to a few hours (free molecular collision rate limited) due to reactions in sea-salt aerosols. Since the DMSO oxidation products are less volatile than DMSO, aqueous-phase oxidation of DMSO can contribute to particle growth via droplet formation/evaporation cycling.

(ii) The lifetime of MSI^- in the aqueous phase is estimated to be much less than an hour, which is considerably faster than gas-phase oxidation and uptake into the condensed phase. On the basis of the present calculations the reaction of MSI^- with OH radicals would be the most important removal pathway in the aqueous phase since it accounts for elimination of 75% of MSI^- while the $MSI^- + Cl_2^-$ reaction removes the remaining 25%. However, if the levels of Cl_2^- reported by Zhu et al.[254] are valid for the marine atmosphere, reaction of MSI^- with Cl_2^- radicals would account for 55% of the MSI^- removal while the $MSI^- + OH$ reaction would contribute only 30%.

(iii) The data presented in Table 20 suggest that OH is the only important oxidant for $DMSO_2$ and MS^- in the aqueous phase, leading to a lifetime of 10 days, which is similar to that of marine aerosols (6 days). Therefore, a significant fraction of $DMSO_2$ and MS^- will be oxidized to more stable SO_4^{2-} particularly under free tropospheric conditions where particle lifetimes are longer than in the boundary layer. As first suggested by von Glasow and Crutzen,[216] the OH-radical-initiated oxidation of MS^- to SO_4^{2-} should be taken into account for a correct interpretation of field observations of the MS^- to SO_4^{2-} ratio in aerosols.

Consideration of multiphase chemistry can give insight into the reasons for the observed variations of the MS^-/nss-SO_4^{2-} ratio with temperature and latitude. As outlined in the section of the review dealing with gas-phase reactions, DMSO production is favored at low temperatures since DMSO is the main product of the addition channel of the DMS/OH reaction (Arsene et al.[84] and Hynes et al.[31]). Arsene et al.[83] and Kukui et al.[197] reported that the main product of the DMSO/OH-initiated oxidation is MSIA. Both MSIA and DMSO can participate in multiphase reactions, mainly with OH radicals, leading to formation MS^-. Thus, multiphase reactions are expected to increase the MS^-/nss-SO_4^{2-} ratio at lower temperatures, which is in agreement with field observations.

4.5. Recommendations for Modeling Studies

The previous sections have clearly highlighted the need for including multiphase chemistry in 3-dimensional models of atmospheric DMS chemistry. It is suggested that the following aqueous-phase reactions, with the rate coefficients

and product distributions reported in Table 19, should be incorporated into DMS atmospheric reaction schemes for a better description of the atmospheric fate of DMS

$$\mathrm{DMS} + \mathrm{O_3} \rightarrow \mathrm{DMSO} + \mathrm{O_2}$$

$$\mathrm{DMSO} + \mathrm{OH} \rightarrow \mathrm{MSIA} + {}^{\bullet}\mathrm{CH_3}$$

$$\mathrm{MSIA} + \mathrm{OH} \rightarrow \mathrm{MSA} + \mathrm{HO_2}$$

$$\mathrm{MSIA} + \mathrm{Cl_2}^{-} \rightarrow \text{Not known}$$

$$\mathrm{MSA} + \mathrm{OH} \rightarrow \mathrm{SO_4}^{2-} + {}^{\bullet}\mathrm{CH_3}$$

Detailed descriptions of aqueous-phase chemical mechanisms coupled with gas-phase chemistry and gas-droplet transfer are computationally expensive to integrate in 3-D models, and their usefulness may be limited by insufficient characterization of the condensed phase. Thus, in the case of DMSO and MSIA which are highly soluble and react very rapidly in the liquid,phase the following simple reaction probability parametrization to describe their uptake by aerosols and clouds can be used as recommended by Jacob[234]

$$k = (d/D_g + 4/u\gamma)^{-1}A$$

where k is the first-order rate constant for heterogeneous loss of a gas to the aerosols, d the aerosol diameter, D_g the gas-phase molecular diffusion coefficient, u the mean molecular speed, γ the reaction probability, and A the aerosol surface. The reaction probability γ is defined as the probability that a molecule impacting the aerosol surface undergoes reaction (Ravishankara[207]). For highly soluble and reactive species $\gamma = \alpha$ (Sander[257]), and thus, the accommodation coefficients calculated by De Bruyn et al.[198] can be used for MSA and DMSO. As a first approximation the γ of MSIA can be considered equal to that of MSA; however, it is clear that an independent determination for MSIA is needed.

Although a detailed description of the aqueous-phase reaction of DMS with O_3 is needed, a more simplistic first-step approach (similar to that used by Boucher et al.[256]) could be computation of the concentrations of DMS and O_3 in the cloud phase assuming a Henry's law equilibrium.

5. Acknowledgment

The authors are very grateful to A. Hynes and co-workers (University of Miami) for supplementary information and helpful discussions on various aspects of DMS chemistry and also to A. R. Ravishankara (NOAA, Boulder) for the initial impetus to write the review. The authors also acknowledge financial support from the European Commission within the 5th Framework Program and the German BMBF within AFO2000 which contributed substantially toward the production of some of the recent data on DMS/DMSO chemistry reviewed in this article.

6. References

(1) Andreae, M. O. *Mar. Chem.* **1990**, *30*, 1.
(2) Bates, T. S.; Lamb, B. K.; Guenther, A.; Dignon, J.; Stoiber, R. E. *J. Atmos. Chem.* **1992**, *14*, 315.
(3) Spiro, P. A.; Jacob, D. J.; Logan, J. A. *J. Geophys. Res.* **1992**, *97*, 6023.
(4) Bates, T. S.; Keene, R. P.; Wolfe, G. V.; Matrai, P. A.; Chavez, F. P.; Buck, K. R.; Blomquist, B. W.; Cunel, R. L. *Geophys. Res.* **1994**, *99*, 7835.
(5) Wilson, C.; Hirst, D. M. *Prog. React. Kinet.* **1996**, *21*, 69.
(6) DeMore, W. B.; Sander, S. P.; Golden, D. M.; Hampson, R. F.; Kurylo, M. J.; Howard, C. J.; Ravishankara, A. R.; Kolb, C. E.; Molina, M. J. *JPL Publication 97−4* **1997**, 1.
(7) Atkinson, R.; Baulch, D. L.; Cox, R. A.; Hampson, R. F., Jr.; Kerr, J. A.; Rossi, M. J.; Troe, J. *J. Phys. Chem. Ref. Data* **1997**, *26*, 1329.
(8) Barone, S. B.; Turnipseed, A. A.; Ravishankara, A. R. *Faraday Discuss.* **1995**, *100*, 39.
(9) Ravishankara, A. R.; Rudich, Y.; Talukdar, R.; Barone, S. B. *Philos. Trans. R. Soc. London B* **1997**, *352*, 171.
(10) Urbanski, S. P.; Wine, P. H. *S-Centered Radicals*; Alfassi, Z., Ed.; John Wiley and Sons: New York, 1999; p 97.
(11) Berresheim, H.; Wine, P. H.; Davis, D. D. *Composition, Chemistry, and Climate of the Atmosphere*; Singh, H. B., Ed.; Van Nostrand Reinhold: New York, 1995.
(12) Atkinson, R. *J. Phys. Chem. Ref. Data, Monograph No. 2* **1994**, 135.
(13) Tyndall, G. S.; Ravishankara, A. R. *Int. J. Chem. Kinet.* **1991**, *23*, 183.
(14) Plane, J. M. C. *Biogenic Sulfur in the Environment;* Saltzman, E. S., Cooper, W. J., Eds.; American Chemical Society: Washington, DC, 1989; p 404.
(15) Atkinson, R. *J. Phys. Chem. Ref. Data, Monograph No. 1* **1989**, 171.
(16) Atkinson, R.; Carter, W. P. L. *Chem. Rev.* **1984**, *84*, 437.
(17) Bentley, R.; Chasteen, T. G. *Chemosphere* **2004**, *55*, 291.
(18) Charlson, R. J.; Lovelock, J. E.; Andreae, M. O.; Warren, S. G. *Nature* **1987**, *326*, 655.
(19) Andreae, T. W.; Andreae, M. O.; Schebeska, G. *J. Geophys. Res.* **1994**, *99*, *22*, 819.
(20) Cainey, J. M.; Ayers, G. P.; Gillett, R. W.; Gras, J. L.; Ivey, J. P.; Selleck, P. W. *Baseline Atmos. Program.* **1996**, 58.
(21) Intergovernmental Panel on Climate Change. *Climate Change 1995, The Science of Climate Change*; Houghton, J. T., et al., Eds.; Cambridge University Press: New York, 1995.
(22) Chin, M.; Rood, R. B.; Allen, D. J.; Andreae, M. O.; Thompson, A. M.; Lin, S.-J.; Atlas, R. M.; Ardizzone, J. V. *J. Geophys. Res.* **1998**, *103*, 8341.
(23) Atkinson, R.; Perry, R. A.; Pitts, J. N., Jr. *Chem Phys. Lett.* **1978**, *54*, 14.
(24) Kurylo, M. J. *Chem. Phys. Lett.* **1978**, *58*, 233.
(25) Cox, R. A.; Sheppard, D. *Nature* **1980**, *284*, 330.
(26) Wine, P. H.; Kreutter, N. M.; Gump, C. A.; Ravishankara, A. R. *J. Phys. Chem.* **1981**, *85*, 2660.
(27) Macleod, H.; Poulet, G.; LeBras, G. *J. Chim. Phys.* **1983**, *80*, 287.
(28) Atkinson, R.; Pitts, J. N., Jr.; Aschmann, S. M. *J. Phys. Chem.* **1984**, *88*, 1584.
(29) Martin, D.; Jourdain, J. L.; LeBras, G. *Int. J. Chem. Kinet.* **1985**, *17*, 1247.
(30) Wallington, T. J.; Atkinson, R.; Tuazon, E. C.; Aschmann, S. M. *Int. J. Chem. Kinet.* **1986**, *18*, 837.
(31) Hynes, A. J.; Wine, P. H.; Semmes, D. H. *J. Phys. Chem.* **1986**, *90*, 4148.
(32) Hsu, Y.-C.; Chen, D.-S.; Lee, Y.-P. *Int. J. Chem. Kinet.* **1987** *19*, 1073.
(33) Barnes, I.; Bastian, V.; Becker, K. H. *Int. J. Chem. Kinet.* **1988**, *20*, 415.
(34) Nielsen, O. J.; Sidebottom, H. W.; Nelson, L.; Treacy, J. J.; O'Farrell, D. J. *Int. J. Chem. Kinet.* **1989**, *21*, 1101.
(35) Barnes, I.; Bastian, V.; Becker, K. H.; Fink, E. *Proceeding, 3rd European Symposium on the Physico-Chemical Behavior of Atmospheric Pollutants, 1984*; D. Riedel Publishing Co.: Dordrecht, Holland, 1984; p 149.
(36) Witte, F.; Zetzsch, C. 9th International Symposium on Gas Kinetics, University of Bordeaux, Bordeaux, France, July 20−25, 1986.
(37) Nielsen, O. J.; Treacy, J.; Nelsen, L.; Sidebottom, H. *Proceeding, 4th European Symposium on the Physico-Chemical Behavior of Atmospheric Pollutants, 1986*; D. Riedel Publishing Co.: Dordrecht, Holland, 1987; p 205.
(38) Abbatt, J. P. D.; Fenter, F. F.; Anderson, J. G. *J. Phys. Chem.* **1992**, *96*, 1780.
(39) Hynes, A. J.; Stocker, R. B.; Pounds, A. J.; Mckay, T.; Bradshaw, J. D.; Nicovich, J. M.; Wine, P. H. *J. Phys. Chem.* **1995**, *99*, 16967.
(40) Barone, S. B.; Turnipseed, A. A.; Ravishankara, A. R. *J. Phys. Chem.* **1996**, *100*, 14694.
(41) Sekušak, S.; Piecuch, P.; Bartlett, R. J.; Cory, M. G. *J. Phys. Chem. A* **2000**, *104*, 8779.
(42) El-Nahas, A. M.; Uchimaru, T.; Sugie, M.; Tokuhashi, K.; Sekiya, A. *J. Mol. Struct. (THEOCHEM)* **2005**, *722*, 9.
(43) Hynes, A. J.; Stickel, R. E.; Pounds, A. J.; Zhao, Z.; McKay, T.; Bradshaw, J. D.; Wine, P. H. In *Dimethylsulfide: Oceans, Atmo-*

sphere, and Climate; Restelli, G., Angeletti, G., Eds.; Kluwer Academic Publishers: Brussels, 1993; pp 211−221.
(44) McKee, M. L. *J. Phys. Chem.* **1993**, *98*, 10971.
(45) Gu, M.; Turecek, F. *J. Am. Chem. Soc.* **1992**, *114*, 7146.
(46) Turecek, F. *J. Am. Chem. Soc.* **1994**, *98*, 3701.
(47) Turecek, F. *Collect. Czech. Chem. Commun.* **2000**, *65*, 455
(48) Wang, L.; Zhang, J. *J. Mol. Struct. (THEOCHEM)* **2001**, *543*, 167.
(49) McKee, M. L. *J. Phys. Chem. A* **2003**, *107*, 6819.
(50) Uchimaru, T.; Tsuzuki, S.; Sugie, M.; Tokuhashi, K.; Sekiya, A. *Chem. Phys. Lett.* **2005**, *408*, 216.
(51) Gross, A.; Barnes, I.; Sørensen, R. M.; Kongsted,; Mikkelsen, K. V. *J. Phys. Chem. A* **2004**, *108*, 8659.
(52) Williams, M. B.; Campuzano-Jost, P.; Bauer, D.; Hynes, A. *J. Chem. Phys. Lett.* **2001**, *344*, 61.
(53) Silvente, E.; Richter, R. C.; Hynes, A, J. *J. Chem. Soc., Faraday Trans.* **1997**, *93*, 2821.
(54) Williams, M. B.; Campuzano-Jost, P.; Hynes, A. J. In *Proceedings of the 16th International Symposium on Gas Kinetics*; Cambridge, U.K., July 2000.
(55) Atkinson R.; Baulch, D. L.; Cox, R. A.; Crowley, J. N.; Hampson, R. F.; Hynes, R. G.; Jenkin, M. E.; Rossi, M. J.; Troe, J. *Atmos. Chem. Phys. Discuss.* **2003**, *3*, 6179.
(56) Albu, M.; Barnes, I.; Becker, K. H.; Patroescu-Klotz, I.; Mocanu, R.; Benter, Th. *Phys. Chem. Chem. Phys.* **2005**, in press.
(57) Putaud, J. P.; Mihalopoulos, N.; Nguyen, C.; Campin, J. M.; Belviso, S. *J. Atmos. Environ.* **1992**, *15*, 117.
(58) Bandy, A. R.; Scott, D. L.; Blomquist, B. W.; Chen, S. M.; Thornton, D. C. *Geophys. Res. Lett.* **1992**, *19*, 1125.
(59) Berresheim, H.; Tanner, D. J.; Eisele, F. L. *Anal. Chem.* **1993**, *65*, 84.
(60) Berresheim, H.; Tanner, D. J.; Eisele, F. L. *Anal. Chem.* **1993**, *65*, 3168.
(61) Berresheim, H.; Tanner, D. J.; Eisele, F. L.; McInnes, L. M.; Ramseybell, D. C.; Covert, D. S. *J. Geophys. Res.* **1993**, *98*, 12701.
(62) Bandy, A. R.; Thornton, D. C.; Blomquist, B. W.; Chen, S.; Wade, T. P.; Ianni, J. C.; Mitchell, G. M.; Nadler, W. *Geophys. Res. Lett.* **1996**, *23*, 741.
(63) Berresheim, H.; Huey, J. W.; Thorn, R. P.; Eisele, F. L.; Tanner, D. J.; Jefferson, A. *J. Geophys. Res.* **1998**, *103*, 1629.
(64) Davis, D.; Chen, G.; Kasibhatla, P.; Jefferson, A.; Tanner, D.; Eisele, F.; Lenschow, D.; Neff, W.; Berresheim, H. *J. Geophys. Res.* **1998**, *103*, 1657.
(65) Jefferson, A.; Tanner, D. J.; Eisele, F. L.; Davis, D. D.; Chen, G.; Crawford, J.; Huey, J. W.; Torres, A. L.; Berresheim, H. *J. Geophys. Res.* **1998**, *103*, 1647.
(66) Davis, D.; Chen, G.; Bandy, A.; Thornton, D.; Eisele, F.; Mauldin, L.; Tanner, D.; Lenschow, D.; Fuelberg, H.; Huebert, B.; Heath, J.; Clarke, A.; Blake, D. *J. Geophys. Res.* **1999**, *104*, 5765.
(67) Mauldin, R. L., III; Tanner, D. J.; Heath, J. A.; Huebert, B. J.; Eisele, F. L. *J. Geophys. Res.* **1999**, *104*, 5801.
(68) Chen, G.; Davis, D. D.; Kasibhatla, P.; Bandy, A. R.; Thornton, D. C.; Huebert, B. J.; Clarke, A. D.; Blomquist, B. W. *J. Atmos. Chem.* **2000**, *37*, 137.
(69) De Bruyn, W. J.; Harvey, M.; Cainey, J. M.; Saltzman, E. S. *J. Atmos. Chem.* **2002**, *41*, 189.
(70) Prospero, J. M.; Savoie, D. L.; Saltzman, E. S.; Larsen, B. R. *Nature* **1991**, *350*, 221.
(71) Minikin, A.; Legrand, M.; Hall, J.; Wagenbach, D.; Kleefeld, C.; Wolff, E.; Pasteur, E. C.; Ducroz, F. *J. Geophys. Res.* **1998**, *103*, 10975.
(72) Legrand, M.; Pasteur, E. C. *J. Geophys. Res.* **1998**, *103*, 10991.
(73) Koga, S.; Tanaka, H. *J. Geophys. Res.* **1999**, *104*, 13735.
(74) Legrand, M. In *Ice Core Studies of Global Biogeochemical Cycles*; Delmas, R., Ed.; NATO ASI Series I; Springer-Verlag: New York, 1995; Vol. 30.
(75) Legrand, M. *Philos. Trans. R. Soc. London B* **1997**, *352*, 241.
(76) Legrand, M.; Hammer, C.; DeAngelis, M.; Savarino, M.; Delmas, R.; Clausen, H.; Johnsen, S. J. *J. Geophys. Res.* **1997**, *102*, 26663.
(77) Saltzman, E. S.; Whung, P. Y.; Mayewski, P. A. *Geophys. Res. Lett.* **1997**, *102*, 26649.
(78) Hatakeyama, S.; Izumi, K.; Akimoto, H. *J. Phys. Chem.* **1985**, *15*, 135.
(79) Barnes, I.; Bastian, V.; Becker, K. H.; Wirtz, K. In *Formation, Distribution and Chemical Transformation of Air Pollutants*; Zellner, R., Ed.; VCH: Verlagsgesellschaft, 1987; Dechema Monographie Vol. 104, pp 59−77.
(80) Sørensen, S.; Falbe-Hansen, H.; Mangoni, M.; Hjorth, J.; Jensen, N. R. *J. Atmos. Chem.* **1996**, *24*, 299.
(81) Barnes, I.; Becker, K. H.; Patroescu, I. V. *Atmos. Environ.* **1996**, *30*, 1805.
(82) Patroescu, I. V.; Barnes, I.; Becker, K. H.; Mihalopoulos, N. *Atmos. Environ.* **1999**, *33*, 25.
(83) Arsene, C.; Barnes, I.; Becker, K. H. *Phys. Chem. Chem. Phys.* **1999**, *1*, 5463.
(84) Arsene, C.; Barnes, I.; Becker, K. H.; Mocanu, R. *Atmos. Environ.* **2001**, *35*, 3769.
(85) Urbanski, S. P.; Stickel, R. E.; Wine, P. H. *J. Phys. Chem. A* **1998**, *102*, 10522.
(86) Barnes, I.; Becker, K. H.; Patroescu, I. *Geophys. Res. Lett.* **1994**, *21*, 2389.
(87) Patroescu, I. V.; Barnes, I.; Becker, K. H. *J. Phys. Chem.* **1996**, *100*, 17207.
(88) Yin, F.; Grosjean, D.; Seinfeld, J. H. *J. Atmos. Chem.* **1990**, *11*, 309.
(89) Yin, F.; Grosjean, D.; Flagan, R. C.; Seinfeld, J. H. *J. Atmos. Chem.* **1990**, *11*, 365.
(90) Koga, S.; Tanaka, H. *J. Atmos. Chem.* **1993**, *17*, 201.
(91) Hertel, O.; Christensen, J.; Hov, Ø. *Atmos. Environ.* **1994**, *28*, 2387.
(92) Saltelli, A.; Hjorth, J. *J. Atmos. Chem.* **1995**, *21*, 187.
(93) Campolongo, F.; Saltelli, N. R.; Jensen, J.; Wilson, J.; Hjorth, J. *J. Atmos. Chem.* **1999**, *32*, 327.
(94) Lucas, D. D.; Prinn, R. G. *J. Geophys. Res.* **2002**, *107*, *D14*, ACH 12.
(95) Chin, M.; Jacob, D.; Gardner, G.; Foreman-Fowler, M.; Spiro, P.; Savoie, D. *J. Geophys. Res.* **1996**, *101*, 18667.
(96) Mari, C.; Suhre, K.; Rosset, R.; Bates, T. S.; Huebert, B. J.; Bandy, A. R.; Thornton, D. C.; Businger, S. *J. Geophys. Res.* **1999**, *104*, 21733.
(97) Capaldo, K. P.; Pandis, S. N. *J. Geophys. Res.* **1997**, *102*, 23251.
(98) Wallington, T. J.; Ellermann, T.; Nielsen, O. J. *J. Phys. Chem.* **1993**, *97*, 8442.
(99) Butkovskaya, N. I.; Le Bras, G. *J. Phys. Chem.* **1994**, *98*, 2582.
(100) Turnipseed, A. A.; Barone, S. B.; Ravishankara, A. R. *J. Phys. Chem.* **1996**, *100*, 14703.
(101) Nielsen, O. J.; Sehested, J.; Wallington, T. J. *Chem. Phys. Lett.* **1995**, *236*, 385.
(102) Urbanski, S. P.; Stickel, R. E.; Zhao, Z.; Wine, P. H. *J. Chem. Soc., Faraday Trans.* **1997**, *93*, 2813.
(103) Turnipseed, A. A.; Barone, S. B.; Ravishankara, A. R. *J. Phys. Chem.* **1993**, *97*, 5926.
(104) Vaghjiani, G. L.; Ravishankara, A. R. *J. Geophys. Res.* **1989**, *94*, 3487.
(105) Baker, J.; Dyke, J. M. *Chem. Phys. Lett.* **1993**, *213*, 257.
(106) McKee, M. L. *J. Phys. Chem.* **1993**, *97*, 10971.
(107) Kuhns, D. W.; Tran, T. B.; Shaffer, S. A.; Turecek, F. *J. Phys. Chem.* **1994**, *98*, 4845.
(108) Turecek, F. *J. Phys. Chem.* **1994**, *98*, 3701.
(109) Mousavipour, S. H.; Emad, L.; Fakhraee, S. *J. Phys. Chem. A* **2002**, *106*, 2489.
(110) Resende, S. M.; De Almeida, W. B. *J. Phys. Chem. A* **1999**, *103*, 4195.
(111) Bilde, M.; Orlando, J. J.; Tyndall, G. S.; Wallington, T. J.; Hurley, M. D.; Kaiser, E. W. *J. Phys. Chem. A* **1999**, *103*, 3963.
(112) Butkovskaya, N.; Barnes, I. In *Evaluation of the Climate Impact of Dimethyl Sulphide* (EL CID), contract number EVK2−CT-1999-00033, final report to the European Commission, Brussels, 2003.
(113) Resende, S. M.; De Almeida, W. B. *Phys. Chem. Chem. Phys.* **1999**, *1*, 2953.
(114) Jensen, N. R.; Hjorth, J.; Lohse, C.; Skov, H.; Restelli, G. *Atmos. Environ.* **1991**, *25A*, 1897.
(115) Jensen, N. R.; Hjorth, J.; Lohse, C.; Skov, H.; Restelli, G. *J. Atmos. Chem.* **1992**, *14*, 95.
(116) Mayer-Figge, A. *Thermischer Zerfall von Peroxynitraten verschiedener Struktur: Experimentelle Untersuchungen und Berechnungen*. Ph.D. Thesis, Bergische University Wuppertal, Germany, 1997.
(117) Resende, S. M.; De Almeida, W. B. *Phys. Chem. Chem. Phys.* **1999**, *1*, 2953.
(118) Turnipseed, A. A.; Barone, S. B.; Ravishankara, A. R. *J. Phys. Chem.* **1992**, *96*, 7502.
(119) Martínez, E.; Albaladejo, J.; Notario, A.; Jiménez, E. *Atmos. Environ.* **2000**, *34*, 5295.
(120) Dominé, F.; Ravishankara, A. R.; Howard, C. J. *J. Phys. Chem.* **1992**, *96*, 2171.
(121) Tyndall, G. S.; Ravishankara, A. R. *J. Phys. Chem.* **1989**, *93*, 2426.
(122) Chang, P.-F.; Wang, T. T.; Wang, N. S.; Hwang, Y.-L.; Lee, Y.-P. *J. Phys. Chem. A* **2000**, *104*, 5525.
(123) Martínez, E.; Albaladejo, J.; Jiménez, E.; Notario, A.; Aranda, A. *Chem. Phys. Lett.* **1999**, *308*, 37.
(124) Dominé, F.; Murrells, T. P.; Howard, C. J. *J. Phys. Chem.* **1990**, *94*, 5839.
(125) Balla, R. J.; Nelson, H. H.; McDonald, J. R. *Chem. Phys.* **1986**, *109*, 101.
(126) Barnes, I.; Bastian, V.; Becker, K. H. *Chem. Phys. Lett.* **1987**, *140*, 451.

(127) Turnipseed, A. A.; Ravishankara, A. R. The Atmospheric Oxidation of Dimethyl Sulfide: Elementary Steps in a Complex Mechanism. In *Dimethylsulphide: Oceans, Atmosphere and Climate*; Restelli, G., Angeletti, A., Eds.; Kluwer: Dordrecht, 1992; p 185.
(128) McKee, M. L. *Chem. Phys. Lett*. **1993**, *211*, 643.
(129) Borissenko, D.; Kukui, A.; Laverdet, G.; Le Bras, G. *J. Phys. Chem. A* **2003**, *107*, 1155.
(130) Kukui, A.; Bossoutrot, V.; Laverdet, G.; Le Bras, G. *J. Phys. Chem. A* **2000**, *104*, 935.
(131) Mellouki, A.; Jourdain, J. L.; Le Bras, G. *Chem. Phys. Lett.* **1988**, *148*, 231.
(132) Hjorth, J.; Jensen, N. R.; Raes, F.; Van Dingenen, R. In *Dimethylsulphide: Oceans, Atmosphere and Climate*; Restelli, G., Angeletti, A., Eds.; Kluwer Academic Publishers: New York, 1993; pp 261−272.
(133) Van Dingenen, R.; Jensen, N. R.; Hjorth, J.; Raes, F. *J. Atmos. Chem.* **1994**, *18*, 211.
(134) Ray, A.; Vassalli, I.; Laverdet, G.; Le Bras, G. *J. Phys. Chem*. **1996**, *100*, 8895.
(135) Butkovskaya, N. I.; Barnes, I. In Proceedings of 8th European Symposium on the Physico-Chemical Behaviour of Atmospheric Pollutants, 17−20 Sep 2001, Torino, Italy, European Commission, CD-ROM proceedings.
(136) Butkovskaya, N. I.; Barnes, I. In *Proceedings of the NATO Advanced Research Workshop on Global Atmospheric Change and its Impact on Regional Air Quality, Irkutsk, Russian Federation, Aug 21−27, 2002*; Barnes, I., Ed.; NATO Science Series IV (Earth and Environmental Sciences); Kluwer Academic Publishers: The Netherlands, 2002; Vol. 16.
(137) Wang, L.; Zhang, J. *J. Mol. Struct. (THEOCHEM)* **2002**, *581*, 129.
(138) Wallington, T. J.; Atkinson, R.; Winer, A. M.; Pitts, J. N., Jr. *J. Phys. Chem*. **1986**, *90*, 4646.
(139) Wallington, T. J.; Atkinson, R.; Winer, A. M.; Pitts, J. N., Jr. *J. Phys. Chem*. **1986**, *90*, 5393.
(140) Tyndall, G. S.; Burrows, J. P.; Schneider, W.; Moortgat, G. K. *Chem. Phys. Lett*. **1986**, *130*, 463.
(141) Dlugokencky, E. J.; Howard, C. J. *J. Phys. Chem*. **1988**, *92*, 1188.
(142) Atkinson, R.; Pitts, J. N., Jr.; Aschmann, S. M. *J. Phys. Chem*. **1984**, *88*, 1584.
(143) Daykin, E. P.; Wine, P. H. *Int. J. Chem. Kinet.* **1990**, *22*, 1083.
(144) Tyndall, G. S.; Ravishankara, A. R. *Int. J. Chem. Kinet.* **1991**, *23*, 483.
(145) Jensen, N. R.; Hjorth, J.; Lohse, C.; Skov, H.; Restelli, G. *J. Atmos. Chem*. **1992**, *14*, 95.
(146) Jensen, N. R.; Hjorth, J.; Skov, H.; Restelli, G. *Atmos. Environ*. **1991**, *25A*, 1897.
(147) Arsene, C.; Barnes, I.; Albu, M. in Evaluation of the Climatic impact of Dimethyl Sulphide (EL CID), contract Nr. EVK2−CT-1999-00033, final report to the European Commission, Brussels, 2003.
(148) MacLeod, H.; Aschmann, S. M.; Atkinson, R.; Tuazon, E. C.; Sweetman, J. A.; Winer, A. M.; Pitts, J. N., Jr. *J. Geophys. Res*. **1986**, *91*, 5338.
(149) Pszenny, A. A.; P., Keene, W. C.; Jacob, D. J.; Fan, S.; Maben, J. R.; Zetwo, M. P.; Springer-Young, M.; Galloway, J. N. *Geophys. Res. Lett.* **1993**, *20*, 699.
(150) Singh, H. B. In *Composition, Chemistry and Climate of the Atmosphere*; Singh, H. B., Ed.; Van Nostrand Reinhold: New York, 1995; ISBN 0-442-01264-0, pp 216−245.
(151) Singh, H. B.; Thakur, A. N.; Chen, Y. E.; Kanakidou, M. *Geophys. Res. Lett*. **1966**, *23*, 1529.
(152) Spicer, C. W.; Chapman, E. G.; Finlayson-Pitts, B. J.; Plastridge, R. A.; Hubbe, J. M.; Berkowitz, C. M. *Nature* **1998**, *394*, 353
(153) Toumi, R. *Geophys. Res. Lett.* **1994**, *21*, 117.
(154) Finlayson-Pitts, B. J.; Pitts, J. N., Jr. *Chemistry of the upper and lower atmosphere*; Academic Press: San Diego, CA, 2000; p 328.
(155) Nielsen, O. J.; Sidebottom, H. W.; Nelson, L.; Rattigan, O.; Treacy, J. J.; O'Farrell, D. J. *Int. J. Chem. Kinet.*, **1990**, *22*, 603.
(156) Stickel, R. E.; Nicovich, J. M.; Wang, S.; Zhao, Z.; Wine, P. H. *J. Phys. Chem*. **1992**, *96*, 9875.
(157) Kinnison, D. J.; Mengon, W.; Kerr, J. A. *J. Chem. Soc., Faraday Trans*. **1996**, *92*, 369.
(158) Butkovskaya, N. I.; Poulet, G.; Le Bras, G. *J. Phys. Chem*. **1995**, *99*, 4536.
(159) Zhao, Z.; Stickel, R. E.; Wine, P. H. *Chem. Phys. Lett*. **1996**, *251*, 59.
(160) Díaz-de-Mera, Y.; Aranda, A.; Rodríiguez, D.; López, R.; Cabaòas, B.; Martíez, E. *J. Phys. Chem*. **2002**, *106*, 8627.
(161) Arsene, C.; Barnes, I.; Becker, K. H.; Benter, Th. *Int. J. Chem. Kinet*. **2005**, *37*, 66.
(162) Enami, S.; Nakano, Y.; Hashimoto, S.; Kawasaki, M.; Aloisio, S.; Francisco, J. S. *J. Phys. Chem. A* **2004**, *108*, 7785.
(163) Dyke, J. M.; Ghosh, M. V.; Kinnison, D. J.; Levita, G.; Morris, A.; Shallcross, D. E. *Phys. Chem. Chem. Phys*. **2005**, *7*, 866.
(164) Langer, S.; McGovney, B. T.; Finlayson-Pitts, B. *J. Geophys. Res. Lett*. **1996**, *23*, 1661.
(165) Urbanski, S. P.; Wine, P. H. *J. Phys. Chem. A* **1999**, *103*, 10935.
(166) Arsene, C.; Barnes, I.; Albu, M. In Proceedings of the IGAC, Greece; Final report of the EL CID (Evaluation of the Climatic Impact of Dimethyl Sulphide (contract number: EVK2−CT-1999−00033) to the European Commission, Brussels, 2003.
(167) Wilson, C.; Hirst, D. M. *J. Chem. Soc., Faraday Trans*. **1997**, *93*, 2831.
(168) Resende, S. M.; De Almeida, W. B. *J. Phys. Chem. A* **1997**, *101*, 9738.
(169) Thompson, K. C.; Canosa-Mas, C. E.; Wayne, R. W. *Phys. Chem. Chem. Phys*. **2002**, *4*, 4133.
(170) Sayin, H.; McKee, M. L. *J. Phys. Chem. A* **2004**, *108*, 7613.
(171) Gravestock, T.; Blitz, M. A.; Heard, D. E. *Phys. Chem. Chem. Phys*. **2005**, *7*, 2173.
(172) Barnes, I.; Bastian, V.; Becker, K. H.; Overath, R. D. *Int. J. Chem. Kinet*. **1991**, *23*, 579.
(173) Wine, P. H.; Nicovich, J. M.; Stickel, R. E.; Zhao, Z.; Shackelford, C. J.; Kreutter, K. D.; Daykin, E. P.; Wang, S. In *The Tropospheric Chemistry of Ozone in Polar Regions*; Niki, H., Becker, K. H., Eds.; NATO ASI Series I (Global Environmental Change); Springer-Verlag: Berlin Heidelberg 1993; Vol. 7, pp 385−395.
(174) Nakano, Y.; Goto, M.; Hashimoto, S.; Kawasaki, M.; Wallington, T. J. *J. Phys. Chem. A* **2001**, *105*. 11045.
(175) Jefferson, A.; Nicovich, J. M.; Wine, P. H. *J. Phys. Chem*. **1994**, *98*, 7128.
(176) Ingham, T.; Bauer, D.; Sander, R.; Crutzen, P. J.; Crowley, J. N. *J. Phys. Chem. A* **1999**, *103*, 7199.
(177) Maurer, T.; Barnes, I.; Becker, K. H. *Int. J. Chem. Kinet*. **1999**, *31*, 1097.
(178) Ballesteros, B.; Jensen, N. R.; Hjorth, J. *J. Atmos. Chem*. **2002**, *43*, 135.
(179) Bedjanian, Y.; Poulet, G.; Le Bras, G. *Int. J. Chem. Kinet*. **1996**, *28*, 383.
(180) Shum, L. G. S.; Benson, S. W. *Int. J. Chem. Kinet.* **1985**, *17*, 27.
(181) Martin, D.; Jourdain, J. L.; Laverdet, G.; Le Bras, G. *Int. J. Chem. Kinet*. **1987**, *19*, 503.
(182) Barnes, I.; Becker, K. H.; Carlier, P.; Mouvier, G. *Int. J. Chem. Kinet*. **1987**, *19*, 489.
(183) Daykin, E. P.; Wine, P. H. *J. Geophys. Res.*. **1990**, *95*, 18547.
(184) Maguin, F.; Mellouki, W.; Laverdet, G.; Poulet, G.; Le Bras, G. *Int. J. Chem. Kinet*. **1991**, *23*, 237.
(185) Knight, G. P.; Crowley, J. N. *Phys. Chem. Chem. Phys*. **2001**, *3*, 393.
(186) Nakano, Y.; Enami, S.; Nakamichi, S.; Aloisio, S.; Hashimoto, S.; Kawasaki, M. *J. Phys. Chem. A* **2003**, *107*, 6381.
(187) Lucas, D. D.; Prinn, R. G. *Atmos. Chem. Phys. Discuss*. **2004**, *4*, 6379.
(188) von Glasow, R.; Crutzen, P. J. *Atmos. Chem. Phys. Discuss*. **2003**, *3*, 6733.
(189) Toyota, K.; Kanaya, Y.; Takahashi, M.; Akimoto, H. *Atmos. Chem. Phys. Discuss*. **2004**, *4*, 1961.
(190) Bandy, A. R.; Thornton, D. C.; Blomquist, B. W.; Chen, S.; Wade, T. P.; Ianni, J. C.; Mitchell, G. M.; Nadler, W. *Geophys. Res. Lett*. **1996**, *23*, 741.
(191) Berresheim, H.; Huey, J. W.; Thorn, R. P.; Eisele, F. L.; Tanner, D. J.; Jefferson, A. *J. Geophys. Res.* **1998**, *103*, 1629.
(192) Sciare, J.; Baboukas, E.; Hancy, R.; Mihalopoulos, N.; Nguyen, B. C. *J. Atmos. Chem.* **1998**, *30*, 229.
(193) Barnes, I.; Bastian, V.; Becker, K. H.; Martin, D. In *Dimethylsulphide: Oceans, Atmosphere and Climate*; Restelli, G., Angeletti, A., Eds.; Kluwer Academic Publishers: New York, 1993; pp 476−488.
(194) Hynes, A. J.; Wine, P. H. *J. Atmos. Chem*. **1996**, *24*, 23.
(195) Le Bras G.; Kukui, A.; Bedjanian, Y.; Riffault, V. In *Evaluation of the Climate Impact of Dimethyl Sulphide* (EL CID), contract number EVK2−CT-1999-00033, final report to the European Commission, Brussels, 2003.
(196) Falbe-Hansen, H.; Sørensen, Jensen, N. R.; Pedersen, T.; Hjorth, J. *Atmos. Environ*. **2000**, *34*, 1543.
(197) Kukui, A.; Borissenko, D.; Laverdet, G.; Le Bras, G. *J. Phys. Chem. A* **2003**, *107*, 5732.
(198) De Bruyn, W. J.; Shorter, J. A.; Davidovits, P.; Worsnop, D. R.; Zahniser, M. S.; Kolb, C. E. *J. Geophys. Res.* **1994**, *99*, 16927.
(199) Barnes, I.; Bastian, V.; Becker, K. H.; Martin, D. In *Biogenic Sulphur in the Environment*; Saltzman, E. S., Cooper, W. J., Eds.; ACS Symposium Series 393; American Chemical Society: Washington, DC, 1989; pp 476−488.
(200) Wang, L.; Zhang, J. *Chem. Phys. Lett*. **2002**, *356*, 490.
(201) Arsene, C.; Barnes, I.; Becker, K. H.; Schneider, W. F.; Wallington, T. T.; Mihalopoulos, N.; Patroescu-Klotz, I. V. *Environ. Sci. Technol*. **2002**, *36*, 5155.

(202) EUPHORE Report 2001 (available at www.physchem.uni-wuppertal.de).
(203) Martínez, E.; Aranda, A.; Díaz de Mera, Y.; Rodríguez, D.; López, M. R.; Albaladejo, J. *Environ. Sci. Technol.* **2002**, *36*, 1226.
(204) Riffault, V. Y.; Bedjanian, Y.; Le Bras, G. *J. Phys. Chem. A* **2003**, *107*, 5404.
(205) Arsene, C.; Albu, M.; Barnes, I. In Proceedings of the International Symposium on Gas Kinetics, July 2002, Essen, Germany.
(206) Wine, P. H.; Nicovich, J. M.; McKee, M. L.; Kleissas, K. M.; Parthasarathy, S.; Pope, F. D.; Pegus, A. T. In Proceedings of the International Sysmposium on Gas Kinetics, Aug 7−12, 2004, Bristol, U.K.; p 21.
(207) Ravishankara, A. R. *Science* **1997**, *276*, 1058.
(208) Seinfeld, J.; Pandis, S. *Atmospheric Chemistry and Physics: From Air Pollution to Climate Changes*; John Wiley and Sons: London, 1997.
(209) Yvon, S. A.; Saltzman, E. S.; Cooper, D. J.; Bates, T. S.; Thompson, A. M. *J. Geophys. Res.* **1996**, *101*, 6899.
(210) Sciare, J.; Baboukas, E.; Kanakidou, M.; Krischke, U.; Belviso, S.; Bardouki, H.; Mihalopoulos, N. *J. Geophys. Res.* **2000**, *105*, *14*, 433.
(211) James, J. D.; Harrison, R. M.; Savage, N. H.; Allen, A. G.; Grenfell, J. L.; Allan, B. J.; Plane, J. M. C.; Hewitt, C. N.; Davison, B.; Robertson, L. *J. Geophys. Res*. **2000**, *105*, *D21*, 26, 379.
(212) Vogt, R.; Crutzen, P. J.; Sander, R. *Nature* **1996**, *383*, 327.
(213) Ayers, G. P.; Gillett, R. W.; Cainey, J. M.; Dick, A. L. *J. Atmos. Chem.* **1999**, *33*, 299.
(214) Dickerson, R. R.; Rhoads, K.; Carsey, T.; Oltmans, S.; Burrows, J.; Crutzen, P. J. *J. Geophys. Res.* **1999**, *104*, 21385.
(215) von Glasow, R.; von Kuhlmann, R.; Lawrence, M. G.; Platt, U.; Crutzen, P. J.; *Atmos. Chem. Phys*. **2004**, *4*, 2481.
(216) von Glasow, R.; Crutzen, P. J. *Atmos. Chem. Phys.* **2004**, *4*, 589.
(217) Wagner, T.; Leue, C.; Wenig, M.; Pfeilsticker, K.; Platt, U. *J. Geophys. Res*. **2001**, *106*, 24225.
(218) Richter, A.; Wittrock, F.; Ladstaeter-Weissenmayer, A.; Burrows, J. P. *Adv. Space Res*. **2002**, *29*, 1667.
(219) Van Roozendael, M.; Wagner, T.; Richter, A.; Pundt, J.; Arlander, D. W.; Burrows, J. P.; Chipperfield, M.; Fayt, C.; Johnston, P. V.; Lambert, J.-C.; Kreher, K.; Pfeilsticker, K.; Platt, U.; Pommereau, J. P.; Sinnhuber, B. M.; Tornkvist, K. K.; Wittrock, F. *Adv. Space Res.* **2002**, *29*, 1661.
(220) Bardouki, H.; Berresheim, H.; Sciare, J.; Vrekoussis, M.; Kouvarakis, G.; Oikonomou, C.; Schneider, J.; Mihalopoulos, N. *Atmos. Chem. Phys.* **2003**, *3*, 1871.
(221) Sciare, J.; Kanakidou, M.; Mihalopoulos, N. *J. Geophys. Res.* **2000**, *105*, *17*, 257.
(222) Legrand, M.; Sciare, J.; Jourdain, B.; Genthon, *J. Geophys. Res.* **2001**, *106*, 14409.
(223) Saltzman, E. S.; Savoie, D. L.; Prospero, J. M.; Zika, R. G. *J. Atmos Chem*. **1986**, *4*, 227.
(224) Savoie, D.; Prospero, J. M. *Nature* **1989**, *339*, 685.
(225) Bates, T. S.; Calhoun, J. A.; Quinn, P. K. *J. Geophys. Res*. **1992**, *97*, 9859.
(226) Legrand, M.; Pasteur, E. C. *J. Geophys. Res*. **1998**, *103*, 10991.
(227) Ayers, G.; Cainey, J. M.; Granek, H.; Leck, C. *J. Atmos. Chem.* **1996**, *25*, 307.
(228) Campolongo, F.; Saltelli, A.; Jensen, N. R.; Wilson, J.; Hjorth, J. *J. Atmos. Chem.* **1999**, *32*, 327.
(229) Dacey, J. W. H.; Wakeham, S. G.; Howes, B. L. *Geophys. Res. Lett.* **1984**, *11*, 991.
(230) Watts, S. F.; Brimblecomble, P. *Environ. Technol. Lett.* **1987**, *8*, 483.
(231) Lee, Y. N.; Zhou, X. *J. Geophys. Res*. **1994**, *99*, 3597.
(232) Clegg, S. L.; Brimblecomble, P. *Environ. Technol. Lett.* **1985**, *6*, 269.
(233) Sander, R. http://www.mpch-mainz.mpg.de/∼sander/res/henry.html.
(234) Jacob, D. *Atmos. Environ.* **2000**, *34*, 2131.
(235) Nathanson, G. M.; Davidovits, P.; Worsnop, D. R.; Kolb, C. E. *J. Phys. Chem*. **1996**, *100*, 13007.
(236) Kolb, C. E.; Worsnop, D. R.; Zahniser, M. S.; Davidovits, P.; Keyser, L. F.; Leu, M. T.; Molina, M. J.; Hanson, D. R.; Ravishankara, A. R. In *Progress and Problems in Atmospheric Chemistry*; Baker, J. R., Ed.; Adv. Ser. Physical Chemistry; 1995; Vol. 3, World Scientific Publishing Co.: Hackensack, NJ, 771.
(237) Dentener, F. J.; Crutzen, P. J. *J. Geophys. Res.* **1993**, *98*, 7149.
(238) Bonifacic, M.; Moeckel, H.; Bahnemann, D.; Asmus, K. D. *J. Chem. Soc., Perkin Trans.* **1975**, *2*, 675.
(239) Gershenzon, M.; Davidovits, P.; Jayne, J. T.; Kolb, C. E.; Worsnop, D. R. *J. Phys. Chem. A* **2001**, *105*, 7031.
(240) Andreae, M. O. *Limnol. Oceanogr*. **1980**, *25*, 1054.
(241) Jacob, D. J. *J. Geophys. Res.* **1986**, *91*, 9807.
(242) Kleiman, L. I. *J. Geophys. Res.* **1986**, *91*, 10889.
(243) Brimblecombe, P.; Watts, S.; Shooter, D. *Proc. 194th ACS Mtg*. **1987**, 96.
(244) Brimblecombe, P.; Shooter, D. *Mar. Chem*. **1986**, *19*, 343.
(245) Bardouki, H. Ph.D. Thesis, University of Crete, 2003; p 198.
(246) Amels, P.; Elias, H.; Wannowius, K.-J. *J. Chem. Soc., Faraday Trans.* **1997**, *93* (15), 2537.
(247) Bardouki, H.; Barcellos da Rosa, M.; Mihalopoulos, N.; Palm, U.; Zetzsch, C. *Atmos. Environ.* **2002**, *36*, 4627.
(248) Milne, P. J.; Zika R. G.; Saltzman, E. S. *ACS Symp. Ser*. **1989**, 518.
(249) Zhu, L.; Nicovich, J. M.; Wine, P. H. *Aquat. Sci.* **2003**, *65*, 425.
(250) Olson, T. M.; Fessenden, R. W. *J. Phys. Chem*. **1992**, *96*, 3317.
(251) Ross, A. B.; Mallard, W. G.; Helman, W. P.; Bielski, B. H. J.; Buxton, G. V.; Cabelli, D. E.; Greenstock, C. L.; Huie, R. E.; Neta, P. *NDRL-NIST Solution Kinetics Database*, Version 1; National Insititute of Standards and Technology: Gaithersburg, MD, 1992.
(252) Sehested, K.; Holcman, J. *Radiat. Phys. Chem*. **1996**, *47*, 357.
(253) Le Bras, G.; Barnes, I.; Hjorth, J.; Zetzsch, C.; Martinez, E.; Mihalopoulos, N. *Dimethyl sulphide (DMS), Air pollution research report EUR 19569 EN*, Commission of the European Communities, 2000, p 114.
(254) Zhu, L.; Nicovich, J. M.; Wine, P. H. *J. Phys. Chem. A* **2005**, *109*, 3903.
(255) Zhu, L.; Nicovich, J. M.; Wine, P. H. *J. Photochem. Photobiol. A: Chem.* **2003**, *157*, 311,
(256) Boucher, O.; Moulin, C.; Belviso, S.; Aumont, O.; Bopp, L.; Cosme, E.; von Kuhlmann, R.; Lawrence, M. G.; Pham, M.; Reddy, M. S.; Sciare, J.; Venkataraman, C. *ACP* **2003**, *3*, 49.
(257) Sander, R. *Surveys Geophys.* **1999**, *20*, 1.
(258) Mozurkewich, M. *Geophys. Res. Lett.* **1997**, *24*, 3209.
(259) Katoshevski, D.; Nenes, A.; Seinfeld, J. H. *J. Aerosol Sci*. **1999**, *30*, 503.
(260) Masuda, N.; Nagano, Y.; Sakiyama, M. *J. Chem. Thermodyn*. **1994**, *26*, 971.
(261) McKee, M. L. *Chem. Phys. Lett.* **1994**, *231*, 257.
(262) Nicovich, J. M.; Kreutter, K. D.; van Dijk, C. A.; Wine, P. H. *J. Phys. Chem*. **1992**, *96*, 2518.
(263) Turecek, F.; Brabec, L.; Vondrak, T.; Hanus, V.; Hajicek, J.; Havlas, Z. *Collect. Czech. Chem. Commun.* **1988**, *53*, 2140.
(264) Gurthrie, J. P.; Gallant, R. T. *Can. J. Chem*. **2000**, *78*, 1295.
(265) Atkinson, R.; Plum, C. N.; Carter, W. P. L.; Winer, A. M.; Pitts, J. N., Jr. *J. Phys. Chem.* **1984**, *88*, 1210.
(266) Aschmann, S. M.; Atkinson, R. *Int. J. Chem. Kinet*. **1995**, *27*, 613.
(267) Atkinson, R.; Aschmann, S. M. *Int. J. Chem. Kinet*. **1985**, *17*, 33.
(268) Barnes, I.; Bastian, V.; Becker, K. H.; Overrath, R.; Tong, Z. *Int. J. Chem. Kinet*. **1989**, *21*, 499.
(269) Yarwood, G.; Peng, N.; Niki, H. *Int. J. Chem. Kinet*. **1992**, *24*, 369.
(270) Platt, U.; Hönninger, G. *Chemosphere* **2003**, *32*, 325.
(271) Tuckermann, M.; Ackermann, R.; Gölz, C.; Lorenzen-Schmidt, H.; Senne, T.; Stutz, J.; Trost, B.; Unold, W.; Platt, U. *Tellus* **1997**, *49B*, 533.
(272) Prinn, R. G.; Huang, J.; Weiss R. F.; Cunnold, D. M.; Fraser, P. J.; Simmonds, P. G.; McCulloch, A.; Harth, C.; Reimann, S.; Salameh, P.; O'Doherty, S.; Wang, R. H. J.; Porter, L. W.; Miller, B. R.; Krummel, P. B. *Geophys. Res. Lett.* **2005**. *32*, L07809; doi 10.1029/2004GL022228.
(273) Adewuyi, Y. G.; Carmichael, G. R. *Environ. Sci. Technol*. **1986**, *20*, 1017.
(274) Krol, M.; Van Leeuwen, P. J.; Lelieveld, J. *J. Geophys. Res.* **1998**, *103*, 10697.
(275) Logan, J. A. *J. Geophys. Res.* **1999**, *104*, 16115.
(276) Wingenter, O. W.; Kubo, M. K.; Blake, N. J.; Smith, T. W.; Rowland, F. S. *J. Geophys. Res*. **1996**, *101*, 4331.
(277) Herrmann, H.; Ervens, B.; Jacobi, H. W.; Wolke, R.; Nowacki, P.; Selner, R.; *J. Atmos. Chem.* **2000**, *36*, 231.
(278) Lelieveld, J.; Crutzen, P. J. *J. Atmos. Chem.* **1991**, *12*, 229.

CR020529+